

CHARACTERIZATION OF A FAMILY OF PROTEIN TYROSINE PHOSPHATASES FROM
MICROPLITIS DEMOLITOR BRACOVIRUS

by

ARDINA JANNETJE PRUIJSSERS

(Under the Direction of Michael Strand)

ABSTRACT

Among the most virulent pathogens of insects are symbiotic polydnnaviruses (PDVs) which are associated with parasitoid wasps. Characterization of the virulence molecules PDVs produce and functional studies are essential to understanding how PDVs kill insect pests. Many gene products encoded by these pathogens target conserved signaling pathways, making them valuable tools for understanding processes regulating the insect immune system. My dissertation project focused on the parasitoid *Microplitis demolitor*, its associated PDV named *M. demolitor* bracovirus (MdBV), and a family of viral genes called protein tyrosine phosphatases (PTPs). Specific aims of my project were to: 1) characterize the structure, function and expression of MdBV PTPs, 2) assess whether any PTP family members play a role in immunosuppression, and 3) understand how MdBV infection inhibits insect growth and pupation. Analysis of PTP expression indicated that most members of this family are expressed in hemocytes (immune cells) of its insect host. MdBV-infected hemocytes also exhibited higher levels of tyrosine phosphatase activity than non-infected hemocytes. Functional studies indicated that two PTPs have tyrosine phosphatase activity, whereas two other did not. The catalytically active PTPs co-localize to focal adhesions and inhibit phagocytosis of several foreign targets in hemocyte-like

cell lines, suggesting that focal adhesion kinase or related proteins are candidate substrates for these viral PTPs. I also found that the catalytically active PTPs caused apoptosis when expressed in Sf-21 cells. My findings suggest that the anti-phagocytic activity of PTP-H2 is conserved but that its apoptosis-inducing activity is restricted and depends in part on intrinsic differences between cell types. The results of my endocrine studies indicate that MdBV blocks pupation by disabling production of ecdysteroids by prothoracic glands (PGs) and the production or release of brain hormones that trigger PGs to produce ecdysteroids. My metabolic studies also indicate that infected larvae undergo a shift in carbohydrate metabolism that resembles the shift observed during starvation. In summary, my dissertation work provides important insights into the mechanisms by which PDVs cause disease in insects and provides evidence for a role of two PTP family members in immunosuppression.

INDEX WORDS: Protein tyrosine phosphatases, *Pseudoplusia includens* hemocytes, Lepidopteran host, *Drosophila*, Polydnavirus, Phagocytosis, Apoptosis, Disruption, Development, Prothoracic glands, Ecdysone, Sugar metabolism, Glycogen, Trehalose

CHARACTERIZATION OF A FAMILY OF PROTEIN TYROSINE PHOSPHATASES FROM
MICROPLITIS DEMOLITOR BRACOVIRUS

by

ARDINA JANNETJE PRUIJSSERS

B.S., Wageningen University, The Netherlands, 2003

A Dissertation Submitted to the Graduate Faculty of The University of Georgia in Partial
Fulfillment of the Requirements for the Degree

DOCTOR OF PHILOSOPHY

ATHENS, GEORGIA

2008

© 2008

Ardina Jannetje Pruijssers

All Rights Reserved

CHARACTERIZATION OF A FAMILY OF PROTEIN TYROSINE PHOSPHATASES FROM
MICROPLITIS DEMOLITOR BRACOVIRUS

by

ARDINA J. PRUIJSSERS

Major Professor: Michael Strand

Committee: Mark Brown
Rick Tarleton

Electronic Version Approved:

Maureen Grasso
Dean of the Graduate School
The University of Georgia
May 2008

To mom and dad
For your love and support

Aan papa en mama
In dank voor jullie liefde en steun

ACKNOWLEDGEMENTS

Now my time as a doctoral student has come to an end, I get to look back and identify the people who have helped me get to this point. First and foremost, there was my major advisor. Thank you, Mike, for believing in me and for supporting my choices throughout the years. I believe you were the driving force behind most good that has come my way professionally. For wet lab issues and trouble shooting, there was always Markus and later also Richard. Thank you both for helping me along and for being patient in doing so. Mark Brown, thank you for being an active member of my committee. Working with you has been a great pleasure thanks to your great enthusiasm, humbleness and generosity. Jena, Kevin, Anne, Patrizia and Lihua: you helped make my daily life in the lab cheery and sunny. Thanks for smiles also to Jodie, Shira, Hans-Peter, and all the other beautiful souls that have crossed my path during my time in Athens. Thanks to my parents, brothers, and extended family for supporting me throughout the years and for keeping me with two feet on the ground. Last but not least, I thank Max: my love, my best friend. Without you, the past four years would have been cloudier and certainly more doubtful.

The years in graduate school have taught me many things and occasionally inspired me to adjust my views. But when it comes to life, I still believe that the only way to live happily ever after is in the here and now.

TABLE OF CONTENTS

	Page
ACKNOWLEDGEMENTS	v
LIST OF TABLES	viii
LIST OF FIGURES	ix
CHAPTER	
1 LITERATURE REVIEW	1
1.1 The polydnavirus lifecycle	1
1.2 General organizational features of PDV genomes	3
1.3 PDV gene families.....	4
1.4 Immunological interactions between PDV-carrying parasitoids and Lepidoptera.....	5
1.5 Developmental interactions between PDV-carrying parasitoids and Lepidoptera.....	7
1.6 <i>Microplitis demolitor</i> Bracovirus is associated with the microgastrine braconid wasp <i>Microplitis demolitor</i>	8
1.7 The MdBV genome encodes multiple gene families	9
1.8 PTPs are structurally and functionally diverse.....	10
1.9 Role of phosphorylation in immune signaling and other physiological processes.....	15
1.10 PTPs as virulence factors	20

1.11 Chapter contents	23
2 CHARACTERIZATION OF PTP SEQUENCE, EXPRESSION, CATALYSIS AND ROLE IN MDBV INDUCED INHIBITION OF PHAGOCYTOSIS	25
2.1 Introduction	25
2.2 Materials and methods.....	26
2.3 Results	34
2.4 Discussion	49
3 ROLE OF MDBV GENES IN APOPTOSIS OF INSECT IMMUNE CELLS	54
3.1 Introduction	54
3.2 Materials and methods.....	55
3.3 Results	60
3.4 Discussion	72
4 THE EFFECT OF VIRAL INFECTION ON HOST GROWTH, METABOLISM AND DEVELOPMENT	76
4.1 Introduction	76
4.2 Materials and methods.....	78
4.3 Results	82
4.4 Discussion	91
REFERENCES	94

LIST OF TABLES

	Page
Table 2:1 Predicted properties of <i>M. demolitor</i> PTP family members	29
Table 2:2 Gene specific primers used for real time PCR reactions	35

LIST OF FIGURES

	Page
Figure 1:1 Polydnavirus lifecycle	2
Figure 1:2 Schematic representation of PTP1B catalytic site.....	12
Figure 2.1 Sequence analysis of MdBV PTP family members	37
Figure 2.2 PTP expression analysis	39
Figure 2.3 MdBV-infected host hemocytes exhibit elevated levels of tyrosine phosphatase activity	42
Figure 2.4 Expression of PTP-H2 and -H3 significantly increases tyrosine phosphatase activity in <i>Drosophila</i> S2 cells	44
Figure 2.5 Localization of PTP-H1, -H2, -H3 and J-1 in <i>Drosophila</i> S2 cells.....	45
Figure 2.6 PTP-H2 and -H3 significantly reduces phagocytosis of <i>E. coli</i> and polystyrene beads by S2 cells	48
Figure 3.1 MdBV infection induces apoptosis of granulocytes.....	62
Figure 3.2 PTP-H2 expression induces apoptosis of Sf-21 cells.....	64
Figure 3.3 PTP-H2 expression increases annexin V binding and mitochondrial membrane depolarization	65
Figure 3.4 PTP-H2 mediated cell death induces caspase activation and requires phosphatase activity	68
Figure 3.5 Apoptosis of Sf-21 cells is unaffected by culture on agarose-coated plates but PTP-H2 expression reduces cell proliferation.....	71

Figure 4.1 Ecdysteroid production by *P. includens* PGs during the fifth instar84

Figure 4.2 Effect of MdBV infection on ecdysteroid production by *P. includens* PGs86

Figure 4.3 MdBV infection alters host carbohydrate metabolism.....89

Figure 4.4 MdBV infection causes an inhibition of weight gain and a loss of appetite90

CHAPTER 1

LITERATURE REVIEW

1.1 The polydnavirus life cycle

Polydnaviruses (PDVs) are enveloped, double stranded DNA viruses that coexist with an estimated 40,000 species of parasitoid wasps [1]. PDVs are divided into two genera, Ichnoviruses (IVs) and Bracoviruses (BVs), on the basis of their association with hymenopteran species in the families *Ichneumonidae* and *Braconidae*, respectively [2]. The biology of PDVs is unique in that PDV genomes persist as proviruses that are stably integrated in the genome of the wasp. Transmission from one wasp generation to the next occurs vertically via inheritance of proviral DNA in eggs and sperm (Figure 1). Viral replication is restricted to the female wasps and occurs in specialized cells that form in a region of the reproductive tract called the calyx. Replication is first detected in the late pupal stage and usually continues after the female emerges as an adult (see [3]). BV virions consist of a single unit membrane enveloping one or more cylindrical nucleocapsids of variable length that are released from calyx cells by cell lysis [4]. IV virions from camplegine ichneumonids consist of two unit membranes that envelop a single fusiform nucleocapsid of uniform size that are released from the calyx cells by budding [5]. Virions from only one banchine ichneumonid have been examined to date. They too consist of two unit membranes but envelop multiple fusiform-shaped nucleocapsids [6]. Following replication and release from calyx cells, virions accumulate to high concentrations in the lumen

of the lateral oviducts to form a suspension of virus called calyx fluid. When a wasp lays an egg into the host, she injects a quantity of calyx fluid into a host, usually a lepidopteran larva. Once inside this host, the virus infects virtually all tissues and begins gene expression. PDV gene products protect the developing parasitoid by suppressing the host immune response. Thus, a true mutualism exists as the virus is dependent on the survival of the parasitoid egg for transmission and the parasitoid depends on viral gene expression for survival inside the host.

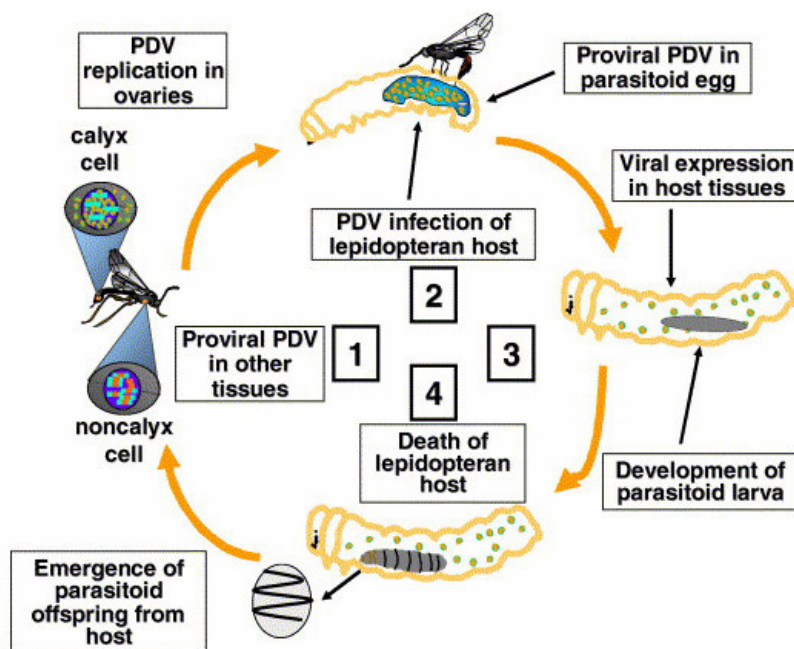


Figure 1.1. Polydnavirus lifecycle (adapted from Webb *et. al.* [7]). (1) PDVs exist as proviruses in all cells of their associated wasp. Virus replicates specifically in calyx cells of the female ovary and encapsidated virus accumulates in the lumen of the lateral oviducts. (2) At oviposition, the wasp injects one or more eggs into the host along with a quantity of virus and secretions from the venom gland. PDV virions infect hemocytes, fat body and other tissues of the parasitized host. The proviral form of the virus is integrated into the DNA of the wasp's egg. (3) PDV genes are expressed in host tissues beginning as early as 1 h post-parasitism and continuing

as the parasitoid egg and larva develops. (4) The parasitoid offspring completes its juvenile development, pupates and emerges as an adult wasp while the host dies as a consequence of PDV infection and feeding by the parasitoid larva.

1.2 General organizational features of PDV genomes

As mentioned above, PDV genomes exist in two states: an episomal form that is packaged into nucleocapsids during replication and a linear proviral form that is integrated into the wasp genome. The episomal form of BV and IV genomes consists of multiple, circular double stranded DNA segments that range in size from 2.0 to over 30 kilobases (kb) [3, 8]. The number of DNA segments varies among PDV isolates from as few as 6 in some BVs to well over 100 in viruses from banchine ichneumonids [6, 9]. Generally, BV genomes consist of fewer but larger DNA segments while IV genomes consist of a larger number of smaller segments. Aggregate genome sizes for PDVs vary from 180 kb to more than 500 kb [6, 7, 10].

Sequence analysis indicates that in the proviral form, the episomal segments of BVs are integrated into the wasp genome as one or more tandem arrays that form macroloci [11, 12]. The proviral segments of IVs on the other hand appear to be dispersed within the genomes of ichneumonoids [13]. Studies with BVs suggest macroloci are amplified before excision of individual segments and packaged into virions [14-16]. Studies with *Chelonus ananitus* bracovirus (CiBV) also suggest the more abundant episomal segments are present in greater copy number in the non-excised proviral form [17]. Webb [18] in contrast suggests that IV replication may occur in a rolling-circle- type mechanism with excision of proviral DNA being followed by amplification of circular episomes.

1.3 PDV gene families

To date, the encapsidated genomes of two BVs from microgastrine braconids (*Cotesia congregata* BV (CcBV) and *Microplitis demolitor* BV (MdBV)), three IVs from campoplegine ichneumonids (*Campoletis sonorensis* IV (CsIV), *Hyposoter fugitives* IV (HfIV), *Tranosema rostrale* IV (TrIV) and one isolate from the banchine ichneumonid *Glypta fumiferanae* (GfIV) have been fully or nearly fully sequenced [6, 7, 10, 19]. Database studies further indicate that several other BVs and IVs have been partially sequenced. These data collectively reveal shared features in addition to the general genomic properties discussed above. These include very low coding densities, strong A + T biases, and the finding that the majority of predicted genes encoded by PDVs form families of related variants. The encapsidated genomes of PDVs also notably lack genes encoding for polymerases or other proteins required for replication which accounts for why PDVs do not replicate in parasitized host insects. PDVs also encode a number of novel, single copy genes or gene families that are currently restricted to single species.

Comparisons within the same or closely related wasp genera reveal that PDVs associated with closely related wasps encode similar gene families, whereas viruses associated with more distantly related wasps exhibit greater differences. PDV gene families appear to have arisen through a combination of gene duplication and inter-genomic recombination events [7, 10, 20]. The size of gene families varies among species. Why this is the case is currently unknown although it potentially reflects differences in host range of the associated parasitoids or the function of a given virus in parasitism. The novel genes and species-specific gene families present in individual species likely also reflect positive selective pressure for functions unique to the particular host species parasitized by a given wasp. It is currently unclear whether the

virulence genes encoded by PDVs have origins from an ancestral virus or have been acquired from their associated wasp or other sources.

That BVs share more similarities with one another than IVs and vice versa is fully consistent with the phylogeny of their associated wasps under conditions of Mendelian inheritance as proviruses. Sequence data combined with differences in morphology also suggest, however, that BVs, IVs from campoplegine ichneumonid, and IVs from banchine ichneumonids may have different origins. If true, similarities in the life cycle and general organization of their genomes reflect convergence driven by the similar roles each of these viral groups play in parasitism.

1.4 Immunological interactions between PDV-carrying parasitoids and Lepidoptera

The most important function of PDVs is to protect the developing parasitoid from the host's immune system. Like other insects, the innate immune system of lepidopteran larvae consists of both humoral and cellular effector responses. Humoral effector responses refer to soluble molecules with defense activities such as antimicrobial peptides (AMPs), complement-like proteins, and products like melanin that are generated by the phenoloxidase (PO) cascade [21-24]. Cellular defenses include phagocytosis, encapsulation, and clotting. These processes directly involve hemocytes. [25, 26]. Hemocytes found in circulation in Lepidoptera consist of four populations called granulocytes (=granular cells), plasmatocytes, spherule cells and oenocytoids ([26-28]. Granulocytes are the most abundant hemocyte type in circulation and function as professional phagocytes. Plasmatocytes are usually larger than granulocytes and are the main capsule-forming hemocytes. Non-adhesive hemocytes include oenocytoids that contain

PO, and spherule cells that are potential sources of cuticular components (see [27]). Progenitor cells called prohemocytes reside in hematopoietic organs as well as at low frequency in circulation [29-32].

1.4.1 Host defense against parasitoid attack

The primary defense against parasitoids is encapsulation that begins when the host recognizes the parasitoid egg or larva as foreign [26]. Recognition of parasitoids and other invaders involves both receptors on the surface of hemocytes as well as humoral pattern recognition molecules that enhance the recognition of foreign targets by binding to their surface (i.e. opsonization). Recognition triggers a small number of hemocytes, usually granulocytes, to bind the surface of the parasitoid and also stimulates proliferation and differentiation of additional hemocytes [33, 34]. Bound hemocytes release cytokines and recruit additional hemocytes, primarily plasmatocytes, that form the bulk of the capsule that envelops the parasitoid. In the last phase of encapsulation, capsules often melanize due to activation of the phenoloxidase (PO) cascade. The parasitoid is then killed by asphyxiation and/or compounds generated as a consequence of producing melanin.

1.4.2 PDV mediated defense against host immune system

Most studies indicate that PDVs prevent their associated parasitoid from being recognized and encapsulated by expressing immunosuppressive gene products in the parasitized host [35-40]. In some parasitoid-host systems, viral infection appears to only suppress

encapsulation of the wasp [41], whereas in others infection results in broader immunosuppressive effects that prevent encapsulation and phagocytosis of any foreign target as well as suppression of humoral responses like melanization, antimicrobial peptide production, and antiviral defenses (summarized by [39, 40]).

1.5 Developmental interactions between PDV-carrying parasitoids and Lepidoptera

The second effect on host physiology that is strongly linked to PDV gene expression is changes in the growth and development of parasitized hosts. All PDV-carrying ichneumonids are solitary (one offspring produced per host), while PDV-carrying braconids are either solitary or gregarious (multiple offspring per host). Chelonine braconids oviposit into the egg stage of Lepidoptera, but almost all other PDV-carrying wasps parasitize larvae during multiple instars. The progeny of PDV-carrying parasitoids either complete their immature development in the host's final instar or develop rapidly and complete development in an earlier instar [42]. Lepidoptera parasitized by solitary species usually exhibit dramatic reductions in weight gain, delays in molting, and are unable to pupate. Hosts parasitized by gregarious species are also inhibited from pupating but usually exhibit less severe alterations in weight gain. The exception to this trend is chelonine braconids that cause the host to initiate precocious metamorphosis one instar earlier than normal but prevent the host from actually pupating [43].

The physiological alterations described above are associated with changes in both endocrine and metabolic physiology [42, 44, 45]. Endocrine alterations include increases in hemolymph juvenile hormone (JH) titers and a failure for ecdysteroid titers to rise to levels that normally occur in non-parasitized hosts during larval-larval or larval-pupal molt. Most studies

indicate that elevated JH titers correlate with reductions in the activity of host metabolic enzymes like JH esterase [46-48] or the secretion of JH from the parasitoid [49]. Only a few studies report decreases in the synthesis and secretion of JH from the host's corpora allata [49, 50]. In contrast, a diversity of alterations have been implicated in suppression of ecdysteroid production including reduced synthesis and release of prothoracothrophic hormone (PTTH) [51, 52], insensitivity of prothoracic glands (PGs) to PTTH stimulation [53], reduced biosynthetic activity in the PGs [52, 54], and premature death of PG cells [55]. Metabolic alterations include changes in the abundance of hemolymph proteins, free amino acids, and carbohydrate levels [45, 56]. For example, triglycerides and glycogen deposits in fat body are greatly reduced in hosts parasitized by *C. sonorensis* while free sugar levels in hemolymph increase. Similar alterations have also been reported in hosts parasitized by braconids (see [42]).

1.6 *Microplitis demolitor* Bracovirus is associated with the microgastrine braconid wasp

Microplitis demolitor

Microplitis demolitor bracovirus (MdBV) is a PDV carried by the microgastrine braconid wasp *Microplitis demolitor*. This wasp parasitizes the larval stage of several moth species including the soybean looper *Pseudoplusia includens* [57]. Development of parasitoid offspring within the host takes 7 days to complete. Viral transcripts are detected by 2 hours post-infection and in *P. includens*, expression continues throughout the 7 day period required for offspring development [58]. MdBV broadly immunosuppresses host insects by inhibiting hemocytes binding to foreign targets, blocking phagocytosis, inducing apoptosis of granulocytes, and

inhibiting humoral defenses [40]. MdBV-infected *P. includens* larvae also exhibit delays in growth and inhibition of pupation [59].

1.7 The MdBV genome encodes multiple gene families

The MdBV genome consists of 15 unique, double stranded, circular DNA segments ranging from 3.1kb (segment A) to 34.3 kb (segment O) [60]. Sequencing of the MdBV genome identified 61 predicted genes encoding 100 amino acids or more. Like other PDV, most of these genes form families of related variants. Transcriptome analysis also indicates most gene family members are expressed in parasitized host insects [7]. Most if not all of these gene products are likely involved in virulence given the absence of replication. Previous studies implicate three MdBV gene families in immunosuppression. The *glc* genes encode cell surface mucins that block encapsulation and phagocytosis by disrupting cell adhesion and the actin cytoskeleton of infected immune cells [61]. A second MdBV gene family encodes ankyrin repeat domain containing genes that are homologs of insect and mammalian inhibitor κ Bs (IkBs). IkBs function as negative regulators of nuclear factor- κ Bs transcription factors (NF- κ Bs). In insects, NF- κ Bs mediate the expression of a diversity of immune factors including antimicrobial peptide genes. Two MdBV IkBs-like family members, IkBs-*H4* and IkBs-*H5*, were shown to bind NF- κ Bs associated with the Toll and Imd signaling pathways and suppress expression of multiple antimicrobial peptide genes [62]. A third MdBV gene family encodes TIL-domain containing genes that act as serine protease inhibitors. These genes, originally named Egf-like genes due to sequence similarity with the gene encoding the human epidermal growth factor, block the phenol oxidase cascade by specifically inhibiting the enzymes that process prophenoloxidase (PPO) to

active PO [63]. Finally, the fourth and largest MdBV gene family encodes thirteen predicted proteins related to protein tyrosine phosphatases (PTPs) [7]. This gene family is the focus of my dissertation.

1.8 PTPs are structurally and functionally diverse

Initially viewed as housekeeping enzymes, the PTP gene family constitutes a growing number of structurally diverse signal transduction enzymes that counteract protein tyrosine kinases (PTKs) in modulating the levels of cellular phosphorylation. Phosphorylation can regulate enzyme function, mediate protein-protein interactions, alter subcellular localization, and control protein stability. Disruption of the balance between PTP and PTK function has been implicated in several human diseases, including cancer, diabetes and chronic inflammation. To better understand what effects the MdBV encoded PTPs could potentially have on the host, I will first review the PTP literature at large.

1.8.1 Structural classification

Members of the PTP family of enzymes are characterized by a unique signature domain (H/V)C(X)₅R(S/T). PTPs are subdivided into classical, dual-specificity and low molecular weight phosphatases. The members of the three groups show no primary sequence conservation beyond the PTP signature domain. Classical PTPs specifically dephosphorylate tyrosine residues in proteins and are subdivided into transmembrane or receptor types and non-receptor or cytosolic PTPs based on the presence or absence of a hydrophobic transmembrane domain.

Unlike cytoplasmic PTPs, which contain only one catalytic domain, receptor type PTPs typically contain two catalytic domains. The membrane distal domain is catalytically inactive but plays a role in modulating activity and stability of the enzyme [64, 65]. Both subtypes play important regulatory roles in fundamental processes such as DNA replication, metabolism, cell growth and differentiation, cell signaling and immune response (reviewed in [66]). The dual specificity PTPs can dephosphorylate both tyrosine and serine/threonine residues. Both classical and dual specificity PTPs play important roles in regulating signaling cascades involved in immune response, cell cycle and metabolism. Low molecular weight phosphatases differ from dual-specificity and classical phosphatases in that they are smaller with a size averaging around 150 amino acids.

1.8.2 Catalytic domain structure, catalysis and substrate specificity

Crystal structure analyses have provided important insight into PTP form and function. The PTPs identified from the MdBV genome share homology with the classical, tyrosine specific subtype. The prototype of this subtype is the human PTP1B. The analysis of more than a dozen crystal structures of PTP1B in the presence and absence of substrate has led to a detailed understanding of catalytic domain architecture, catalysis and substrate specificity.

1.8.3 Catalytic domain structure and catalysis

Classical PTPs are characterized by the presence of a conserved catalytic domain of approximately 240 residues that has a conserved tertiary fold composed of a highly twisted

mixed β -sheet flanked by α -helices on both sides (Figure 2a). The active site is located at the base of a cleft lined by three loops that aid in substrate recognition and binding [67, 68]. In PTP1B, binding of a phosphotyrosine substrate induces a conformational change that brings the surface loop containing the general acid/base (Asp 181) deeper into the catalytic cleft, bringing the general acid in close proximity to the reactive cysteine residue on the base of the catalytic cleft (Figure 2b,c). The side chain of active site Arg 221 positions the substrate phosphor close to the sulphur of the thiolate side chain cysteinyl residue, which then performs a nucleophilic attack on the substrate phosphor [69]. The tyrosyl leaving group becomes protonated by Asp 181 acting as a general acid, formation of a cysteinyl-phosphate intermediate occurs. Gln 262 coordinates a water molecule that forms hydrogen bonds with the amide side chain of Gln266, the amide nitrogen of Phe 182 and the bound phosphate group to stabilize the closed conformation. Subsequent action of Asp 181 as a general base induces hydrolysis of the catalytic intermediate followed by release of the phosphate [67].

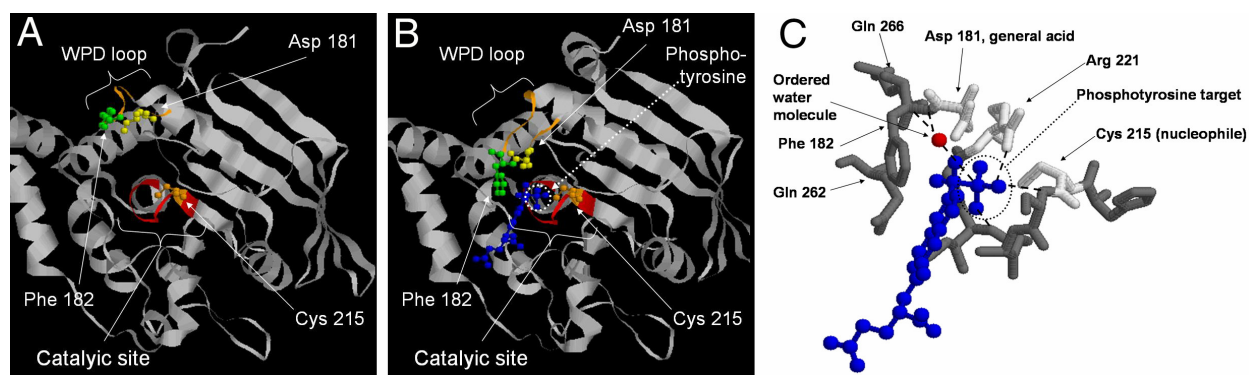


Figure 1.2. Schematic representation of PTP1B catalytic site a) Catalytic site in absence of substrate (modified from PDB file 1BZH) b) catalytic site in presence of phosphorylated tyrosine

substrate (modified from PDB file 1BZC) c) Active site residues that play a role in catalysis reaction in the presence of phosphorylated tyrosine substrate (modified from PDB file 1BZC)

1.8.4 PTP substrate specificity

The depth of the catalytic cleft of the enzyme provides a structural basis for the specific recognition of phosphorylated tyrosine residues. Crystal structure analysis of the first dual specificity phosphatase, human Vaccinia H1 related protein phosphatase (VHR), revealed a shallow active site pocket of at most 6Å compared to a 9Å pocket of the tyrosine-specific, classical PTP1B [70]. The significantly deeper active site pocket in the tyrosine-specific phosphatases is thought to restrict dephosphorylation of tyrosine substrates only [67, 71], while the more shallow active site cleft of dual specificity phosphatases can accommodate phosphorylated tyrosine as well as serine/threonine residues [70]. Besides the depth of the catalytic cleft, PTP substrate specificity is acquired by targeting of the PTPs to a specific subcellular location [72, 73]. *In vitro* substrate coimmunoprecipitation assays using PTP1B illustrate a level of promiscuity that is restricted by the array of the substrates available to the enzyme *in vivo* [74].

1.8.5 Substrate-trapping mutants for identification of PTP substrates

Dephosphorylation reactions performed by catalytically active PTPs are transient, making coimmunoprecipitation of enzyme substrate complexes for the purpose of substrate identification very inefficient. Detailed understanding of PTP catalysis and the key residues involved has

enhanced the generation of catalytically impaired enzymes that bind their substrates but are not able to finish the dephosphorylation reaction and release the substrate. These substrate-trapping mutants include enzymes in which the nucleophilic cysteine is substituted for a serine or alanine [67], enzymes in which the general acid/base aspartic acid is substituted for an alanine [74], and double mutants in which both the aspartic acid and one of the water molecule coordinating glutamates are substituted for an alanine [75]. The substrate trapping efficiency of these mutants depends on the subject PTP. Together, these substrate trapping mutants have played an important role in the identification of PTP substrates [76-78] .

1.8.6 Most PTP gene families contain pseudophosphatases

The human genome encodes 38 PTPs, and an estimated 38 and 36 PTPs are present in the *Drosophila* and honeybee genomes, respectively [79, 80]. Interestingly, most PTP families contain pseudophosphatases: PTPs that share core features with PTPs but lack essential residues required for catalysis [81-86]. Pseudophosphatases could theoretically stabilize or increase the basal phosphorylation level of their target substrates and promote ligand-independent signaling. Alternatively, if the site of tyrosine phosphorylation is critical for protein-protein interaction required for signaling, or if the substrate is an enzyme and the site of phosphorylation is located close to the active site, binding of a catalytically inactive phosphatase may cause an effect that is functionally similar to protein dephosphorylation [74]. Pseudophosphatases are most prevalent in the myotubularin subfamily of vertebrate dual-specificity phosphatases (MTMs). It has recently been demonstrated that inactive MTMs form complexes with active MTMs and that these interactions regulate both enzymatic activity and subcellular localization [87-89].

1.9 Role of phosphorylation in immune signaling and other physiological processes

The reversible phosphorylation of tyrosine residues is a key component in both vertebrate and insect immune signaling, as well as a variety of other physiological processes. The PTPs encoded by MdBV could thus potentially interfere with any of these processes in the infected host.

1.9.1 Role of tyrosine phosphorylation in immune signaling

The cellular immune response is composed of a series of cell signaling events that are regulated by the reversible phosphorylation of tyrosine residues in proteins in immune cells. The phagocytosis response is initiated by recognition of a conserved pathogen-associated molecular pattern (PAMP) molecules present on the surface of microorganisms by pattern recognition receptors (PRRs) on the surface of phagocytes. Two bacteria specific macrophage transmembrane PRRs have been identified in insects, the family of scavenger receptors (SRs) and the family of peptidoglycan recognition proteins (PGRPs). *Drosophila* SR-C1 (dSR-C1) [90, 91] is involved in phagocytosis of gram-negative bacteria, whereas the PGRP-SA recognizes gram-positive bacteria [92] and PGRP-LC recognizes gram negative bacteria [93]. Binding of the particle to its receptor on the phagocyte elicits a signaling cascade that activates downstream proteins through a series of tyrosine phosphorylation events, including proteins of the FAK/Src signaling complex and regulators of the antimicrobial pathways. Tyrosine phosphorylation of focal adhesion proteins results in local actin-polymerization at the cytoplasmic side of the plasmamembrane, followed by ingestion of the particle and formation of a phagosome containing the particle [94]. The phagosome then matures and fuses with a lysosome to form the

phagolysosome. In vertebrates, the lysosome contains reactive oxygen intermediates (ROI) and reactive nitrogen intermediates (RNI) that are toxic to many microorganisms [95, 96]. Intruders that are too large to be phagocytized, such as eggs of parasitic wasps, become encapsulated by plasmatocytes [27]. Plasmatocytes form a capsule by attaching to the target and forming multiple layers. When isolation is complete, the hemocytes adjacent to the egg kill the eggs by secretion of nitric oxide produced through the phenol oxidase cascade [37]. Encapsulation is also thought to involve phosphorylation dependent signaling pathways similar to the ones activated during phagocytosis. The JAK-STAT and JNK pathway are other important in insect and mammalian immune responses that are regulated by tyrosine phosphorylation. JAK-STAT signaling generally results in delayed, transient induction following immune challenge, whereas JNK was indicated to regulate the rapid upregulation of cytoskeletal genes in response to infection [97].

Another level of defense against microbial infection in insects is the humoral response. Two distinct pathways are activated upon infection with bacteria, Toll and IMD, and both signaling pathways depend heavily on tyrosine phosphorylation events. Binding of a ligand to the Toll pathway receptor dSR-C1 or to IMD pathway receptor PGRP-LC initiates a cytoplasmic signaling cascade that depends in part on the reversible phosphorylation of tyrosine residues. One key step in this pathway is the tyrosine phosphorylation and subsequent proteolytic degradation of I κ B-like proteins. Tyrosine phosphorylation induces the release of the I κ B-like proteins from the NF κ B-like proteins and permits the NF κ B-like proteins to translocate to the nucleus, where they act as transcription factors to activate antimicrobial peptide genes [98]. Antimicrobial peptides are produced in the fat body and secreted in the blood where they work

by disrupting bacterial membranes. Mutants that are impaired in IMD and Toll signaling pathways are severely immunosuppressed [99].

1.9.2 Role of tyrosine phosphorylation in growth and development

PTPs have also been implicated in a number of signaling pathways that regulate growth and development. Two phosphorylation dependent signal transduction pathways that are important for the growth and development of immature insects are the insulin signaling pathway and the PTTH-dependent ecdysteroid biosynthesis pathway.

1.9.2.1 Role of tyrosine phosphorylation in insulin signaling

The conserved insulin pathway plays an important role in growth and metabolism. Experimental evidence from vertebrate systems supports a role for the receptor-type PTP LAR and the non-receptor types TC-PTP and PTP1B in the negative regulation of insulin signaling by dephosphorylating the insulin receptor (IR) and post-receptor substrates in the insulin signaling pathway (reviewed in [100, 101]). Like in vertebrates, activation of a *Drosophila* IR results in the activation of a downstream signaling cascade that depends heavily on the tyrosine phosphorylation of various homologues in the signaling pathway (reviewed in [102]). In both vertebrates and insects, IR activation results in tyrosine phosphorylation of its β -subunit, which then stimulates interaction of the receptor with insulin receptor substrates [103]. These substrates become tyrosine phosphorylated by the kinase domain of the receptor, and can then bind and activate growth factor receptor-bound protein (GRB2) and phosphatidylinositol-3-

kinase (PI3K). In vertebrates, GRB2 activates the mitogen-activated protein kinase (MAPK) pathway. There is however no strong evidence for MAPK activation through IR signaling in insects. The role of PI3K in insect insulin signaling, on the other hand, is more evident [104]. PI3K consists of two subunits: the catalytic p110 and the non-catalytic p85 subunit, which stabilizes and inactivates p110. The inhibitory effect of p85 is released upon activation of the IR by phosphorylation of a tyrosine by a Src-kinase. Activated PI3K then mediates the phosphorylation of phosphatidylinositol-4,5-bisphosphate (PIP2) to phosphatidylinositol-3,4,5-trisphosphate (PIP3), a process that can be reversed by endogenous lipid phosphatase PTEN [105]. The resulting messenger activates a series of phosphorylation events that activate downstream effectors such as phosphorylation of S6 kinase and the ribosomal protein S6 [106]. Activation of the insulin signaling pathway ultimately leads to protein and lipid synthesis and the expression of insulin-responsive genes.

1.9.2.2 Role of tyrosine phosphorylation in ecdysteroid biosynthesis

Molting and metamorphosis are key developmental processes in holometabolous insects that are driven by the production of the molting hormone ecdysone by the prothoracic glands (PGs). The sequence of events leading up to the production of ecdysteroids has been well studied in *Manduca sexta*, *Bombyx mori* and *Drosophila melanogaster*. At the end of each instar, juvenile hormone levels in the hemolymph drop and prothoracicotrophic hormone (PTTH) is secreted by the brain. PTTH activates ecdysteroid production by the PGs through a cAMP and protein kinase A dependent signaling cascade, eventually leading to the activation of S6 kinase and the synthesis of proteins required for ecdysteroid biosynthesis (reviewed by [107]). Studies

with *M. sexta* PGs indicate that the PTTH induced signaling cascade depends on multiple tyrosine phosphorylation events [108]. In lepidopteran species, PG production can be activated by the application of dbcAMP and inhibited by blocking the calcium influx, indicating that an increase in intracellular cAMP levels is both sufficient and necessary for ecdysteroid production [109]. In contrast, production of ecdysteroids by *Drosophila* PGs is a cAMP independent process [110].

1.9.3 Relationship between insulin signaling and ecdysteroid production by the PGs

Recent work with *Drosophila* suggests that the PG, a component of the ring gland in larvae, functions as the size assessing tissue that determines when the critical weight has been obtained [111]. In this model, ecdysone release depends on both promotion of PG cell growth by PI3K and a Raf-dependent effect that may promote transcription of genes involved in ecdysteroid biosynthesis [112]. Using the GAL4/UAS system to modulate PG signaling pathway, Caldwell *et. al.* [112] report that PG specific expression of activated Ras, PI3 kinase (PI3K) but not Raf reduces adult body size, whereas expression of double-negative Ras, Raf and PI3K increases adult body size. Down regulation of the insulin signaling pathway also prolonged the larval instar. Taken together, these data suggest that in *Drosophila*, a delay in maturation of the PGs leads to a delay in the onset of metamorphosis.

1.10 PTPs as virulence factors

Considering the highly regulated level of tyrosine phosphorylation in the cell and the importance of this mechanism in controlling a large variety of cellular processes, PTPs qualify as potentially powerful virulence factors. The following paragraphs summarize what is currently known about how PTPs are applied in virulence by vertebrate and invertebrate pathogens.

1.10.1 PTPs involved in virulence of non-viral pathogens

A well known example of a PTP used to promote pathogenesis is encoded by the human plague bacterium *Yersinia pestis*. *Y. pestis* induces pathogenesis by binding to cell surface receptors of macrophages and T-lymphocytes followed by translocation of a set of effector molecules known as Yops into the cell via a type III secretion system. YopH is a highly active classical, non-receptor type PTP [113] that induces inhibition of phagocytosis [114], suppression of the oxidative burst [115], disruption of stress fibers and focal adhesions [116, 117], and reduced calcium signaling [118]. The inhibition of phagocytosis is induced by the dephosphorylation of several focal complex proteins including focal adhesion kinase and Crk-associated substrate (Cas) [119]. Additional substrates found in macrophages are Fyn-binding/SLP-76-associated protein and SKAP-HOM [120]. The related bacterial pathogen *Salmonella typhimurium* uses the same type of secretion system to translocate SptP into human macrophages. SptP modulates a number of cellular responses induced by *Salmonella* infection including recovery of the actin cytoskeletal changes induced by the bacterium in epithelial cells and the infection-stimulated activation of ERK in the MAPK pathway [121, 122]. The SptP

induced pathogenesis is largely due to both its tyrosine phosphatase and GTPase activity dependent inhibition of Raf-1 activation [123].

1.10.2 PTPs involved in viral pathogenesis

The Interpro database predicts more than 200 PTPs are encoded by various dsDNA viruses in the family *Poxviridae*, *Iridoviridae*, arthropod-specific viruses in the families *Baculoviridae*, *Polydnviridae*, an amoeba virus, an algae virus, and a bacteriophage. The best studied viral PTP is the Vaccinia H1 dual specificity phosphatase (VH-1). Although required for infectivity of the virus [124], VH-1 does not strictly function as virulence factor. Instead, VH-1 is essential for early gene expression and targeted repression of VH1 expression caused strongly reduced viral infectivity [125].

1.10.2.1 PTPs in insect virus genomes

As previously discussed, PTPs can be subdivided into classical PTPs, dual specificity PTPs, and low molecular weight PTPs [126]. Interestingly, the type of PTP encoded in viral genomes differs between insect virus families. Classical tyrosine specific PTPs are restricted to polydnviruses, whereas baculoviruses and iridoviruses encode exclusively dual specificity phosphatases. Although dual specificity PTPs and classical PTPs belong to the same superfamily of enzymes, overall sequence similarity is limited to the conserved signature motif in the catalytic site. Insect viruses are thus likely to have acquired PTPs independently during evolution.

1.10.2.1.1 PTPs in PDV genomes

Protein tyrosine phosphatase homologues to date have been found in one ichnovirus and five bracoviruses. The GfIV genome is the first genome characterized from an IV associated with wasps of the subfamily Banchinae. Twenty three PTP genes have been identified from the genome of the banchine PDV *Glypta fumiferanae* Ichnovirus [127]. The other available ichnovirus genomes found in wasps associated with the Ichneumonid subfamily *Campopleginae* do not contain PTP gene families. Current data suggest all BVs encode PTPs. For example, 27 PTP-like genes are encoded by *Cotesia congregata* BV (CcBV)[128], 14 by *Cotesia plutellae* (CpBV) [129], 13 by *Toxoneuron nigriceps* (TnBV)[128], and 9 by *Glyptapanteles indiensis* BV (GiBV)[130]. All PDV-encoded PTPs belong to the classical, tyrosine specific subtype. To date, no functional studies on PDV PTPs have been published besides the work described in this document.

1.10.2.1.2 PTPs in baculovirus genomes

While PDV genomes contain only genes involved in virulence, baculoviruses and iridovirus replicate in the infected host and their genomes contain all the necessary tools for replication. The dual specificity phosphatases encoded by these viruses could thus potentially play a role in either replication or virulence, or both. The family *Iridoviridae* is composed of genera that contain species that infect insects and a few invertebrates (Iridoviruses, Chloriridoviruses), but also genera that infect vertebrates. PTP genes are found in Iridoviruses with both invertebrate and vertebrate hosts but no function has been identified. The literature provides two examples of baculovirus PTPs involved in virulence. The first example is BVP, a

dual-specificity PTP encoded by the *Autographa californica* nuclear polyhedrosis virus (AcMNPV). BVP mutants typically form viral occlusion bodies less efficiently and generate reduced virus titers in Sf-21 cells [131, 132]. Although BVP was initially shown to be capable of dephosphorylating tyrosine, serine and threonine residues from proteins, the enzyme was later found to be much more potent as an RNA 5'-tri- and diphosphatase [133-136]. Another example of a baculovirus dual-specificity phosphatase involved in virulence is BmNPV *ptp* from *Bombyx mori* nucleopolyhedrovirus (BmNPV). Wild-type BmNPV infection induces enhanced locomotory activity (ELA) in silkworms [137], a behavior that is believed to enhance virus transmission and spread. BmNPV *ptp* plays an important role in ELA, as BmNPV *ptp* knockout mutants do not induce light induced ELA. Interestingly, the deduced amino acid sequence of BmNPV *ptp* indicates an 80.7% similarity with a *B. mori* derived PTP (Bmptp-h). The observation that replacement of the baculovirus *ptp* by Bmptp-h partially recovered ELA led the authors to suggest that the baculovirus may have acquired this *ptp* gene from an ancestral host and selectively maintained because of its role in virus transmission [137].

1.11 Chapter contents

The working hypothesis for my dissertation research is that one or more members of the MdBV PTP family play an important role in parasitism. The preceding literature review shows that PTPs are essential signaling molecules that have been co-opted by selected pathogens and function as virulence factors. The following chapters describe the results of my studies. Chapter 2 describes the characterization of PTP family structure and an analysis of the expression of individual PTP family members in different tissues of the infected host, the characterization of

catalytic activity and the effect on phagocytosis of selected PTPs. Chapter 3 reports the results of a screen to determine the effect of various MdBV genes on apoptosis, and Chapter 4 describes the effect of viral infection on host endocrine and metabolic processes.

CHAPTER 2

CHARACTERIZATION OF PTP SEQUENCE, EXPRESSION, CATALYSIS AND ROLE IN MDBV INDUCED INHIBITION OF PHAGOCYTOSIS

2.1 Introduction

As described in Chapter 1, the most important role of MdBV infection in parasitism is the protection of the parasitoid offspring against the host immune system. The hallmarks of inhibition of the cellular immune response are the loss of hemocytes adherence, the inability of hemocytes to phagocytize or encapsulate foreign targets, and the apoptosis of granular cells. Although we have made progress in understanding how MdBV causes these effects and what virulence factors are involved, we do not fully understand how MdBV immunosuppresses the host.

The largest MdBV gene family encodes predicted proteins related to protein tyrosine phosphatases (PTPs) [7, 39]. Notably, several other BVs also encode multiple predicted PTPs, suggesting that this gene family is important in parasitism [128, 138]. Given the importance of PTPs in various signaling pathways including those controlling immune responses, one could picture a role for the virulence factors in immunosuppression. In this chapter, I report that most members of the MdBV PTP gene family are expressed in virus-infected hosts. I also present evidence that two family members are active tyrosine phosphatases that inhibit phagocytosis and localize to the focal adhesions in insect immune cells.

2.2 Materials and methods

2.2.1 Insects and cell cultures

M. demolitor was reared by parasitizing third instar *Pseudoplusia includens* at $27 \pm 1^\circ\text{C}$ with a 16 h light (L): 8 h dark (D) photoperiod as previously described [139]. *Drosophila* S2 cells (American Type Culture Collection) were maintained in HyQ medium (Hyclone) and passaged as adherent cells in Corning 75 cm² tissue-culture flasks. Most experiments were conducted in 12-well culture plates (Corning). Cells were seeded into wells at specific densities, cultured for 18-24 h, and then used in bioassays.

2.2.2 Sequence analysis

PTP-related gene family members were aligned with selected insect and mammalian PTPs using Lasergene software (DNASTAR, Inc.) and the CLUSTAL W method with gap creation penalties of 10.00 and gap extension penalties of 0.20. Motifs and other structural features were identified using the PFAM (<http://www.sanger.ac.uk/Software/Pfam/>) or NCBI conserved domain (<http://www.ncbi.nlm.nih.gov/Structure/cdd/wrpsb.cgi>) databases.

Transmembrane domains were identified using the “DAS” transmembrane prediction server (<http://mendel.imp.univie.ac.at/sat/DAS/DAS.html>). The sequence of selected MdBV-PTP genes was reconfirmed by partial or full sequencing of genomic and/or cDNA clones using the chain termination method and ABI Prism BigDye Termination Cycle kit (Applied Biosystems). Sequence reactions were run at the University of Wisconsin-Madison sequencing facility.

2.2.3 Calyx fluid collection and host infection.

M. demolitor calyx fluid consists almost entirely of MdBV which is the only factor in calyx fluid that is infectious and immunosuppressive [57, 139]. During the current study, calyx fluid was collected from wasps and used to infect host cells as previously described [61, 140]. Following convention in the PDV literature, the amount of calyx fluid (=MdBV) from a single wasp is defined as one wasp equivalent with *M. demolitor* normally injecting 0.1-0.02 wasp equivalents of MdBV per host [58, 141, 142]. For infection of cells, MdBV isolated from wasps was diluted in TC-100 medium (Sigma), sterilized using a 0.2 µm syringe Acrodisc filter (Pall), and 0.05 wasp equivalents was injected into fifth instar *P. includens*. Injection of this amount of virus results in infection levels of hemocytes in vivo or cultured cells in vitro of greater than >95% [139]. Mock infected hosts were injected with TC-100 medium only. Hemocytes were subsequently collected for use in PTP activity assays. For real time PCR studies, third instar *P. includens* or *T. ni* larvae (6-12 h post-ecdysis) were singly parasitized by *M. demolitor*.

2.2.4 Total RNA isolation and real time PCR.

For real-time PCR studies, third instar *P. includens* larvae (6 to 12 h postecdysis) were singly parasitized by *M. demolitor*. Parasitized and nonparasitized larvae were then CO₂ anesthetized and processed at 18 h postparasitism. For tissue samples, host larvae were dissected in physiological saline to collect the fat body, gut (digestive tract plus Malpighian tubules), salivary glands, nervous system (brain plus ventral nerve cord) removed [143]. Hemocytes were collected by bleeding larvae from a cut proleg and pelleting the cells by centrifugation as described above. Total RNA was extracted from each tissue sample using TRIzol Reagent

(Invitrogen) according to the manufacturer's instructions with slight modifications. To remove contaminating genomic DNA, the isolated RNA was treated with DNase I (Ambion), extracted with phenol/ chloroform, isopropanol precipitated, and resuspended in RNase-free water. RiboGreen RNA (Molecular Probes), in combination with a fluorescence microplate reader (FLUOstar Galaxy; BMG), were used to quantitate RNA amounts [144, 145].

For first-strand cDNA synthesis, 500 ng of total RNA per samples was reverse transcribed Superscript II (Invitrogen) and random hexamer in 20 μ l reactions according to the manufacturer's recommendations. Relative quantitative real time PCR (rqRT-PCR) reactions were run on a Rotor-Gene 3000 Real-Time PCR Thermal Cycler (Corbett Research) in 10 μ l reactions as described previously [142]. Briefly, each 10 μ l reaction contained 4 μ l cDNA template, 5 μ l iQ SYBR Green Supermix (BioRad), and each of the corresponding gene specific forward and reverse primers (Table 2.1). To normalize differences in total RNA amounts that were reverse transcribed and added to each reaction, an 18 S ribosomal gene from *P. includens* (GenBank Accession No. AY298945) was used as an active endogenous control [145]. Cycling conditions were the same for all primer combinations: 3 min initial denaturation at 95 °C, followed by 40 cycles of 20 sec denaturation at 95 °C, 20 sec annealing at 50 °C, and 20 sec extension at 72 °C except for PTP-J2 the annealing temperature was 52 °C. Data were acquired during the extension step, and analyzed with the Rotor-Gene application software (Version 6.0.27). For every amplicon, reactions were carried out in quadruplicate, from which the mean threshold cycle (CT) values plus standard deviations were calculated. Relative transcript amounts were calculated applying the comparative CT or $2^{-\delta\delta CT}$ -method as previously described [143]. For the visualization of PCR products on agarose gels, conditions were identical as above

but reactions were stopped at 25 cycles for each PTP and at 15 cycles for the 18S ribosomal control.

Table 2.1 Gene specific primers used for real time PCR reactions

Family member	Forward (F) and reverse (R) primer sequences (5'-3')	Expected product size (bp)	Primer efficiency
ptp-H1	(F) TATATAATGCGTTATCACAAGTGCG (R) ACCTTGTCTTGGAATGCAGAGAAT	201	92%
ptp-H2	(F) CGTTGCAGCAGACAGCCTAC (R) CTTAAGTGAGTTTCTATTTGGGTGGT	187	104%
ptp-H3	(F) CAGGCTATTGTTTCGAAATCTTTAAC (R) GGAGTTATCCCAACACGTTACATCA	194	102%
ptp-H5	(F) GATCCATCACATATAACCCTAACACC (R) TCTTCCAAATATCTCCATACCTTCC	258	95%
ptp-J1	(F) CCAATTCGGAAGGGTCTCG (R) GGGGTAGCACTTTTGTTTGTATCT	198	96%
ptp-J2	(F) TATACGCTGATTTAAGAAAGCATAAGAC (R) GACATAATCATTTAATCGGTTACATACAA	212	87%
ptp-J3	(F) TGGAACATCCGGTGTTCATTATC (R) TTTGGTGTAATGTACTTCCGCTT	236	96%
ptp-J4	(F) ATAAGCTATCTGCACGAAACTCCC (R) CATAATTCTCCGGCTGACTAATGG	201	93%
ptp-N1	(F) TGTGGTACATTGCAGTGACGG (R) GTTGTAATATTAAGTAATCATCTGGCG	174	98%
ptp-N2	(F) AGAAGAGTTTCATTATATCGTGCTCC (R) CGCCGTTTTTCGACTCTATCA	143	95%
ptp-N3	(F) CTACAACATATCTGCATCATCATCAA (R) CCTCAAAGCTAAAGAAATCTAATTGC	203	93%

2.2.5 Plasmids and expression

The coding sequences for *ptp-H1*, *-H2*, *-H3*, and *-J1* were cloned into the expression vector pIZT/V5-His (Invitrogen) which uses the OpIE2 promoter from the *Orgyia pseudotsugata* baculovirus for constitutive expression of the gene of interest and the OpIE1 promoter to express a Zeocin-green

fluorescent (GFP) gene fusion which can be used for selection and as a marker. This vector also produces recombinant proteins with a V-5 epitope tag. Each PTP family member was PCR amplified using MdBV genomic DNA as template and the following primers: *ptp-H1* 5'-
ATTCTAGAATGGGGCGTCATAGTTTC-3' (forward), *ptp-H1* 5'-
ATCCGCGGATACTTATTATTAAATGAATG-3' (reverse); *ptp-H2* 5'-
AGAATTCATAAAAATGGGTCGATGCAAATT-3' (forward); *ptp-H2* 5'-
TATCCGCGGATAGTTATCTTTTAGATGAAG-3' (reverse); *ptp-H3* 5'-
CTAGTGT**TTTCTAGA**ATGGCAGGCTATTGTTTCG-3' (forward), *ptp-H3* 5'-
GCCGCGGAAGCTGTGAAACCAGATAATAA-3' (reverse), *ptp-J1* 5'-
GCTCTAGAATGGGTTACATTGTTCTAAAAAC-3' (forward), *ptp-J1* 5'-
TCCCGCGGATAACAAGGCGTTGAC-3' (reverse). *Xba*I or *Eco*RI (forward) and *Sac*II site (reverse) were incorporated into the primers (underlined) for directional cloning of each gene. As recommended by the manufacturer, we also modified the sequence around the start codon in some of the forward primers (bold) to create Kozak sequences for proper initiation of translation, and mutated the stop codons in the reverse primers (bold) to express the protein product in frame with the vector-encoded V5 epitope and 6xHis tag. Standard 50 µl reactions contained 2 µl Elongase Enzyme Mix (Invitrogen), 1.5 mM MgCl₂, 250 µM dNTP mix, 200 nM of each primer, and 100 ng of genomic MdBV DNA. After a 3 min initial denaturation at 94°C, the target sequence was amplified by 30 cycles of 30 sec denaturation at 94°C, 30 sec annealing at 50°C, and a 4 min extension step at 68°C. PCR products were first cloned into pCRdual-TOPO (Invitrogen) and then cloned into pIZT/V5-His as previously described [61] to yield the expression constructs pIZT/PTP-H1, pIZT/PTP-H2, pIZT/PTP-H3, and pIZT/PTP-J1. In addition, *ptp-H2* was also cloned into pHSP70polyA [146] under control of the *Drosophila* hsp70 promoter. Briefly, *ptp-H2* plus V5 epitope and 6xHis tag was PCR amplified from pIZT/H2 using the

primers 5' AGATCTATGGGTCGATGCAAATTCAGG-3' (forward) and 5' AGATCTTCAATGGTGATGGTGATGATG-3' (reverse) that each contained *Bg*III restriction sites (incorporated). The *ptp-H2* stop codon was also reintroduced into the reverse primer so as not to express GFP. PCR products were again initially cloned into pCRdual-TOPO followed by cloning into pHSP70polyA to produce pHSP70/PTP-H2. The structure and orientation of all constructs was confirmed by sequencing as described above. A previously made Glc1.8 expression construct (pIZT/Glc1.8) was also used in functional assays [61]. All constructs were transiently expressed in S2 cells by cationic lipid-mediated transfection using a 1 µg of plasmid per ml of medium [61, 147]. Transfection efficiencies averaged 75-80% as measured by GFP expression.

2.2.6 Protein tyrosine phosphatase activity assays

For each replicate, hemocytes from MdBV or mock-infected hosts, and transfected *Drosophila* S2 cells were counted using a hemocytometer. Five x 10⁵ hemocytes and 1 x 10⁶ S2 cells per replicate were then lysed on ice in 250 µl of lysis buffer (50 mM Tris, pH 7.5, 150 mM NaCl, 1% Nonidet P-40 vol/vol (Pierce), plus protease inhibitor cocktail (Roche)). PTP activity in lysates was then measured in 96-well plates (Corning) using the tyrosine phosphatase assay system (Promega) according to the manufacturer's instructions. Briefly, lysates for each replicate were first precleared of free phosphate. Twenty µl of the cleared lysate was then incubated with the tyrosine-containing phosphopeptide END(pY)INASL (0.13 mM) in the presence or absence of 1 mM sodium orthovanadate. The reaction buffer used was Tris-buffered saline containing 1 mM dithiothreitol and 1 mM phenylmethanesulfonyl fluoride (pH 5.5). After 30 min at 30° C, the reaction was terminated by the addition of stop buffer containing a molybdate

dye for visualization of liberated phosphate at 600 nm using a plate reader (BMG). Picograms of phosphate released was then determined by comparison to a standard curve. Each treatment was replicated a minimum of four times using independently prepared and collected samples. The data were then analyzed by one way analysis of variance (ANOVA) and the Tukey Kramer multiple-comparison procedure ($\alpha \leq 0.05$) using JMP 3.0 software (SAS Institute, Gary, NC) [148].

2.2.7 Western blotting

Lysates prepared for PTP activity assays were also used in Western blotting experiments. Protein concentrations in lysates were determined by Bradford assay (Biorad). Forty μg of protein per sample was then added to SDS/PAGE buffer, boiled and separated by SDS-PAGE. After transfer to nitrocellulose, membranes were probed with a mouse anti-V5 antibody (Invitrogen) (1: 10,000) that recognizes the V5 epitope on each recombinant protein. A goat anti-mouse horseradish peroxidase-conjugated secondary antibody (Jackson Labs) (1: 20,000) was then used followed by visualization of bands by HRP-enhanced chemiluminescence (ECL; Amersham Biosciences).

2.2.8 Phagocytosis assays.

We assessed the ability of S2 and Sf-21 cells to phagocytose rhodamine-labeled *Escherichia coli* [61] or inert polystyrene beads (0.5 μm) (Polysciences). S2 cells were first transfected with different pIZT/PTP and/or Glc1.8 expression constructs with empty pIZT vector serving as a negative control. Sf-21 cells were first transfected with pIZT/PTP-H2 or the pIZT empty vector and then maintained for 20 h

in the presence of Z-VAD-FMK. Sf-21 cells were then transferred to new 12-well culture plates in serum free medium plus Z-VAD-FMK at a density of 1×10^5 cells per well. Forty eight h later, S2 or Sf-21 cells were collected and added to new 12-well culture plates in medium without serum at a density of 1×10^5 cells per well. After a 1 h preincubation period, bacteria or microspheres were added to each culture well at a ratio of 15: 1. Cells were allowed to phagocytose for 45 minutes (S2 cells) or 90 minutes (Sf-21 cells) at 27° C followed by transfer of the culture plate to ice. We then scored the percentage of cells with one or more ingested particles [149] by counting 200 cells per well from 4 randomly selected fields of view using a Leica TCS inverted epifluorescent microscope. Particles were red while cells expressing a gene of interest were green. Each treatment was replicated a minimum of five times using independently prepared samples. The proportional data were then arcsin transformed, analyzed by one way ANOVA, and the Tukey Kramer multiple comparison procedure.

2.2.9 Immunofluorescence staining

S2 cells transfected with pHSP70/PTP-H2 and SF21 cells transfected with pIZT/PTP-H2 were processed for immunofluorescence microscopy as previously described [61]. Briefly, 48 h post-transfection (non-heat shocked) S2 cells were washed in PBS and then fixed for 20 min in 4% paraformaldehyde in PBS. Fixed cells were permeabilized with PBS-0.1% Triton X-100 (PBT), blocked in 5% dry milk in PBS. S2 cells were then incubated overnight at 4° C with mouse anti-V5 antiserum (1: 1000) that recognized recombinant PTP-H2 and a rabbit anti-Fak^{Y397} (Biosource) (1: 100) that recognizes Drosophila focal adhesion kinases (Fak56) [150]. After washing in PBT, cells were incubated with Texas-Red-conjugated goat anti-rabbit (1: 2000) and fluorescein isothiocyanate (FITC)-conjugated goat anti-mouse secondary antibody (1:

2000) (Jackson Labs). Incubation of cells in secondary antibodies alone served as the negative control. Samples were examined on a Leica-TCS scanning confocal microscope with images processed using Leica and Adobe Photoshop software.

2.3 Results

2.3.1 MdBV encodes multiple PTP-related genes

Sequencing of the MdBV genome and BlastX analysis (www.ncbi.nlm.nih.gov) previously identified 13 ORFs with significant homology to known PTPs [7]. Each MdBV PTP family member was named by its location in the MdBV genome with one ORF located on genomic segment D (ptp-D1), five on segment H (ptp-H1, 2, 3, 4, 5), four on segment J (ptp-J1, 2, 3, 4), and three on segment N (ptp-N1, 2, 3) (Table 2.2). Further analysis during the current study indicated that all family members except ptp-D1 and ptp-N1 possessed 5' TATA boxes that were located 7-192 bp upstream of the initiation methionine (Table 2.1). Each family member except ptp-D1 also possessed 3' polyadenylation signal sequences (AATAA) that were 4-145 bp downstream of the stop codon. Although several MdBV genes are spliced, none of the PTP-related ORFs contained introns [151]. Predicted proteins encoded by each family member ranged from 183 (ptp-H4) to 337 (ptp-H1) amino acids and had molecular masses of 21.1 to 39.5 kDa (Table 2.2)..

Table 2.2. Predicted properties of *M. demolitor* PTP family members

Family member	Genomic location (segment, position)*	TATA from initiation codon	AATAAA from stop codon	Predicted protein length (amino acids)	Predicted protein size (kilodaltons)
<i>ptp-D1</i>	D, 7778-7823, 1-377	None	None	141	16.9
<i>ptp-H1</i>	H, 1250-2260	-18	10	337	39.5
<i>ptp-H2</i>	H, 2846-3823	-126	29	326	37.9
<i>ptp-H3</i>	H, 4941-5903	-104	24	321	37.2
<i>ptp-H4</i>	H, 9043-9591	-73	88	183	21.1
<i>ptp-H5</i>	H, 10409-11238 1-129	-70	63	319	36.9
<i>ptp-J1</i>	J, 1931-2833	-82	126	301	34.7
<i>ptp-J2</i>	J, 6126-7019	-7	78	298	34.5
<i>ptp-J3</i>	J, 10999-11754	-13	20	251	29.7
<i>ptp-J4</i>	J, 12570-13469	-60	4	299	35.0
<i>ptp-N1</i>	N, 4114-5070	None	46	319	37.1
<i>ptp-N2</i>	N, 5743-6512	-78	136	256	30.3
<i>ptp-N3</i>	N, 14837-15796	-29	37	320	38.0

*GenBank accession numbers for MdBV genomic segments: D (AY875683), H (AY875685), J(AY875686), and N (AY875689)

PTPs form a large superfamily whose members are recognized by the presence of one or two centrally located catalytic domains [66, 126]. Each catalytic domain contains a signature motif (catalytic site) (H/V)C(X)₅R(S/T) that includes an essential cysteine required for protein tyrosine phosphatase activity. The PTP superfamily can be divided into three families: classical PTPs, dual specificity phosphatases, and low molecular weight phosphatases [126]. BlastX results indicated that all of the MdBV PTP family members encode predicted proteins in the classical family. Classical PTPs are further subdivided into 17 subtypes on the basis of sequence similarity of the catalytic domain(s) and other motifs with regulatory or targeting functions. These subtypes also divide themselves into non-transmembrane (NT) (i.e. cytosolic) and transmembrane (T) forms. All predicted MdBV PTPs were of the NT form with the highest

similarity matches ($1 e^{-81}$) being to PTPs encoded by BVs from the wasps *Cotesia congregata* (CcBV) and *Cotesia plutellae* (CpBV) [128, 152]. Conserved domain searches also identified high similarity matches to PTPs encoded by other organisms. For example, the catalytic domain of MdBV PTP-H2 had similarity matches of e^{-65} and e^{-56} to the catalytic domains of human PTP1b and Yop51 from the bacterium *Yersinia pasteurilla* respectively which are both classical NT1 subtype members [126]. Other MdBV PTPs were also most similar to the classical NT1 subtype.

The catalytic domains of classical PTPs contain 10 conserved motifs which include the previously mentioned signature motif (catalytic site, motif 9) plus nine other motifs with proposed roles in substrate recognition, secondary structure, or catalysis [126]. Alignments with a predicted PTP from CcBV (designated PTPR) and with PTP1b indicated that seven MdBV PTP family members possess all 10 motifs: PTP-H1, -H2, -H3, -H5, -J1, -N1, and -N2 (Figure 2.1). However, the aspartic acid in the WPD loop (motif 8) of PTP-H1 is poorly conserved while both the aspartic acid and the catalytic cysteine (Cys236) in motif 9 of PTP-J1 were substituted. PTP-H4 was almost identical to PTP-H3 but lacked motifs 1 to 3 because of truncation of its N-terminus. The remaining family members (PTP-D1, -J3, -J4, and -N3) lacked five or more motifs because of more complex deletions and/or rearrangements. We also noted that PTP-D1 was nearly identical to PTP-J4, except for a small deletion in its N terminus and a large deletion in its C terminus that eliminated motifs 8 to 10. Substitutions and truncations were confirmed by sequencing. In summary, most MdBV PTP family members have features consistent with their being functional genes but only five, ptp-H2, -H3, -H5, -N1, and -N2, encode predicted proteins with fully intact catalytic domains. A severely degenerate catalytic domain combined with the absence of promoter elements or a polyadenylation signal strongly suggested that ptp-D1 is a

pseudogene. Sequence similarity among ptp-H3 and -H4 and between ptp-J4 and -D1 also suggested that diversification of this gene family is due in part to recent duplication events within and between genomic segments.

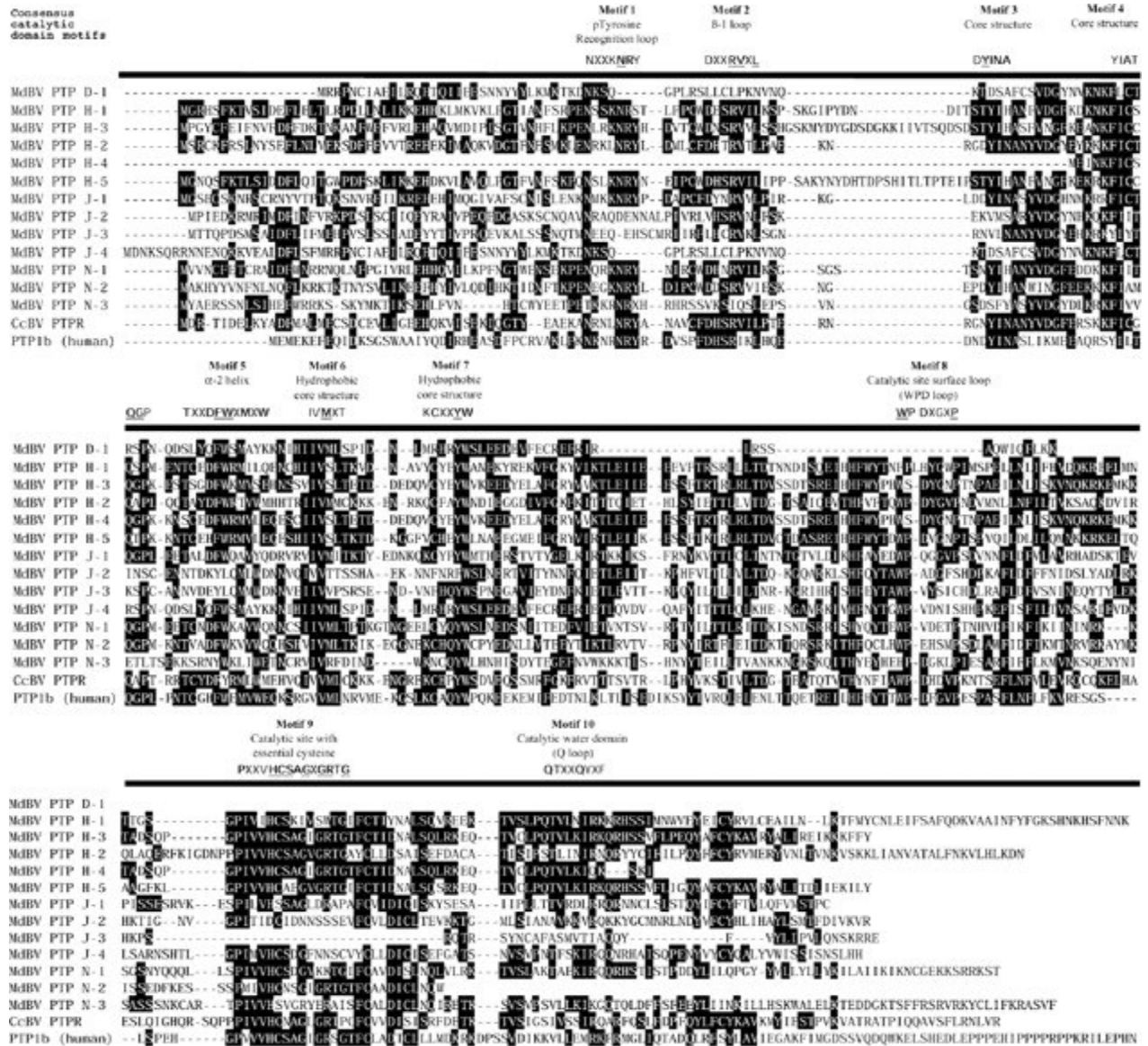
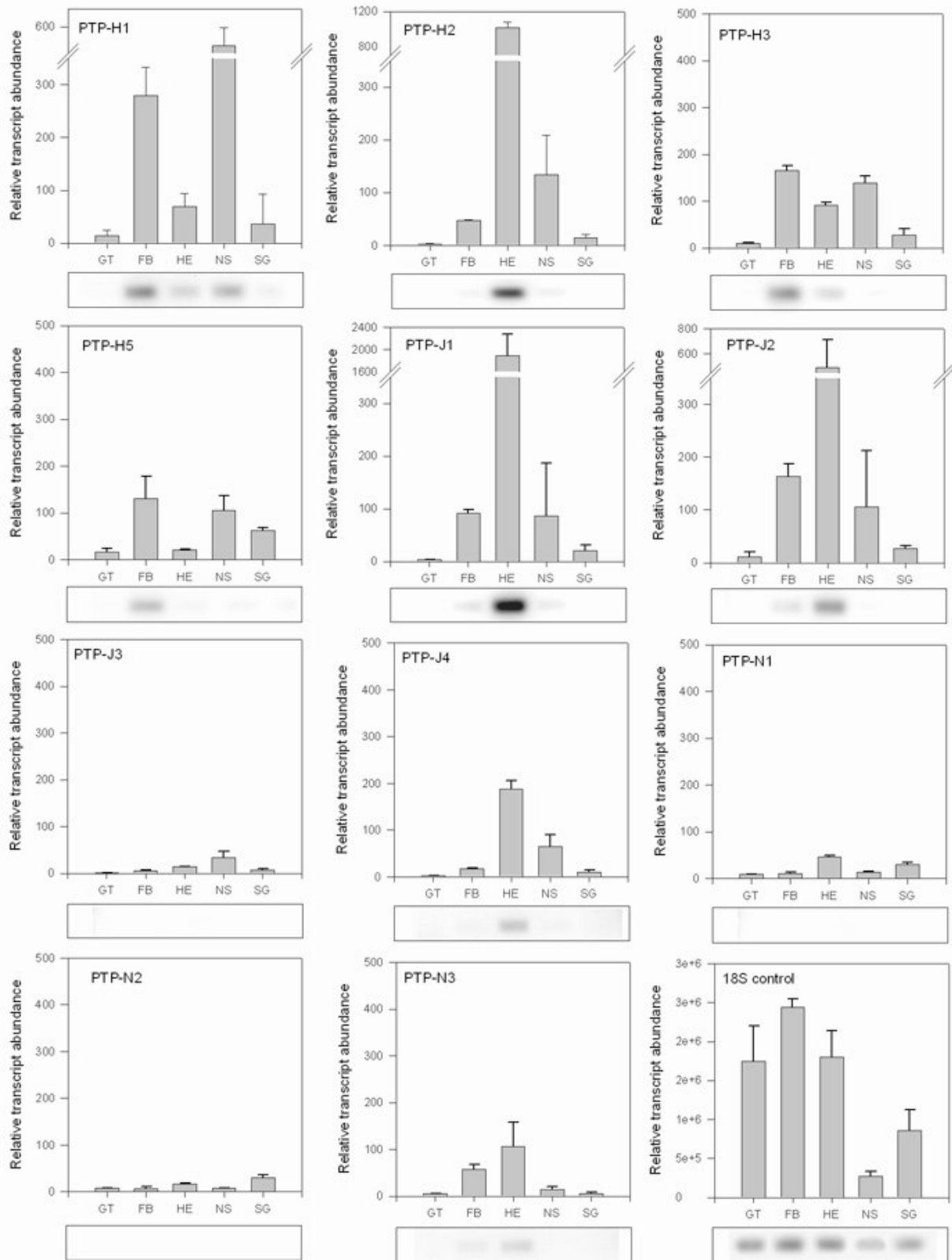


Figure 2.1. Sequence analysis of MdBV PTP family members. The deduced amino acid sequences of MdBV PTP family members are aligned to the deduced sequence of PTPR from *Cotesia congregata* bracovirus (CcBV) (EMBL accession number AJ632310), and PTP1b from humans (Genbank accession number M33689). Residues shared by a majority of genes in the alignment are boxed in black. The consensus sequence of the 10 conserved motifs present in the catalytic domain of most classical PTPs are presented above the alignment [126].

2.3.2 Most PTP family members are expressed in MdBV-infected hosts but not host cell lines

Prior studies indicated that MdBV primarily infects hemocytes, fat body, and the nervous system of host insects with expression of gene products beginning ca. 2 h post-infection and continuing at near steady state levels for several days thereafter [143, 153]. To assess whether MdBV PTPs were expressed in these or other host tissues, I conducted rqRT-PCR experiments using primer pairs specific for individual family members (Table 2.2). All family members were examined except ptp-D1 and ptp-H4 which are truncated but otherwise nearly identical to ptp-J4 and ptp-H3 respectively (see above). These experiments indicated that transcript abundance for ptp-H2, -J1, -J2, -J4, -N1, and -N3 was highest in hemocytes, while transcript abundance for ptp-H1, -H3, -H5, and -J3 was highest in the fat body and/or nervous system (Figure 2.2a). Transcript abundance for all family members was usually lower in the other tissues we sampled. As a control, PTP amplicons were not detected when template from MdBV-infected samples was not reverse-transcribed indicating that our RNA samples were not contaminated with viral DNA. In addition, no amplicons were detected in samples from non-infected hosts (data not presented).

A



B

Relative PTP transcript abundance in infected hemocytes and cell lines

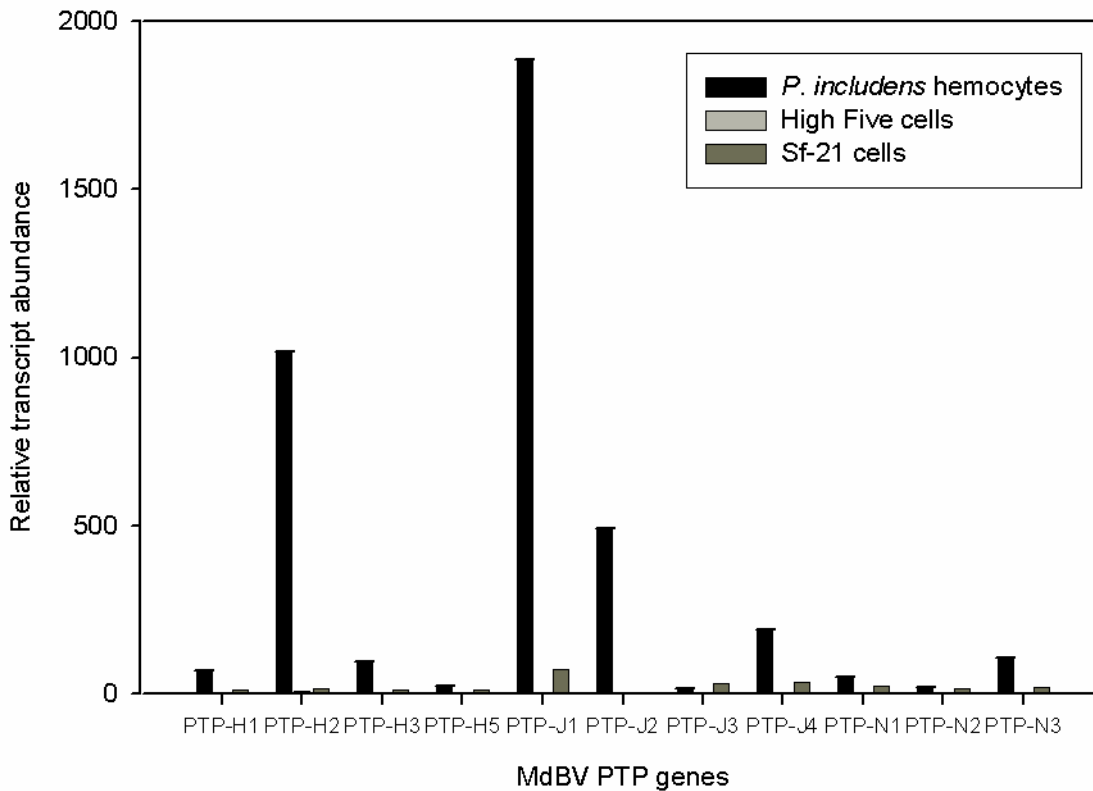


Figure. 2.2. PTP expression analysis. (a) Relative quantitative real-time PCR analysis of MdBV PTP family members *ptp-H1*, *H2*, *H3*, *H5*, *J1-J4*, and *N1-N3* in gut (GT), fat body (FB), hemocytes (HE), nervous system (NS) and salivary glands (SG) from parasitized *P. includens*. All PTPs were expressed in one or more types of infected host tissue. (b) PTP expression in MdBV infected *T. ni* High Five cells and *S. frugiperda* Sf-21 cells. PTP transcript abundance in infected hemocyte-like cell lines was low compared to infected *P. includens* hemocytes. All values were first normalized to 18S ribosomal RNA controls to account for variations in cDNA pools and subsequently calibrated to the sample displaying the lowest value which was set to 1 (see Methods). The abundance of PTP-J3 in the gut sample was standardized to a level of 1. The abundance of each PTP family member in the gut and other tissues was then determined relative to the PTP-J3 gut sample. PCR products were run on 1% agarose gels to verify

the size of each amplicon and to assure that no cross-amplification occurred. Each treatment was replicated four times using tissues collected from different virus-injected larvae. Error bar = 1 SD.

Secondary host cell lines are useful tools for studying PDV genes in loss- and gain-of-function assays [61, 140]. Previous studies exploring the role of individual MdBV genes in immunosuppression have utilized the hemocyte-like cell line High Five from the host *Trichoplusia ni*, a lepidopteran species related to *P. includens* [61, 140]. Another hemocyte like cell line, Sf-21 cells, is derived from related host species *Spodoptera frugiperda*. Both cell lines are susceptible to infection by MdBV and support expression of at least some MdBV genes. To determine if these cell lines are also suitable for loss-of-function assays targeting PTPs, I measured the relative expression levels of individual PTPs. My results indicated that at 24 h post infection, PTP transcript abundance in both MdBV infected High Five and Sf-21 cells was very low compared to those observed in infected *P. includens* hemocytes (Figure 2.2b). In contrast, other MdBV genes were expressed at normal levels and cells showed signs of infection (data not shown).

2.3.3 MdBV-infected host hemocytes and transfected *Drosophila* S2 cells exhibit elevated levels of PTP activity.

Given that transcript abundance was highest in hemocytes for several PTP family members, we first determined if tyrosine phosphatase activity was higher in host hemocytes infected with a physiological dose of virus than hemocytes from mock-infected hosts using a

commercially available kit optimized for studies on cell lysates. After preclearing lysates of free phosphate, we added a tyrosine-containing phosphopeptide (END(pY)INASL) recognized by most PTPs and then measured the free phosphate released after a 30 min incubation period. Addition of the PTP inhibitor sodium orthovanadate to each sample served as a negative control. Our results indicated that MdBV-infected hemocytes released significantly more free phosphate than lysates from mock-infected hemocytes or lysates containing inhibitor suggesting that one or more viral PTPs had tyrosine phosphatase activity (Figure 2.3).

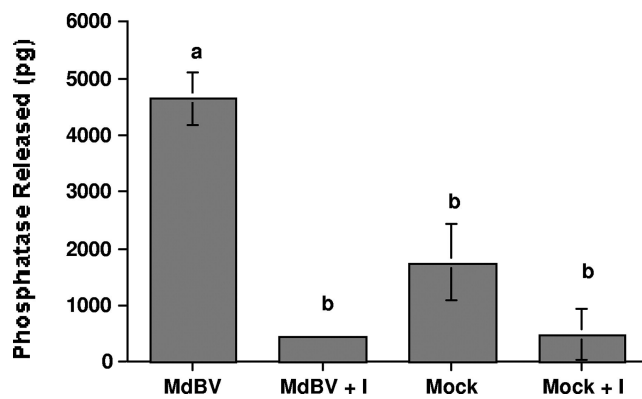


Figure 2.3. MdBV-infected host hemocytes exhibit elevated levels of tyrosine phosphatase activity. Hemocyte lysates from MdBV- or mock-infected *P. includens* larvae were precleared of free phosphate and incubated with a synthetic tyrosine phosphopeptide (Promega). Controls consisted of MdBV- or mock-infected lysates plus the inhibitor sodium orthovanadate (I). Picrograms of free phosphate released \pm SE after a 30 min incubation period was then measured at 600 nm ($n= 5$ per treatment). Means with the same letter are not significantly different ($P<0.05$); Tukey Kramer multiple comparison procedure

2.3.4 PTP-H2 and -H3 are active tyrosine phosphatases whereas PTP-H1 and -J1 are not

Sequence analysis suggested that *ptp-H2*, *-H3*, *-H5*, *-N1* and *-N2* were the strongest candidates for being functional PTPs since they were the only family members with fully intact catalytic domains (see above). My rqRT-PCR studies, however, suggested that transcript abundance for *ptp-H2* and *-H3* was much higher in hemocytes than for *ptp-H5*, *N1*, and *-N2* (Figure 2.2a). I therefore focused on *ptp-H2* and *-H3* by producing the expression constructs pIZT/H2 and pIZT/H3. Since the catalytic cysteine of *ptp-J1* was replaced by a serine, we produced pIZT/J1 as a potential natural loss of function mutant. I also produced an expression construct for *ptp-H1* (pIZT/H1), because it possessed a functional catalytic site but lacked an intact WPD loop (motif 8) which is also considered important for PTP activity [126]. I then used hemocyte-like *Drosophila* S2 cells in bioassays because 1) these cells are excellent models for studies on insect cellular immune function, 2) other MdBV virulence genes have immunosuppressive effects in S2 cells that are very similar to host hemocytes, and 3) more detailed knowledge on the pathway components regulating cellular immune responses is available in *Drosophila* than other insects [34, 140, 154, 155]. Following transfection of each construct into S2 cells, lysates were assayed for protein expression and PTP activity. An anti-V5 antibody detected a single protein band of expected size (Table 2.2) for each recombinant PTP family member on western blots but did not detect any protein in lysates prepared from the empty vector control (Figure 2.4a). Enzymatic assays further indicated that cells transfected with pIZT/H2 and pIZT/H3 produced significantly more free phosphate than lysates from cells transfected with pIZT/H1, J1 or the empty vector (Figure 2.4b). The presence of sodium orthovanadate in contrast reduced free phosphate production in each treatment to almost undetectable levels (Figure 2.4b).

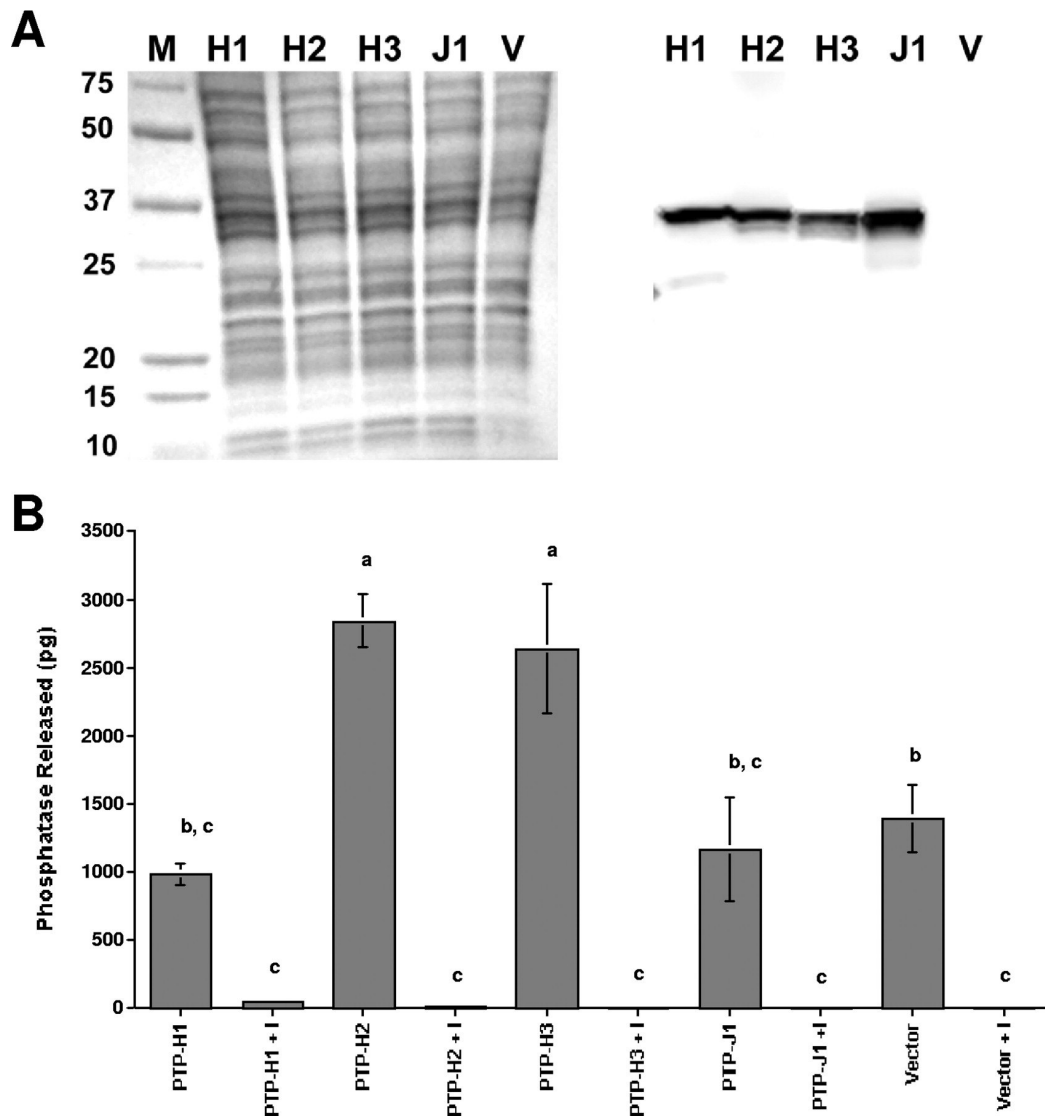


Figure 2.4. Expression of PTP-H2 and -H3 significantly increases tyrosine phosphatase activity in *Drosophila* S2 cells. (A) Protein lysates from cells harvested 48 h post-transfection with different expression constructs were prepared and separated by SDS-PAGE on 8-16% gradient gels. A Coomassie blue stained gel showing molecular weight markers (M) and lysates from cells transfected with pIZT/H1 (H1), H2, H3, J1, or empty vector (V) is shown on the left side of the figure. The corresponding western blot is shown on the right with recombinant PTP-H1, -H2, -H3 and -J1 detected using a mouse anti-V5 antibody. (B) Outcome of tyrosine phosphatase assays using lysates from S2 cells expressing PTP-H1, -H2, -H3, -J1. Lysates from cells

transfected with the empty vector or lysates containing sodium orthovanadate (I) served as controls. Assays were conducted as described in Fig. 3 with picograms of free phosphate released \pm SE after a 30 min incubation period (n= 4 per treatment). Means with the same letter are not significantly different ($P < 0.05$); Tukey Kramer multiple comparison procedure

2.3.5 PTP-H1, -H2, -H3 and -J1 localize to the cytoplasm in insect immune cells

According to the literature, classical, non-receptor type PTPs localize to the cytoplasm. To determine if this is also true for the MdBV PTPs, I visualized PTP-H1, -H2, -H3 and -J1 in *Drosophila* S2 cells using an antibody against the V5 epitope tag on each recombinant PTP protein. The results indicated that all four PTPs localized to the cytoplasm in S2 cells (Figure 2.5). The localization pattern of PTP-H2 and H-3 is focused in specific areas of the cytoplasm, whereas the localization of PTP-H1 and J-1 is more diffuse.

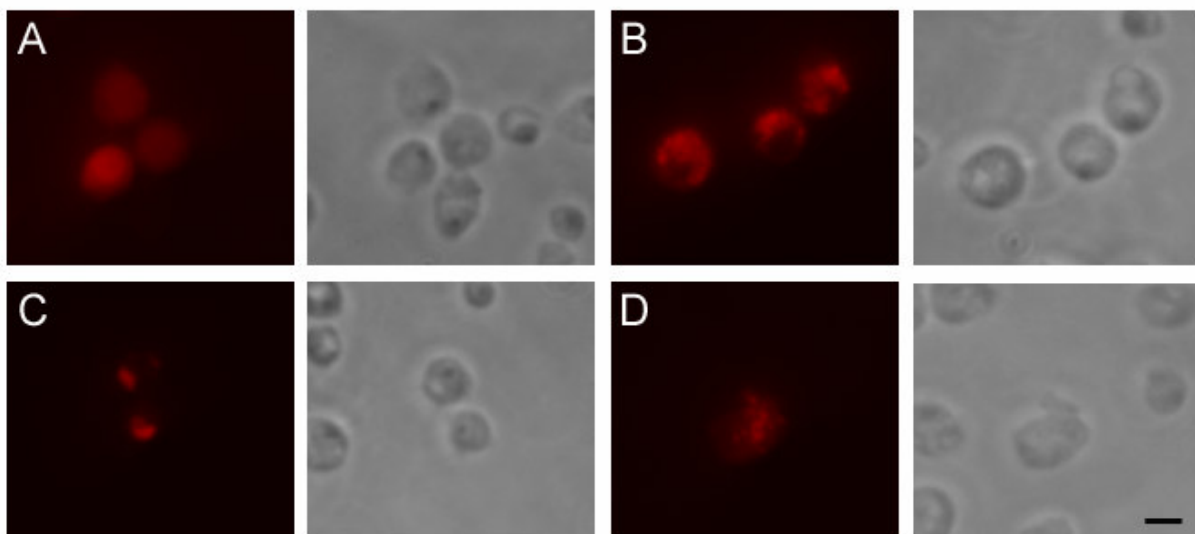


Figure 2.5. Localization of PTP-H1, -H2, -H3 and J-1 in *Drosophila* S2 cells. Cells transfected with pIZT/PTP-H1 (A), -H2 (B), -H3 (C) , -J1 (D) or empty vector (not shown) were immunostained with anti-V5 (red) at 48h post transfection. The stain localizes to the cytoplasmic region of the cell. Empty vector control transfected cells showed no staining. The scale bar in panel D represents 10 μ m.

2.3.6 PTP-H2 and –H3 reduce phagocytosis by S2 cells

Phagocytosis and encapsulation are closely related defense responses that both involve receptor mediated binding of a foreign target to the cell. Insect hemocytes remain bound to the surface of large foreign objects, whereas adhesion of smaller targets activates formation of a phagosome and ingestion of the target via actin-polymerization dependent mechanisms [94, 156]. Linkage to the cell surface and remodeling of the actin cytoskeleton in mammalian immune cells depends on phosphorylation of several proteins localized in focal adhesions [94, 157, 158]. As previously noted, MdBV infection disrupts adhesion and phagocytosis of insect hemocytes and hemocyte-like cell lines including S2 cells [61, 140]. One MdBV protein clearly involved in disrupting these defense responses is Glc1.8 which is expressed on the surface of virus-infected cells [61]. Given the importance of protein phosphorylation in these same processes, however, I assessed whether one or more MdBV PTPs also reduced phagocytosis by transfecting each expression construct into S2 cells. After 48h, I conducted phagocytosis assays by incubating the cells in the presence of bacteria and polystyrene beads that likely bind to cells via different surface receptors [34, 91, 93, 144]. My results indicated that a significantly smaller percentage of S2 cells expressing PTP-H2 or PTP-H3 phagocytized *E. coli* compared to the

empty-vector control, whereas cells expressing PTP-H1 or –J1 did not (Figure 2.6a). PTP-H2 expression also reduced the percentage of cells that phagocytized beads (Figure 2.6b). However, cells expressing PTP-H2 or –H3 alone did not exhibit a reduction in phagocytosis as strong as cells expressing Glc1.8 which as previously reported [57] reduced the number of phagocytic cells to less than 20% (Figure 2.6a, b). However, co-transfection of cells with Glc1.8 and PTP-H2 or –H3 reduced phagocytosis even more strongly with almost no cells being capable of internalizing bacteria or beads (Figure 2.6a, b).

2.3.7 PTP-H2 localizes with focal adhesion kinase to the focal adhesions

One component of focal adhesions in mammalian immune cells is focal adhesion kinase (Fak), which is a non-receptor protein tyrosine kinase (PTK) [94, 157-159]. The homologue of Fak in *Drosophila* (Fak56) also localizes to focal adhesions in adherent cells [107, 150]. Since recombinant PTP-H2 exhibited phosphatase activity and reduced phagocytosis, I examined whether it localized to focal adhesions. Labeling with anti-Fak^{Y397} indicated that Fak56 localized primarily in focal adhesions of S2 cells in a pattern similar to studies using other *Drosophila* cell types (Figure 2.6c) [150]. Visualization of PTP-H2 in transfected S2 cells using our anti-V5 antibody indicated that it too localized to focal adhesions in almost all cells we examined (Figure 2.6c). Identical studies conducted with PTP-H3 yielded an identical result (data not presented) indicating that both family members predominantly localize in focal adhesions in S2 cells.

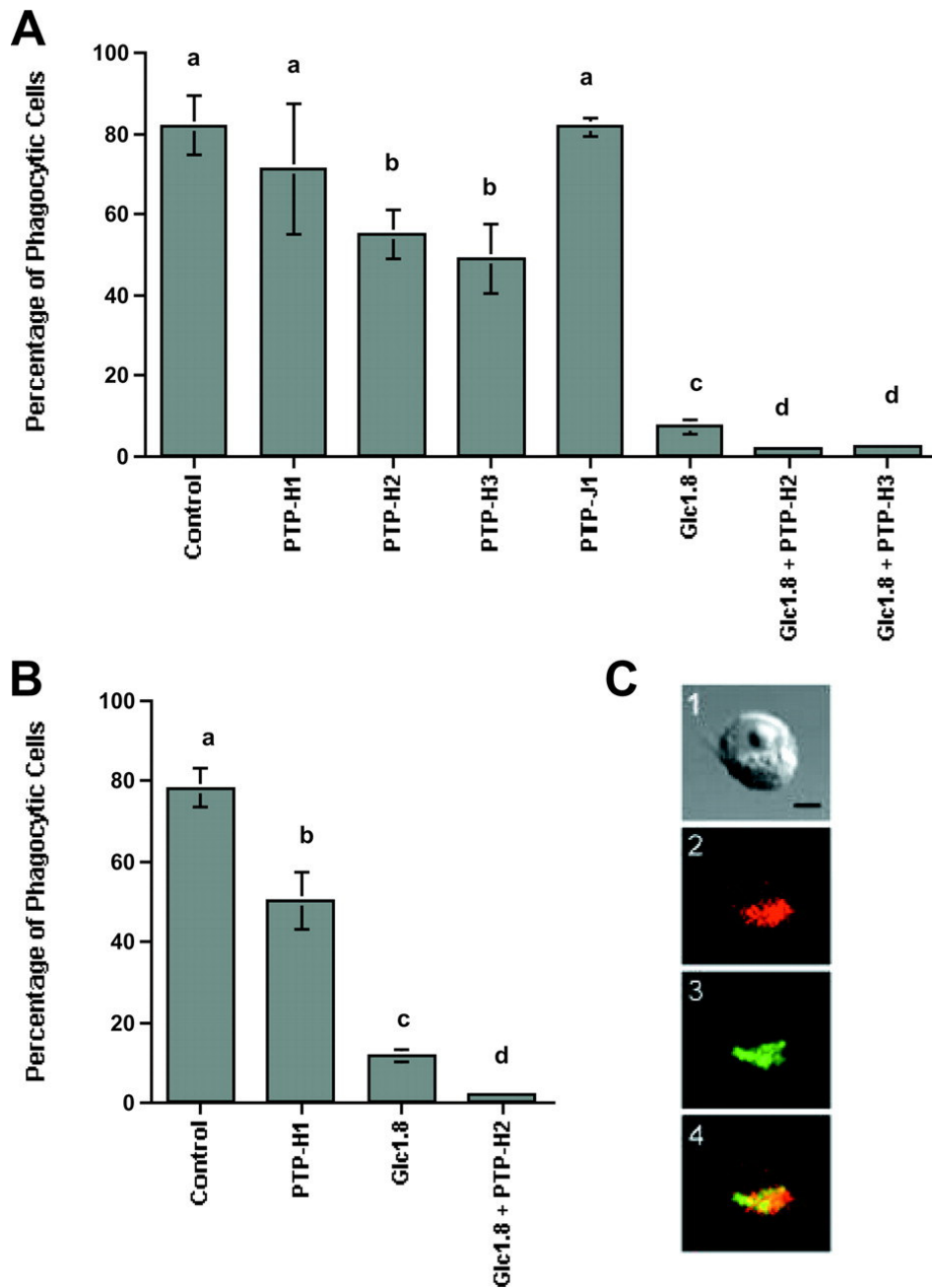


Figure 2.6. PTP-H2 and -H3 significantly reduces phagocytosis of *E. coli* and polystyrene beads by S2 cells. Cells were transfected with pIZT/PTP-H1, -H2, -H3, -J1, or empty vector (Vector), or co-transfected with PTP-H2 or PTP-H3 plus pIZT/Glc1.8. Forty eight h post-transfection, rhodamine-conjugated *E. coli* (A) or fluorescent polystyrene beads (B) were added to cells. Cells were examined 45 min later for phagocytosis by epifluorescent microscopy (n = 6 replicates per treatment). Means with

the same letter in (A) or (B) are not significantly different ($P < 0.05$); Tukey Kramer multiple comparison procedure. C. PTP-H2 co-localizes with Fak in focal adhesions. A light micrograph of a typical S2 cell expressing PTP-H2 is shown in image 1. The same cell after staining with anti-Fak^{Y397} (red) indicates that Fak56 localizes primarily to focal adhesions (arrows) (2). Staining with anti-V5 (green) indicates that PTP-H2 localizes to the same region of the cell (3). Merging of images 2 and 3 results in an orange-yellow signal indicative of co-localization of Fak56 and PTP-H2. Scale bar in (C1) equals 10 μm .

2.4 Discussion

A key regulatory mechanism in immunity and other physiological processes is reversible tyrosine phosphorylation of essential proteins. In mammals, immune cells express more protein tyrosine kinase (PTKs) and PTP genes than any other cell type with the possible exception of neurons [160]. Far less is known about either the number or function of PTKs and PTPs expressed in insect hemocytes. The *Drosophila* genome, for example, contains approximately 32 PTKs and 38 PTPs but only a small number of these enzymes have been directly implicated in regulating a specific immune pathway or effector response [79, 161]. However, conservation between mammals and insects in immune signaling pathways such as Toll, JAK/STAT, and GATA as well as in the protein complexes that regulate adhesion and phagocytosis circumstantially suggests that specific PTKs and PTPs are likely essential in regulating phagocytosis as well as other immune responses [27, 91, 93, 161-163].

Several bacterial pathogens of mammals including *Yersinia* spp., *Salmonella typhimurium*, and *Mycobacterium tuberculosis* encode phosphatases that disrupt phagocytosis, interfere with activation of MAP kinases, or suppress other immune responses [160, 164-166]. In contrast, while all bracoviruses examined to date encode multiple PTP-like genes, no

experimental data prior to the current study reveal whether any function as virulence factors [7, 128, 138, 151, 152]. Previous studies indicate that MdBV immunosuppresses insects by inhibiting several effector functions including phagocytosis. The results from this study indicate that most other MdBV PTP family members are expressed in virus-infected immune cells but only a subset of these genes likely encode catalytically functional PTPs. I also provide evidence that two of these putatively functional PTPs, PTP-H2 and -H3, are preferentially expressed in hemocytes, localize to focal adhesions in S2 cells, and have antiadhesive of phagocytic activity.

Adhesion and phagocytosis of foreign targets involves multiple pathways in both mammals and insects [27, 34, 163]. Opsonin-dependent pathways are regulated by binding of complement-like or other humoral pattern recognition molecules prior to uptake by hemocytes while opsonin-independent pathways involve direct binding of the target to cell-surface receptors like integrins and scavenger receptors [34, 91, 93, 167]. Integrin expression by hemocytes is also implicated in encapsulation of foreign targets including parasitoids [34, 151, 168, 169]. Integrin-mediated adhesion and signaling by mammalian immune cells requires tyrosine phosphorylation of the PTKs Fak or Pyk2, as well as other proteins including p130^{Cas} and paxillin [157-159]. These proteins concentrate primarily in focal adhesions that link integrins and other components of the extracellular matrix to the actin cytoskeleton. Reciprocally, the anti-phagocytic activity of PTP YopH from *Yersinia* sp. is associated with its ability to dephosphorylate Fak, paxillin, p130^{Cas} and several other proteins in mammalian macrophages, neutrophils, and lymphocytes [160, 164, 170]. Far less is known about these processes in insect immune cells but it is likely that adhesion and phagocytosis are regulated in part by similar protein complexes given that *Drosophila* encodes homologs of Fak (Fak56), Pyk2, and paxillin (DpaxA) that also localize to focal adhesions [150, 162, 171, 172]. In turn, the anti-phagocytic

activity of recombinant MdBV PTP-H2 and –H3 combined with their localization in focal adhesions suggest Fak56 or related proteins are candidate substrates for these virally encoded enzymes.

Some adhesion and phagocytic pathways do not require tyrosine phosphorylation for normal function [162]. The ability of YopH to use multiple substrates has been suggested as one way by which *Yersinia* sp. simultaneously disables different phagocytic pathways. Another strategy is that pathogens can introduce multiple virulence factors into immune cells that disrupt phagocytosis and other effector functions by different mechanisms [160, 164, 170]. Disrupting multiple immune pathways is clearly important to MdBV and other PDVs given that encapsulation and killing of the parasitoid, as well as potential clearance of the virus by the host immune system, likely involve multiple effector responses. Our previous studies already indicate that MdBV encodes at least one other virulence gene (*glc1.8*) with anti-adhesive and anti-phagocytic activity that unlike PTP-H2 targets the cell surface [61, 140]. The present study indicates that PTP-H2 and –H3 complement the activity of Glc1.8 since expression of these PTPs and Glc1.8 together have greater effect on adhesion and phagocytosis than either factor alone. Combined with the expression of multiple IκBs that disrupt the Toll and Imd signaling pathways [62], the picture that collectively emerges is that MdBV encodes a suite of virulence factors that suppress multiple immune functions.

Although host hemocytes are the primary target of MdBV infection, other tissues are also infected [3, 58, 141, 143]. Results of the present study further indicate that while transcript abundance of some PTP family members is highest in hemocytes, others are more abundant in the fat body and nervous system. This suggests that MdBV PTP-like gene products interact with other physiological processes of the host besides immunity. One potential target of interest is the

ecdysone biosynthetic pathway, which involves the phosphorylation of several proteins in prothoracic glands [107]. Hosts parasitized by many BV-carrying parasitoids exhibit reduced ecdysteroid titers that result in inhibition of molting and metamorphosis [42, 44], which has led to the suggestion that proteins in the ecdysone pathway are potential substrates for PTPs encoded by *Toxoneuron nigriceps* BV and CcBV [128]. This could be the case for some MdBV PTP family members as well given that virus infection strongly suppresses host ecdysteroid titers [46, 59]. A baculovirus-encoded PTP was also recently implicated in enhancing the locomotor activity of infected larvae [137]. Lepidopteran larvae parasitized by BV-carrying braconid wasps exhibit reduced locomotor activity in concert with suppressed weight gain, but whether any viral gene product is responsible for these alterations is unknown.

Phylogenetic studies indicate that BV-carrying braconid wasps form a monophyletic lineage that now consists of approximately 17,000 species in four subfamilies (*Microgastrinae*, *Miracinae*, *Cardiochilinae*, and *Cheloninae*) (see references [3, 42], and [173] for a summary). Since BVs are only transmitted vertically, the presence of classical PTP genes in all of the BVs from microgastrine and cardiochiline wasps examined to date suggests that one or more PTP genes were acquired by a common ancestor relatively early in the evolution of the BV-braconid association. Subsequent diversification, however, has clearly resulted in pronounced differences among the PTP genes encoded by the thousands of BVs that exist today. The CcBV genome, for example, encodes 27 PTP family members, compared to only 13 in MdBV [7, 10, 128]. Sequence comparisons among MdBV and CcBV PTP family members indicate that most differ considerably from one another. Within-species comparisons also reveal various degrees of similarity. For example, MdBV PTP-D1 and PTP-J4 are very similar and likely reflect a recent duplication event. In contrast, sequence variation is very high among other MdBV family

members (Figure 1), as well as PTP family members encoded by CcBV [128]. The differences in the PTP-like genes encoded by BVs could reflect differences in the host insects their associated wasps parasitize since sequence variation in PTP catalytic domains greatly affects substrate specificities [66, 126]. Most BV-carrying parasitoids also parasitize multiple host species, which further increases the diversity of protein targets with which PTP family members could interact [7, 83, 174, 175]. While MdBV PTP-H2 and -H3 appear to be functional PTPs, sequence analysis suggests that most other family members likely are not. Analyses of PTP gene families in other organisms similarly reveal that catalytically inactive enzyme homologues commonly occur, and in some instances enzymatically inactive family members have assumed functions in other regulatory processes [83]. Thus, some MdBV PTP family members could function as substrate traps or have other novel activities. Key challenges for the future are to determine what these other functions might be and what role they play in successful parasitism.

CHAPTER 3

ROLE OF MDBV GENES IN APOPTOSIS OF INSECT IMMUNE CELLS

In collaboration with Richard J. Suderman

3.1 Introduction

As discussed in Chapter 1, granulocytes are the primary lepidopteran hemocyte type that phagocytizes foreign intruders, whereas encapsulation requires cooperation between granulocytes and a second class of hemocytes called plasmatocytes [33, 147, 176]. The primary role of granulocytes in capsule formation appears to be the recognition of foreign targets and release of cytokines that recruit plasmatocytes. Plasmatocytes then bind and form an overlapping sheath around the target, eventually resulting in death of the parasitoid. In the host *Pseudoplusia includens*, both granulocytes and plasmatocytes lose the capacity to bind foreign surfaces or phagocytize small foreign targets 4–8 h after infection by MdBV [57, 139, 147]. Thereafter, a large proportion of granulocytes, but not plasmatocytes, die by apoptosis [177]. Transcriptionally inactive MdBV has no apoptotic activity, suggesting that expression of one or more viral gene products is required for this response [177]. However to date, no viral genes have been linked to MdBV induced apoptosis.

Considering that many check points in the apoptosis pathway are controlled by phosphorylation, the MdBV encoded PTPs could potentially trigger this process. However, we can not exclude the possibility that other MdBV encoded virulence factors play a role as well.

We therefore sought to determine if any MdBV gene that was previously found to be preferentially expressed in hemocytes plays a role. To this end, we conducted an expression screen of MdBV genes that are preferentially expressed in the host hemocytes or the Sf-21 cell line. This cell line is derived from the lepidopteran host *Spodoptera frugiperda* and is well known to undergo apoptosis in response to different stimuli. This chapter reports that expression of PTP-H2 triggered mitochondrial membrane depolarization and caspase-dependent apoptosis, suggesting that this virulence factor induces apoptosis through a mitochondria-dependent death pathway.

3.2 Materials and methods

3.2.1. Insects and cell lines

Insects and cell lines. *M. demolitor*, *P. includens* and *S. frugiperda* were reared as described previously [57]. IPLB-SF-21 (Sf-21) cells derived from *S. frugiperda* were maintained in TC-100 medium (Invitrogen) with 10% fetal calf serum (Atlanta Biologicals) and 1% antibiotic cocktail (Gibco). Cells were maintained and passaged as adherent cells in Corning 25 cm² tissue-culture flasks. Most experiments were conducted in 24- or 96-well culture plates (Corning).

3.2.2. Virus collection and injection into *S. frugiperda* larvae.

MdBV was collected from wasps and injected into larvae as described previously [58, 140]. As is convention in the PDV literature, the amount of MdBV collected from the reproductive tract of a single adult female is defined as one wasp equivalent. MdBV packages only one genomic segment per virion and the 15 genomic segments that comprise the genome are nonequimolar in abundance [143]. Quantitative data indicate that one wasp equivalent on average equals 161010 virions and that wasps inject 0.01–0.05 wasp equivalents per host during oviposition which equals 16108–56108 virions [143]. For this study, we injected 0.05 wasp equivalents of MdBV into fourth instar *S. frugiperda* larvae as described previously [143]. Negative controls were larvae injected with 0.05 wasp equivalents of MdBV that had been inactivated by treatment with psoralen and UV light [58].

3.2.3. Plasmid expression constructs and cell transfections

ORFs for the MdBV genes *g1c1.8*, *ptp-H1*, *ptp-H2*, *ptp-H3*, *ptp-J1*, *egf0.4*, *egf1.0*, *IκB-H4* and *IκB-N5*, were previously cloned into the vector pIZT/V5-His (Invitrogen) to produce the expression constructs pIZT/G1c1.8, pIZT/PTP-H1, pIZT/PTP-H2, pIZT/PTP-H3 and pIZT/PTP-J1, pIZT/Egf0.4, pIZT/Egf1.0, pIZT/IκB-H4 and pIZT/IκB-N5 [61, 62, 178] (for construct details and transfection strategies see Chapter 2, Methods). We also produced an expression construct of PTP-H2 that lacks PTP activity (pIZT/PTP-H2^{C236A}) by replacing the essential catalytic cysteine with an alanine residue using pcr-based site-directed mutagenesis. Empty pIZT/V5-His vector was used as a negative control. For the colocalization experiments, *ptp-H2* including the C-terminal V5 epitope tag was cloned into GFP-lacking pHSP70polyA under control of the *Drosophila* hsp70 promoter (pHSP/PTP-H2). Constructs were transiently expressed in S2 or Sf-21 cells seeded at 70-80% confluency in 12 or 24-well

culture plates and transfected using Cellfectin (Invitrogen) for S2 cells and Lipofectin (Invitrogen) for Sf-21 cells as previously described [152]. In some experiments using Sf-21 cells, the pan-caspase inhibitor Z-VAD-FMK (Promega) (20 μ M) was added to cultures in fresh medium 5 h post-transfection.

3.2.4. Assessment of apoptosis by *S. frugiperda* hemocytes and Sf-21 cells

Apoptosis of hemocytes was measured by bleeding *S. frugiperda* larvae 3, 18 and 30 h post-infection from a cut proleg. Cells from individual larvae were rinsed 2x in physiological saline and placed into wells of 24-well culture plates [179]. The four major hemocyte types in circulation (granulocytes, plasmatocytes, spherule cells and oenocytoids) were identified by morphology and staining with hemocyte type-specific antibodies [29]. Hemocytes exhibit several classical symptoms during MdBV-mediated apoptosis including DNA fragmentation, alterations in mitochondrial membrane potential and cell blebbing [180]. In the current study, apoptotic hemocytes were identified by staining with fluorescein-conjugated annexin V (BD Biosciences) which detects phosphatidylserine serine on the surface of apoptosing cells and the mitochondrial membrane potential marker JC-1 (5,5',6,6'-tetrachloro-a,a',3,3'-tetraethylbenzimidazolylcarbocyanine Iodide, λ_{ex} = 400 nm, λ_{em} = 505 nm; Biotium) (10 μ g/ml). Annexin V staining was performed as recommended by the manufacturer. Hemocytes were stained with JC-1 as previously outlined with healthy cells fluorescing red due to aggregation of the dye on mitochondria with high membrane potential and apoptosing cells fluorescing green due to the dye forming monomers on mitochondria with reduced membrane potential [181]. The percentage of apoptotic cells for each hemocyte type was determined by counting 200 cells using an epifluorescent, phase-contrast microscope (Leica DM IRB). The

proportion of apoptotic cells for each hemocyte type was then compared between larvae injected with viable and inactivated MdBV by two-tailed binomial test using JMP statistical software (SAS Institute). Since Sf-21 cells undergo extensive blebbing in association with apoptosis [182, 183], we initially screened for apoptosis in this cell line using a cell survival assay in which we counted the proportion of living cells 20 h after a given treatment. This was done by counting the number of intact (non-blebbed) cells present in three randomly selected fields of view at 400X magnification both two hours and 20 hours post-treatment. Percentage cell survival was determined by dividing the number of intact cells present at the end of the experiment by the number of cells at the beginning of the experiment with values greater than 100% indicating that the number of cells per well increased during the 20 h assay. Sf-21 cells were also stained with annexin V and JC-1 as described above. Proportional data were arcsin transformed and analyzed by one-way ANOVA with treatments compared to the negative empty vector control using Dunnett's multiple comparison procedure. Images were captured using Q-imaging and Adobe Photoshop software.

3.2.5. Caspase Activity Assay

Protein extracts for caspase activity assays were prepared by lysing approximately 1.5 x 10⁵ cells at 24 h post transfection by three cycles of freeze-thaw in caspase activity buffer (50 mM HEPES, pH 7.5, 0.1% CHAPS, 10% sucrose, 1 mM EDTA, 0.1 M NaCl, 5 mM DTT), followed by removal of insoluble material by centrifugation at 16,000 x g at 4 °C for 5 min. The supernatants were assayed for protein concentration by modified Bradford assay (Pierce). Concentrations were normalized and 17 µg total protein were incubated in 0.2 ml caspase assay

buffer containing 100 μ M Ac-DEVD-AFC (fluorogenic caspase 3 substrate, Biomol International). Fluorescence due to enzymatic release of AFC [7-amino-(trifluoromethyl)coumarin] from the substrate was measured using a spectrofluorometer (BMC) over 1 h at 37°C (λ_{ex} = 405 nm, λ_{em} = 520 nm). Experiments were carried out in triplicate.

3.2.6. Phagocytosis assays

We assessed the ability of Sf-21 cells to phagocytose heat-killed *Escherichia coli* labeled with rhodamine (see Chapter 2, methods). Cells were first transfected with pIZT/PTP-H2 or the pIZT empty vector and then maintained for 20 h in the presence of Z-VAD-FMK. Cells were then transferred to new 12-well culture plates in serum-free medium plus Z-VAD-FMK at a density of 16105 cells per well. After a 1 h preincubation period, bacteria were added to each culture well at a ratio of 15:1. Cells were allowed to phagocytose for 90 min at 27 °C followed by transfer of the culture plate to ice. We then scored the percentage of cells with one or more ingested bacteria by counting 200 cells per well from four randomly selected fields of view using a Leica TCS inverted epifluorescent microscope. Bacteria were red, while cells expressing a gene of interest were green. Each treatment was replicated a minimum of five times using independently prepared samples. The data were then analysed by Student's t-test.

3.2.7. Immunofluorescence microscopy

Sf-21 cells transfected with pIZT/PTP-H2 or other expression constructs were processed for immunofluorescence microscopy as described in Chapter 2, methods. Briefly, cells cultured

in the presence of Z-VADFMK were washed in PBS 20 h post-transfection and then fixed for 20 min in 4% paraformaldehyde in PBS. Fixed cells were permeabilized with PBS–0.1% Triton X-100 (PBT), blocked in 5% dried milk in PBS, and then incubated overnight at 4 °C with anti-V5 antiserum (1:5000) that recognizes recombinant PTP-H2. After washing in PBT, cells were incubated with Alexa fluor 568-conjugated goat anti-mouse (1:2000) (Invitrogen). Incubation of cells with secondary antibody alone served as the negative control. Samples were examined on a Leica-TCS microscope with images captured as described above.

3.2.8. Cell proliferation assays

Proliferation of Sf-21 cells transfected with pIZT/PTP-H2 and pIZT (empty vector) in the presence of Z-VAD-FMK was assessed by seeding 5000 cells/well into 96 well culture plates (Promega). The mock control were cells transfected with empty vector maintained in medium without caspase inhibitor. At selected times post-transfection, cells were resuspended by gentle pipetting and the number of cells per well determined using a Neubauer hemocytometer. The number of cells present per well in each treatment over a 6 day assay period were then compared by conducting a repeated measures analysis and using the General Linear Model and JMP software.

3.3 Results

3.3.1 MdBV infection induces apoptosis of granulocytes in *S. frugiperda* larvae.

P. includens hemocytes lose the capacity to bind foreign surfaces and phagocytize small targets as early as 4 h post-infection by MdBV followed by apoptosis of granulocytes by 24 h, as measured by DNA fragmentation, annexin V staining and cell blebbing [147, 180]. MdBV-infected hemocytes from the related host *S. frugiperda* similarly lose the capacity to bind foreign surfaces and form capsules [184], but whether infected granulocytes undergo apoptosis had not previously been investigated. In the current study, we determined that, as in *P. includens*, MdBV infection caused *S. frugiperda* granulocytes but not other hemocyte types to apoptose as measured by annexin V binding. Almost no hemocytes bound annexin V at 3 h postinfection but by 18 h significantly more granulocytes from MdBV-infected larvae were stained by annexin V than in control larvae infected with UV-inactivated virus (Figure 3.1a, b). Additional evidence that *S. frugiperda* granulocytes undergo apoptosis included nuclear condensation as visualized by propidium iodide staining and loss of mitochondrial membrane potential as visualized by JC-1 staining (data not presented). By 30 h post-infection, numerous apoptotic bodies from fragmenting granulocytes were observed in the hemolymph resulting in a significant reduction in the number of viable granulocytes per microliter of hemolymph compared to larvae injected with inactive MdBV (Figure 3.1c).

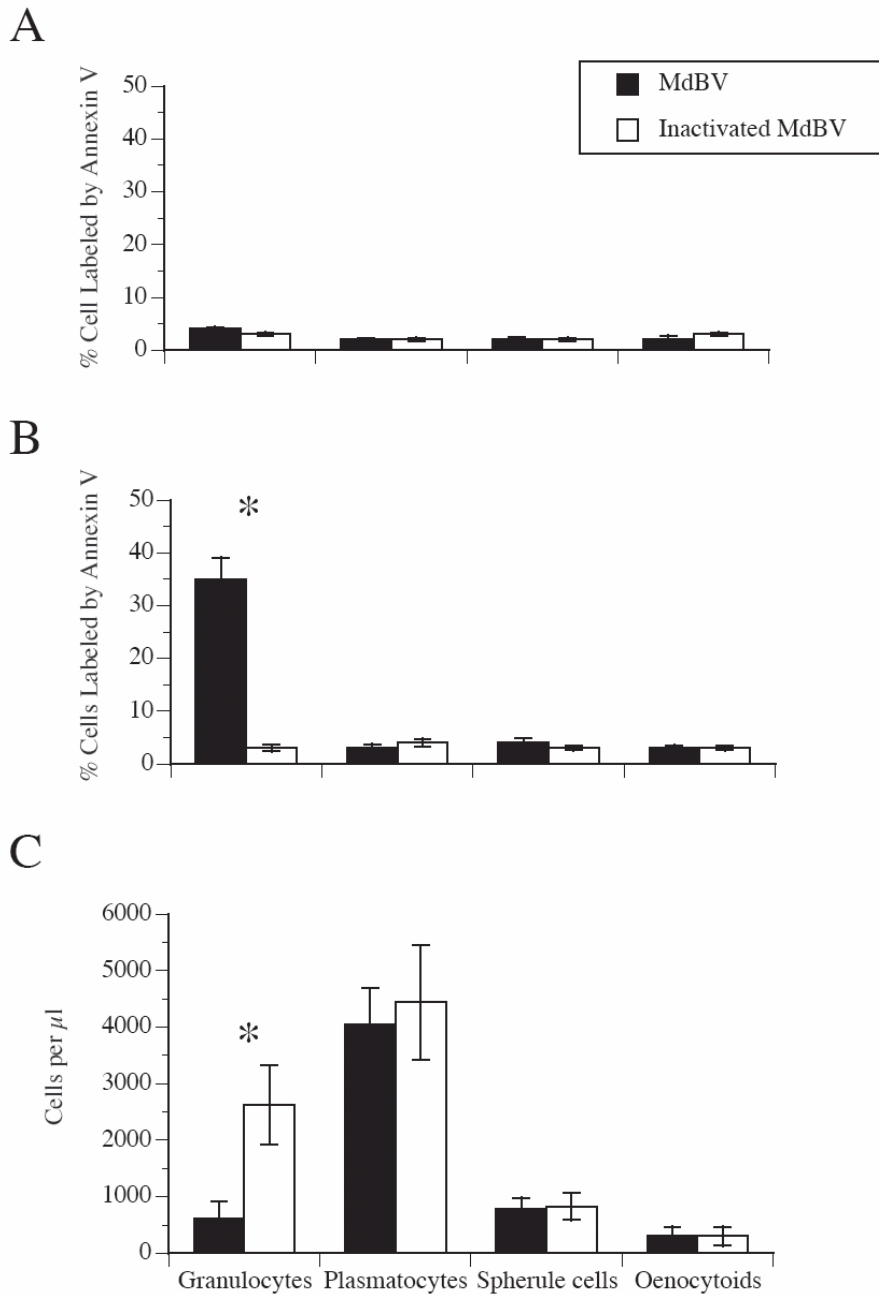


Figure 3.1. MdBV infection induces apoptosis of granulocytes. *S. frugiperda* larvae were infected with 0.05 equivalents of MdBV or MdBV inactivated with psoralin and UV light. Hemocytes were collected 3 h (A) and 18 h (B) post-infection and the percentage of each hemocyte type in circulation (granulocytes, plasmatocytes, spherule cells and oenocytoids) that

bound annexin V was determined by counting the total number of cells in three randomly selected fields of view. An asterisk (*) above a given cell type indicates that the MdBV treatment differs significantly from the inactivated virus control (two way binomial tests, $p < 0.05$, $n = 10$ larvae sampled per treatment). C. Hemocytes were collected from larvae 30 h post-infection and the mean number (\pm SD) of granulocytes, plasmatocytes, spherule cells and oenocytoids per microliter of hemolymph was determined using a hemocytometer. The asterisk (*) indicates that the number of granulocytes in circulation in larvae infected by MdBV differs significantly from larvae injected with the inactivated virus control (t-test, $t = 6.2$, $p = 0.004$, $n = 10$ larvae sampled per treatment).

3.3.2 PTP-H2 induces apoptosis of Sf-21 cells

Since MdBV and other PDVs do not replicate outside of female wasps, it is currently not possible to produce, maintain or screen PDV mutants. Therefore, to assess whether a specific MdBV gene product functions as an apoptosis inducer, we conducted an expression screen in the Sf-21 cell line using plasmid constructs of viral genes that prior studies indicated are preferentially expressed in host insect hemocytes [61, 62, 141, 178, 185]. We reasoned that Sf-21 cells were a good choice for this screen because preliminary experiments indicated that MdBV infection caused Sf-21 cells to undergo apoptosis similar to granulocytes (data not presented). Sf-21 cells are also well known to undergo high levels of apoptosis following infection by baculovirus mutants deficient in anti-apoptotic gene activity [182, 183, 186]. Our screen indicated that Sf-21 cells transfected with pIZT/PTP-H2 exhibited a significant reduction in survival, whereas the other MdBV genes we tested had no effect on survival compared to cells

transfected with the empty vector that expressed only GFP (Figure 3.2a). A large proportion of cells expressing PTP-H2 fragmented into apoptotic bodies resulting in a loss of intact cells and the accumulation of small membrane blebs in assay wells (Figure 3.2b). PTP-H2 expression also resulted in significantly increased binding of annexin V and a pronounced spectral shift from red to green following staining by the mitochondrial marker JC-1 (Figure 3.3). Together, these symptoms suggested that PTP-H2 induced apoptosis of Sf-21 cells rather than necrosis.

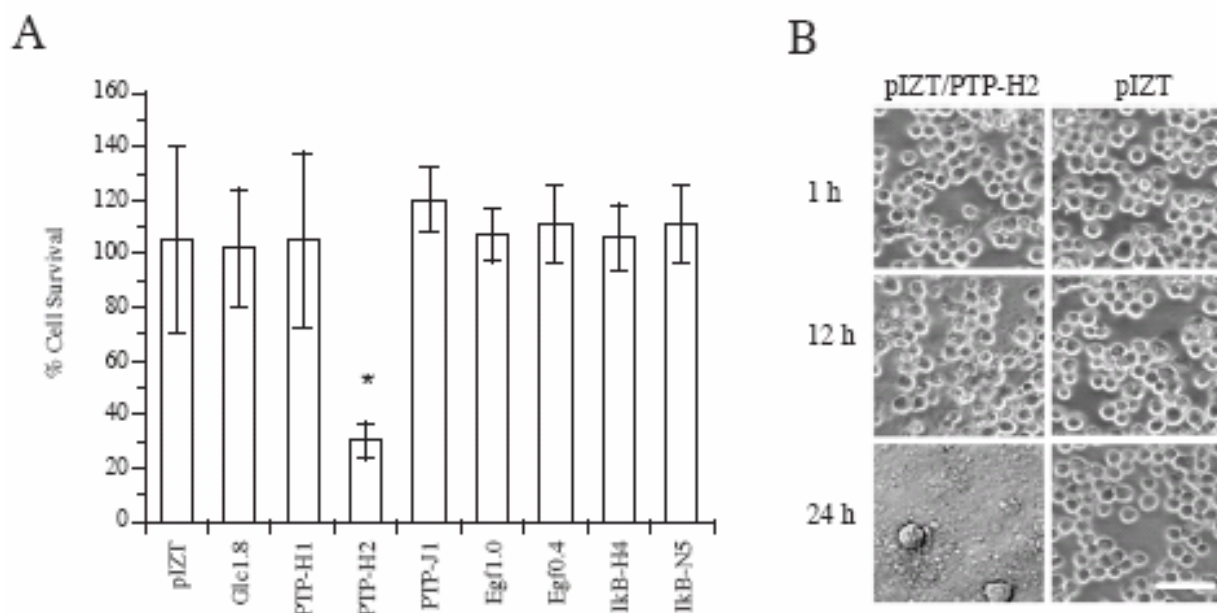


Figure 3.2. PTP-H2 expression induces apoptosis of Sf-21 cells. Sf-21 cells were transiently transfected with 2 μ g of the indicated expression plasmids per ml of medium. A. The mean percentage (\pm SD) cell survival 20 h post-transfection. Cells were counted as viable if they were intact (non-blebbed) and excluded propidium iodide. An asterisk (*) indicates that a given treatment resulted in significantly reduced cell survival compared to cells transfected with pIZT

empty vector (Overall model F8, 26 = 27.5, $p = 0.001$, $n = 3$ independent experiments per treatment followed by Dunnett's multiple comparison procedure, $p < 0.05$). B. Representative phase-contrast micrographs of Sf-21 cells transfected with the expression plasmids pIZT/PTP-H2 or pIZT empty vector at 1, 12 and 24 h post-transfection. Almost all cells are intact and viable at 1 h, whereas a majority of cells expressing PTP-H2 have fragmented into small apoptotic bodies at 24 h. Scale bar in the 24 h pIZT panel equals 200 μm .

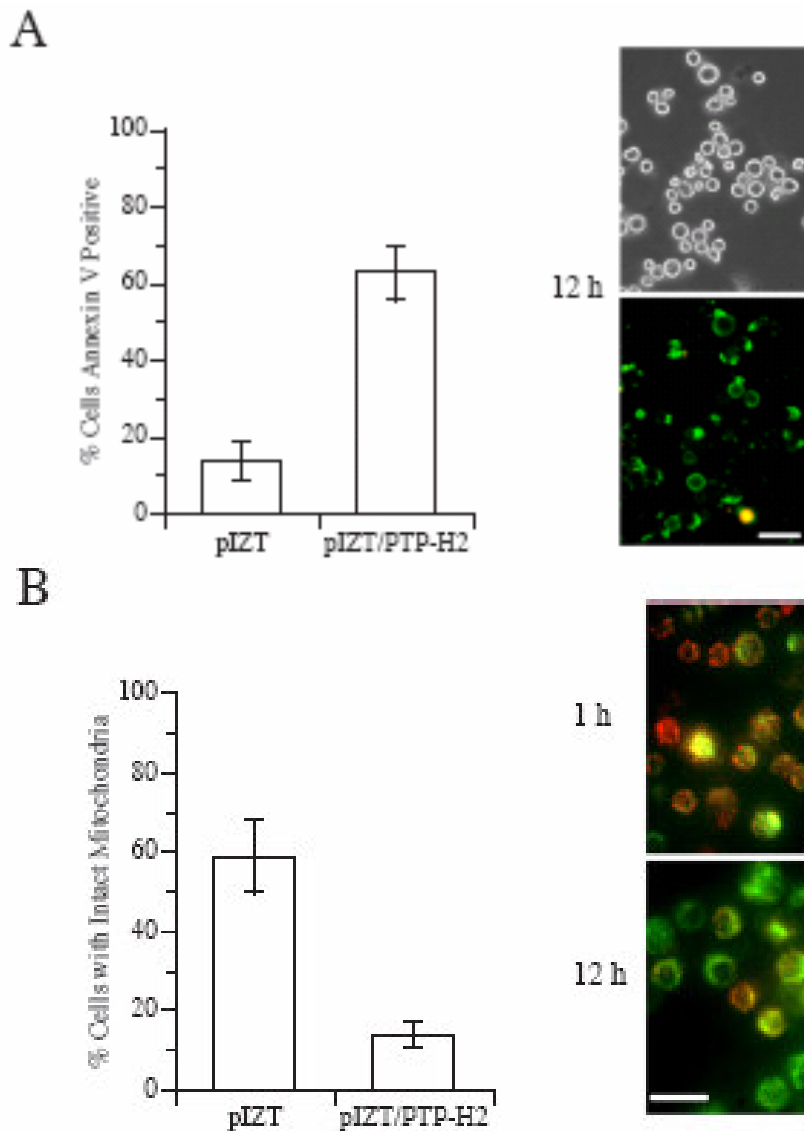


Figure 3.3. PTP-H2 expression increases annexin V binding and mitochondrial membrane depolarization. Sf-21 cells were transiently transfected with 2 μ g pIZT/PTP-H2 or pIZT empty vector per ml of medium. A. The mean percentage (\pm SD) of cells binding annexin V 12 h post-transfection as determined by epifluorescent microscopy. Significantly more cells transfected with pIZT/PTP-H2 bind annexin V than cells transfected with the empty vector ($t = 10.2$, $p = 0.0005$, $n = 3$ replicates per treatment). To the right of the figure are light (upper) and epifluorescent (lower) micrographs of Sf-21 cells 12 h post-transfection with pIZT/PTP-H2 after staining with annexin V and propidium iodide. The majority of cells binds annexin V (green) but is not labeled by propidium iodide (red). Scale bar in lower panel equals 130 μ m. B. The mean percentage (\pm SD) of cells with depolarized mitochondria as determined by JC-1 staining. A total of 200 cells from a randomly selected field of view were examined and scored by epifluorescent microscopy. Significantly more cells transfected with pIZT/PTP-H2 exhibit a green shift in JC-1 fluorescence compared to the empty vector control ($t = 8.1$, $p = 0.001$, $n = 3$ replicates per treatment). To the right of the figure are epifluorescent micrographs of Sf-21 cells 1 h (upper) and 12 h (lower) post-transfection with pIZT/PTP-H2 and staining with JC-1. Most cells at 1 h fluoresce red while cells at 12 h fluoresce green. Scale bar in lower panel equals 100 μ m.

3.3.3 PTP-H2 promotes apoptosis by caspase activation

To determine whether caspases were involved in PTP-H2 mediated cell death, we conducted enzymatic assays using the fluorogenic caspase-3 substrate Ac-DEVD-AFC. These experiments indicated that effector caspase activity was significantly higher in lysates from cells

expressing PTP-H2 than cells transfected with empty vector (Figure 3.4a). Reciprocally, addition of the pan caspase inhibitor Z-VAD-FMK blocked PTP-H2 mediated death as measured by our cell survival assay (Figure 3.4b). Sf-21 cells expressing PTP-H2 in the presence of Z-VAD-FMK were morphologically similar to control cells when examined by phase-contrast microscopy with almost no cell blebbing and more than 90% of cells remaining viable as measured by exclusion of propidium iodide. Depolarization of mitochondria in cells expressing PTP-H2 was also apparently related to caspase activation because we did not observe any change in JC-1 fluorescence of cells transfected with pIZT/PTP-H2 and maintained in the presence of Z-VAD-FMK (data not presented). Immunostaining of Sf-21 cells cultured in the presence of Z-VAD-FMK indicated that PTP-H2 preferentially localized to focal adhesions, as reported previously for hemocytes and hemocyte-like cell lines, such as High Five cells from *Trichoplusia ni*, and S2 cells from *Drosophila* [61, 141, 178] (data not presented). This observation suggested that Z-VAD-FMK did not affect the cellular distribution of PTP-H2 and led to the question of whether Sf-21 cells expressing PTP-H2 lost the capacity to phagocytize foreign targets when prevented from apoptosing, as previously found for High Five and S2 cells [178]. Our results indicated that PTP-H2 had precisely this effect (Figure 3.4c). Since the antiphagocytic activity of PTP-H2 depends on an intact catalytic core and associated phosphatase activity [178], we also assessed whether the phosphatase inactive mutant PTPH2C^{236A} lacked apoptosis-inducing activity. Unlike wild-type PTP-H2, pIZT/PTP-H2^{C236A} had no apoptotic activity in Sf-21 cells (Figure 3.4d).

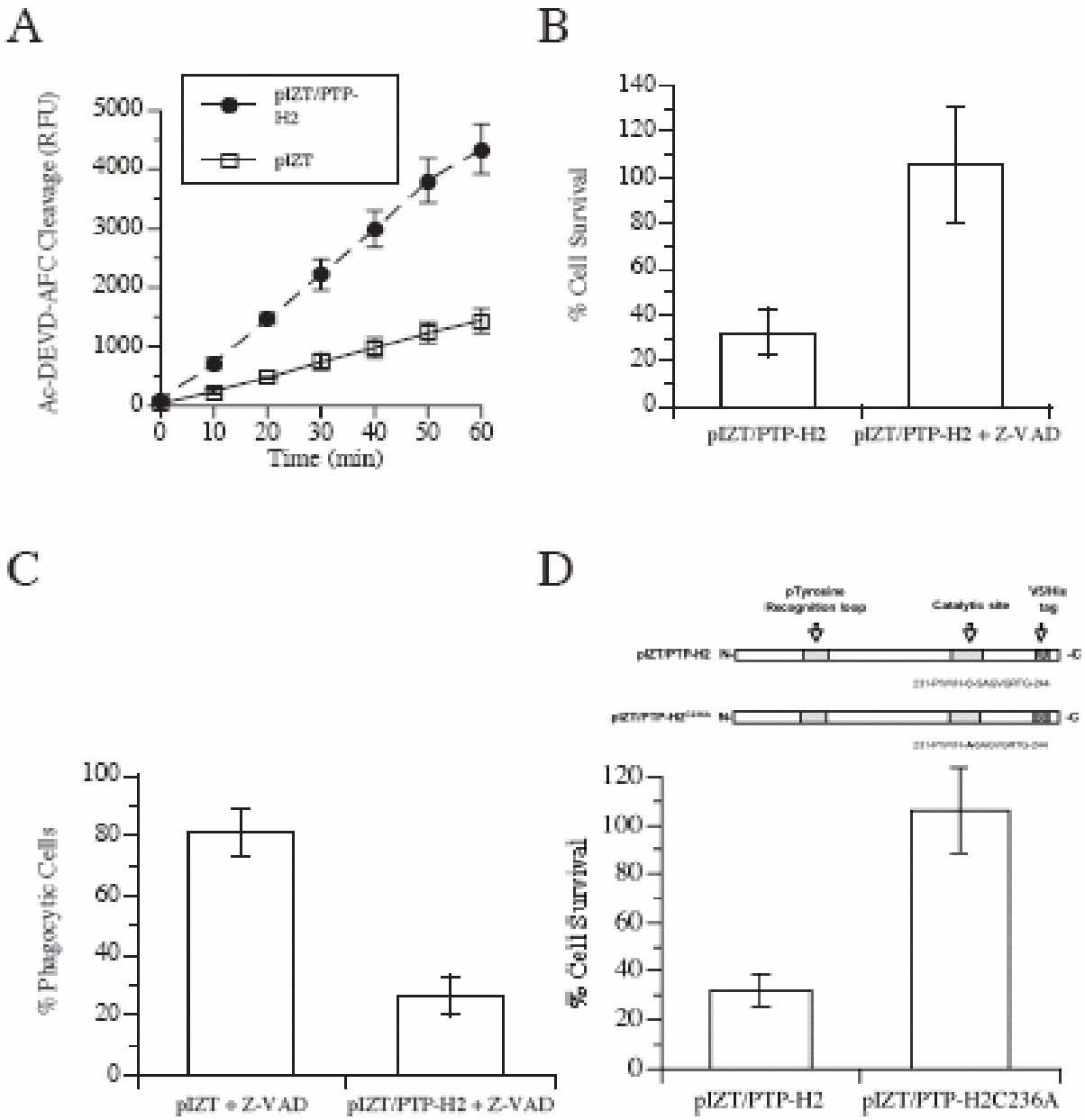


Figure 3.4. PTP-H2 mediated cell death induces caspase activation and requires phosphatase activity. Sf-21 cells were transiently transfected with 2 μ g pIZT/PTP-H2 or pIZT empty vector per ml of medium. A. Caspase activity in lysates prepared from cells 20 h post-transfection. Cleavage of the synthetic caspase substrate Ac-DEVD-AFC was greater in lysates from cells expressing PTP-H2 than from pIZT control cells. B. Mean percentage (\pm SD) cell survival 20 h

post-transfection with pIZT/PTP-H2 when the pan caspase inhibitor Z-VAD-FMK was present or absent. Cell survival was significantly higher in the presence or absence of Z-VAD-FMK ($t = 5.3, p = 0.006, n = 4$ replicates per treatment). C. Mean percentage (\pm SD) of cells that phagocytose *E. coli* 36 h post-transfection with pIZT empty vector or pIZT/PTP-H2. Cells for each treatment were maintained in the presence of Z-VAD-FMK following transfection. Significantly fewer cells expressing PTP-H2 phagocytosed bacteria compared to the empty vector control ($t = 7.6, p = 0.001, n = 4$ replicates per treatment). D. Mean percentage survival (\pm SD) of cells 20 h post-transfection with pIZT/PTP-H2 or pIZT/PTP-H2^{C236A}. Survival was significantly lower in cells expressing wild-type PTP-H2 than the catalytically inactive mutant protein ($t = 9.0, p < 0.0008, n = 4$ independent replicates per treatment). Schematics illustrating the primary structure of PTP-H2 and PTP-H2^{C236A} are illustrated above the figure.

3.3.4 PTP-H2 expression arrests cell proliferation

In addition to disrupting phagocytosis, MdBV also disrupts the ability of immune cells to bind to foreign surfaces which effectively disables the ability of infected hemocytes to bind and encapsulate large foreign targets like parasitoid eggs or to internalize small foreign targets like bacteria [57, 139, 147]. We thus considered the possibility that PTP-H2-mediated apoptosis of Sf-21 cells could potentially involve alterations in adhesion since this triggers apoptosis in some mammalian cells through a response called anoikis [187]. Like many insect cells [144, 168], Sf-21 cells are unable to bind or spread on the surface of culture plates coated with agarose. Sf-21 cells transfected with pIZT/PTP-H2 in agarose coated wells underwent the same high level of apoptosis as cells on non-coated plates, yet cells transfected with empty vector exhibited no

increase in apoptosis (Figure 3.5a). This result suggested that simple loss of adhesion was insufficient to induce Sf-21 cell death. Another factor associated with apoptosis, however, is proliferation and cell cycle arrest. To assess whether PTP-H2 affected proliferation, we compared the growth of Sf-21 cells maintained in the presence of Z-VAD-FMK following transfection with pIZT/PTP-H2 or empty vector to mock control cells transfected with the empty vector but maintained in medium lacking caspase inhibitor. Our repeated measures analysis revealed a significant interaction between treatment and time indicating that cells expressing PTP-H2 proliferated significantly less over the six day assay period than cells transfected with the empty vector (Figure 3.5b). Empty vector and mock treated cells increased from an average of 5.0×10^3 cells per well to more than 40.0×10^4 cells per well over 6 days, whereas cells expressing PTP-H2 increased from 5.0×10^3 cells per well to only 8.7×10^3 cells per well during the same period (Figure 3.5b). As expected in a transient expression assay, PTP-H2 expression thereafter declined, as monitored by the GFP marker in the pIZT vector. Concurrent with this decline, cell proliferation increased to similar levels to those transfected with the empty vector and mock transfected controls (data not shown).

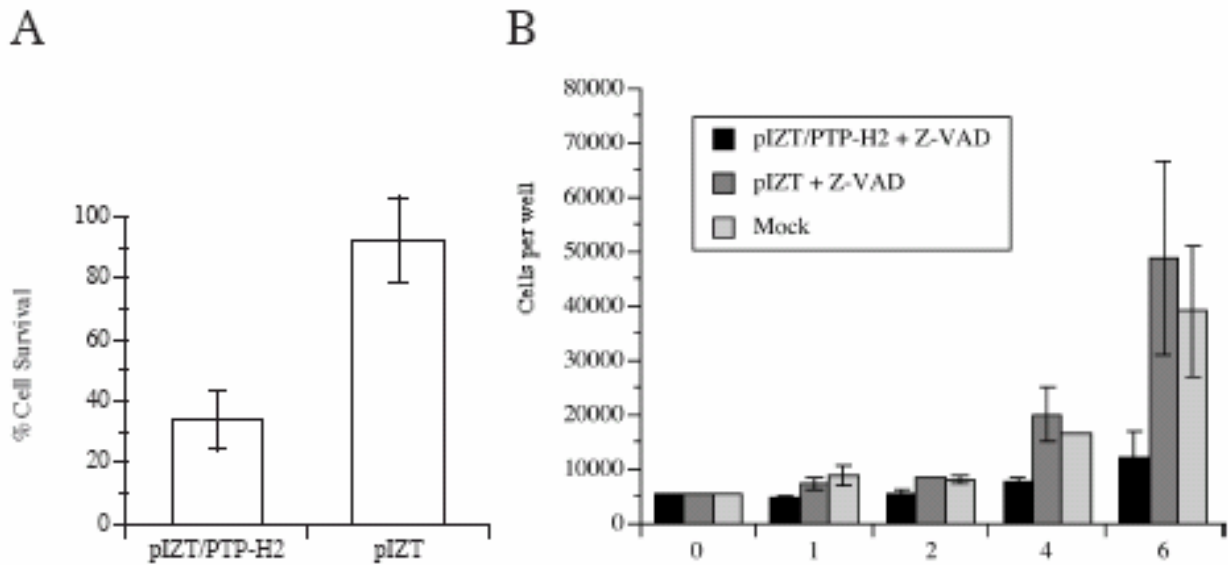


Figure 3.5. Apoptosis of Sf-21 cells is unaffected by culture on agarose-coated plates but PTP-H2 expression reduces cell proliferation. Sf-21 cells were transiently transfected with 2 μ g pIZT/PTP-H2 or pIZT empty vector per ml of medium. A. mean percentage survival of Sf-21 cells cultured on agarose coated plates. Most cells transfected with the empty vector survive despite being unable to adhere to the plate's surface, whereas cells expressing PTP-H2 apoptose ($t = 8.3$, $p = 0.001$, $n = 4$ replicates per treatment). B. Proliferation of cells transfected with pIZT/PTP-H2 or pIZT empty and maintained in the presence of Z-VAD-FMK compared to cells transfected with pIZT and maintained in medium without ZVAD-FMK (mock). Repeated measures analysis indicated a significant interaction between day and treatment ($F = 3.1$, $df = 8$ $p = 0.04$) with cells expressing PTP-H2 proliferating less than the control treatments.

3.4 Discussion

We determined previously that MdBV suppresses several components of the cellular and humoral immune response of host insects and that these immunosuppressive activities are essential for the survival of its associated parasitoid wasp [57, 61, 62, 140, 178, 180]. In the study described in this chapter we took advantage of the Sf-21 cell line, which is well known to undergo apoptosis in response to different stimuli [182], to conduct a screen for candidate apoptosis-inducing genes. Our results identified only one gene, *ptp*-H2, that induced apoptosis, suggesting that apoptosis in Sf-21 cells is not a generalized response to infection by MdBV or viral transcriptional activity. It is also unlikely apoptotic activity is due to overexpression of PTP-H2 in Sf-21 cells given that: 1) granulocytes and Sf-21 cells exhibit a similar response following natural infection and 2) real time PCR analyses indicating that PTP-H2 transcript abundance is actually higher in MdBV-infected hemocytes than in Sf-21 cells transfected with pIZT/PTP-H2 (A. Pruijssers and M. R. Strand, unpublished results).

In mammalian cells, terminal caspases are activated by either the extrinsic pathway that requires death receptors, like the tumor necrosis factor (TNF) receptor, or the intrinsic pathway that involves mitochondrial disruption and release of factors like cytochrome c which stimulate caspase activation [188, 189]. In insects, an extrinsic pathway involving the TNF- α superfamily member Eiger and receptor Wengen has been described from *Drosophila* that stimulates apoptosis through the c-Jun Nterminal kinase (JNK) pathway. An intrinsic apoptotic pathway requiring RHG family proteins like Rpr, Hid, and Grim that promote mitochondrial disruption and terminal caspase activation is also reported [190-192]. Rescue from the apoptotic effects of PTP-H2 by Z-VADFMK combined with high levels of JC-1 monomer fluorescence (green) implicate caspase activation and loss of mitochondrial membrane potential in PTP-H2 induced

apoptosis. Our results with the mutant PTP-H2^{C236A} combined with prior studies [178] further suggest that PTP-H2 associated phosphatase activity is required for both the apoptotic and anti-phagocytic functions of this protein. Recent studies in a related bracovirus, CpBV, also implicate PTPs in disabling haemocyte function [129], while studies in *Toxoneuron nigriceps* bracovirus (TnBV) suggest that other bracovirus gene products induce caspase activation without causing apoptosis [19].

We previously reported that PTP-H2 inhibits phagocytosis by hemocyte-like High Five and S2 cells as well as by primary immune cells like granulocytes and plasmatocytes in caterpillar hosts [57, 61, 178]. Unlike Sf-21 cells and granulocytes [177], however, PTP-H2 does not induce apoptosis of these cell types. This finding suggests that the anti-phagocytic activity of PTP-H2 extends across a diversity of insect cell backgrounds but its apoptosis-inducing activity is restricted and must depend in part on intrinsic differences between cell types. Analogously, TN-368 cells, which served as the parental cell line for developing High Five cells, are similarly resistant to a variety of apoptotic stimuli including baculoviruses deficient in the apoptotic inhibitor P35 [183, 193]. With diverse pathways regulating apoptosis in insect and mammalian cells, it is currently, to our knowledge, not known why PTP-H2 and other apoptotic stimuli trigger apoptosis in one cell type but not another. Intriguingly though, studies with both Sf-21 and S2 cells implicate depletion of inhibitor of apoptosis proteins (IAP) in caspase activation [194, 195]. This suggests the possibility that the differential apoptotic response of Sf-21 and S2 cells to PTP-H2 could reflect differences between these cell types in IAP abundance or a differential effect of PTP-H2 on IAP depletion.

Given the anti-adhesive and antiphagocytic activities of MdBV, we initially hypothesized that PTP-H2-mediated apoptosis of Sf-21 cells could reflect a form of anoikis [187]. However,

Sf-21 cells cultured on nonadhesive surfaces like agarose do not undergo apoptosis in the absence of PTP-H2 expression suggesting loss of adhesion alone is insufficient to induce an apoptotic response. Similar to hemocytes, expression of the MdBV virulence gene *gcl1.8* also causes 30-50 % of Sf-21 cells to detach 20 h post-transfection (R. J. Suderman, A. J. Pruijssers and M. R. Strand, unpublished results) but this gene product had no apoptotic inducing activity (see Figure 3.2). In contrast, our results do indicate that PTP-H2 significantly reduces proliferation when Sf-21 cells are maintained in the presence of Z-VAD-FMK. It is well known that perturbations in the cell cycle can trigger apoptosis and that several caspases involved in apoptosis also function as cell cycle regulators. This includes effector caspases like caspase 3 that inhibits proliferation of certain mammalian cell types [192, 196, 197]. Thus, while the presence of a caspase inhibitor could itself affect cell proliferation, our results indicate this is not the case, since Sf-21 cells transfected with the empty vector and maintained in Z-VAD-FMK proliferated similarly to cells maintained in the absence of caspase inhibitor. Take together, these results suggest that PTP-H2 may induce apoptosis by directly or indirectly perturbing the cell cycle.

PTP-H2 is a classical PTP whose closest homologues include PTPs encoded by other PDVs and cytosolic PTPs from mammals like PTP1B [178]. Although, to our knowledge, no studies in insects implicate PTPs in apoptosis, several phosphatases including PTP1B have been shown to regulate apoptosis of mammalian cells [198-200]. We also note interesting parallels between PTP-H2, the classical, cytosolic phosphatase YopH from the bacterium *Yersinia pestis* and PTP-PEST from the mouse that each induce apoptosis of certain cells while also localizing to focal adhesions and disrupting functions like phagocytosis and cell division that require the actin cytoskeleton [178, 201, 202]. Similar to *Yersinia* sp., PDVs appear to have acquired and

co-opted PTPs from their hosts for use as immunosuppressive virulence factors, while PTP1B and PTP-PEST function as endogenous regulators of related functions.

Our results to date collectively indicate that MdBV encodes a diverse repertoire of virulence factors that synergistically interact to disable host immune defenses. Elimination of granulocytes by apoptosis is likely also a benefit to the parasitoid because of the essential role these cells play in non-self recognition, capsule formation, and the production of different effector molecules [26]. However, apoptosis has also been suggested to function as an antiviral defense by hosts by eliminating infected cells that serve as sites for viral replication. Given the absence of replication by MdBV in the wasp's host, the observation that only certain host cells infected by MdBV apoptose, and that a single viral gene triggered cell death of Sf-21 cells, our results overall favor the hypothesis that MdBV induces apoptosis as part of a larger strategy to disable the host immune system and facilitate successful development of its associated wasp.

CHAPTER 4
THE EFFECT OF VIRAL INFECTION ON HOST GROWTH, METABOLISM AND
DEVELOPMENT

In collaboration with Patrizia Falabella

4.1 Introduction

As discussed in Chapter 1, parasitism by PDV carrying wasps causes changes in the development of hosts that are strongly linked to viral gene expression. These changes are often correlated with alterations in both endocrine and metabolic physiology. Endocrine changes include a increased JH titer and suppression of the ecdysteroid titer, whereas the metabolic alterations include changes in the abundance of hemolymph proteins, free amino acid and carbohydrates. *Microplitis demolitor* successfully parasitizes *P. includens* larvae from the second through the fifth (last) instar [203]. Larvae that are parasitized prior to the last instar exhibit delays in weight gain, undergo larval-larval molts at suboptimal threshold sizes, and fail to pupate. Larvae that are parasitized in the last larval instar prior to critical period stop gaining weight and also never pupate [59, 203].

Few studies have characterized alterations in endocrine and metabolic physiology in *P. includens* larvae following infection by MdBV. One study reports that parasitism of fifth instar *P. includens* larvae causes a 20-fold increase in JH titer that is correlated with a marked decrease in the activity of JH-esterase (JHE) [46]. Although an elevation in JH level could contribute to a

developmental delay, the observation that larvae injected with calyx fluid and venom alone displayed only a small increase in JH titer while still exhibiting delays in growth, development and inhibition of pupation suggested that an increased JH titer was not solely responsible for the juvenilizing effect caused by parasitism [46]. The lack of a phenotype in larvae injected with calyx fluid that was treated with the virus inactivating compound trioxalen provided further evidence for the crucial role of transcriptionally active MdBV in the delay in growth and developmental arrest observed in parasitism [59].

Considering the importance of PTPs in the regulation of physiological processes regulating growth and developmental processes, MdBV encoded PTPs are obvious candidates for mediating both endocrine and metabolic alterations observed following viral infection. However, before any virulence factors can be linked to these effects we need to gain a better understanding of the physiological alterations that occur following viral infection. To this end, we took steps to characterize endocrine and metabolic changes in the infected host.

The key hormone that regulates molting and metamorphosis in insects is called ecdysone. Ecdysone is produced by the prothoracic glands (PGs) in response to hormones produced by the brain, including insulin-like hormones such as PTHH (reviewed in [107]). *In vivo*, ecdysteroid production is inhibited by binding of prothoracicostatic peptides to their receptors in the PGs. Two prothoracicostatic peptides have been identified from *B. mori*, *BomPTSP* and *Bommo-myosuppressin*. The latter peptide is expressed by the medial neurosecretory cells [204].

We hypothesized that the inability of MdBV infected larvae to pupate could be due to an alteration in the production of ecdysteroidogenic or prothoracicostatic hormones from the brain, an inhibition of the PGs to produce ecdysone in response to ecdysteroidogenic stimuli, or an insensitivity of ecdysone responsive tissues. The latter possibility can however be dismissed

because previous observations have indicated MdBV infected fifth instar larvae are able to pupate after the injection of 20-hydroxy ecdysone. Furthermore, the inability of infected larvae to gain weight suggests that viral infection causes a change in nutrient metabolism. We therefore hypothesized that MdBV infection induces a mobilization of nutrient storage or inhibits the assimilation and storage of nutrients.

The results reported in this chapter provide evidence that PGs of MdBV infected *P. includens* larvae produce reduced amounts of ecdysteroids compared to PGs of uninfected larvae. Furthermore, brain extracts from infected larvae are unable to stimulate ecdysteroid production by glands from uninfected larvae. In addition, MdBV infected larvae contained decreased glycogen stores in the fat body and increased hemolymph carbohydrate levels compared to uninfected larvae. Together, these results explain why MdBV infected *P. includens* larvae exhibit a delay in growth and developmental arrest.

4.2 Materials and methods

4.2.1 Rearing

P. includens larvae were reared as described in Chapter 2. For metabolic experiments, larvae were reared one individual per cup and molting time was recorded.

4.2.2 Virus collection and injection into larvae

Virus was collected as described in paragraph 3.2.2. At 32 h post ecdysis into the fifth instar, larvae were anesthetized on ice and injected with 2 μ l of 0.1 wasp equivalent calyx fluid in Grace's medium (Sigma) or 2 μ l Grace's medium alone.

4.2.3 Determination of weight gain and food uptake

At 24 and 48 h post injection, larva, diet and wet weight of frass were weighed using a Galaxy analytical scale. Evaporation of diet was estimated by subtracting the weight of diet, frass and larva from the total weight of diet, frass and larva at the start of the experiment. Food uptake was calculated as a function of diet weight loss and larval weight gain minus frass production and evaporation.

4.2.4 Plasma and fat body sampling and preparation

Hemolymph and fat body samples were obtained at 24 and 48 h post injection, and are represented as the 32, 56, and 80 h time points.

4.2.4.1 Plasma preparation

Hemolymph was collected from larvae by bleeding from a cut proleg and transferred with a pipette to an equal amount of anticoagulant. Samples were gently centrifuged for 2 min. at 800 x g to pellet the hemocytes. Supernatants were transferred to a fresh tube and centrifuged for 15

min. at 14,000 rpm to remove other debris and stored at -80°C until use. Twelve µl of plasma was added to 48 µl ddH₂O and boiled for 5 min. After centrifugation for 5 min at 14,000 rpm, supernatant was added to 10-20 mixed bed resin beads (Sigma) and incubated for 30 min. at 4°C under continuous agitation. Prepared plasma samples were transferred to a clean tube and stored at -80°C until use.

4.2.4.2 Fat body sample preparation

Fat body was dissected in PBS, transferred to a pre-weighed tube and covered with 95% ethanol. Samples were dried under vacuum and dry weight was determined. Tissue was homogenized with a motor-driven pestel in 200 µl of 0.3 M perchloric acid. Samples were assayed immediately or stored at -80°C until use.

4.2.5 Carbohydrate measurements

For free sugar measurements, trehalose was digested to glucose by adding 50 µl of a 1:20 dilution of trehalase (Sigma) in PBS to 2.5- 5 µl prepared plasma sample. PBS was added to a total volume of 100µl. Total glucose was measured by adding 200 µl of glucose oxidase/ peroxidase reagent (Sigma)/ TMB (0.25µg/ml in DMSO) followed by 10 min. incubation at RT. Samples were transferred to a Costar 96 well plate and read at A450. Glycogen was digested into glucose by adding 5 µl of 2 mg/ml amyloglucosidase (AG)(Fluka Biochemika) to 10 µl homogenate and 85µl of 100 mM sodium acetate buffer (pH 5.0), incubated at 37°C for 3 h., and measured using the glucose oxidase method. Sample (10 µl) without AG was used as a control

to correct for glucose in fat body. Means represent at least 5 larvae per treatment condition and time point.

4.2.6 Ecdysteroid biosynthesis in vitro

Larvae were anesthetized in water for 10 min before dissection. Prothoracic glands were dissected in PBS and preincubated in a drop of Grace's insect medium for at least 20 min and at most 1 h to eliminate ecdysteroid production induced by manipulation. For stimulation, glands were incubated in 25 μ l drops of medium in the presence or absence of a stimulator for 3 h at 27°C. For the preparation of brain extract, 10 heads from larvae in the late feeding stage and 10 heads from larvae in the early wandering stage were washed three times with 1 ml of Grace's medium, homogenized on ice in 100 μ l Grace's medium, boiled, and centrifuged for 5 min. at 14000 rpm. Dibutyryl cyclic AMP (dbcAMP) was dissolved in Grace's medium and diluted to create a 10 mM working solution. After incubation, samples were collected and stored at -80°C until use.

4.2.7 Radioimmunoassay (RIA)

Ecdysteroids were quantified by radioimmunoassay as described by Sieglaff *et. al.* [152]. Each assay sample contained 5-10 μ l sample. The anti-ecdysteroid rabbit serum (AS 4919, a generous gift from P. Poncheron, Université P. et M. Curie, Paris, France) was diluted to 1:25,000–1:35,000. Sample values reported for each treatment represent the means of three to five replicates. Because component(s) of brain extract cross react with the anti-ecdysteroid

serum, we ran appropriate dilutions of brain extract as controls and subtracted the control values from the sample values obtained from brain extract stimulated PGs.

4.2.8 Data analysis

Data were analyzed using the General Linear Model and JMP software.

4.3 Results

4.3.1 *P. includens* prothoracic glands become sensitive to stimulation at 50h post ecdysis

Based on our observation that MdBV infection causes developmental arrest in last instar *P. includens* larvae, we hypothesized that MdBV-mediated inhibition of pupation is due to a change in ecdysone production by the PGs or disrupted signaling from the brain. According to the literature, the ability of last instar *B. mori* PGs to produce ecdysteroids depends on the age of the larva. Gu *et. al.* (1996)[205] reported that *B. mori* PGs are refractory to stimulation up to five days post-ecdysis into the last instar, whereas at day six, PGs produce elevated levels of ecdysone in response to either synthetic activators, crude brain extract or partially purified PTTH. To determine when in the last instar the PGs of *P. includens* become responsive, PGs were dissected at 1, 8, 28, 34, 50 and 60 hours post ecdysis and stimulated for 3 hours with 10 mM dbcAMP in Grace's medium. Grace's medium without dbcAMP served as the negative control. *P. includens* PGs produce low levels of ecdysteroids up to 34h post ecdysis (Figure 4.1). Addition of a synthetic stimulator to the medium increased ecdysteroid production, however a

much larger increase in production was detected from glands dissected from larvae at 50 h post ecdysis. The release of endogenous stimuli by the brain and the corresponding production and release of ecdysone by the PGs triggers lepidopteran larvae to purge their guts and initiate metamorphosis, a stage referred to as early wandering. The high ecdysone levels produced in the absence of dbcAMP from PGs dissected at 60 h post ecdysis can be explained by the observation that larvae from this group had entered the early wandering stage. In summary, our results indicate that similar to *B. mori* PGs, *P. includens* PGs do not produce elevated levels of ecdysteroids in response to a stimulus until the late feeding stage, approximately 50h post ecdysis. This means that experiments towards determining if MdBV infection affects hormone stimulated ecdysteroid production should be performed between 50 and 60h post ecdysis.

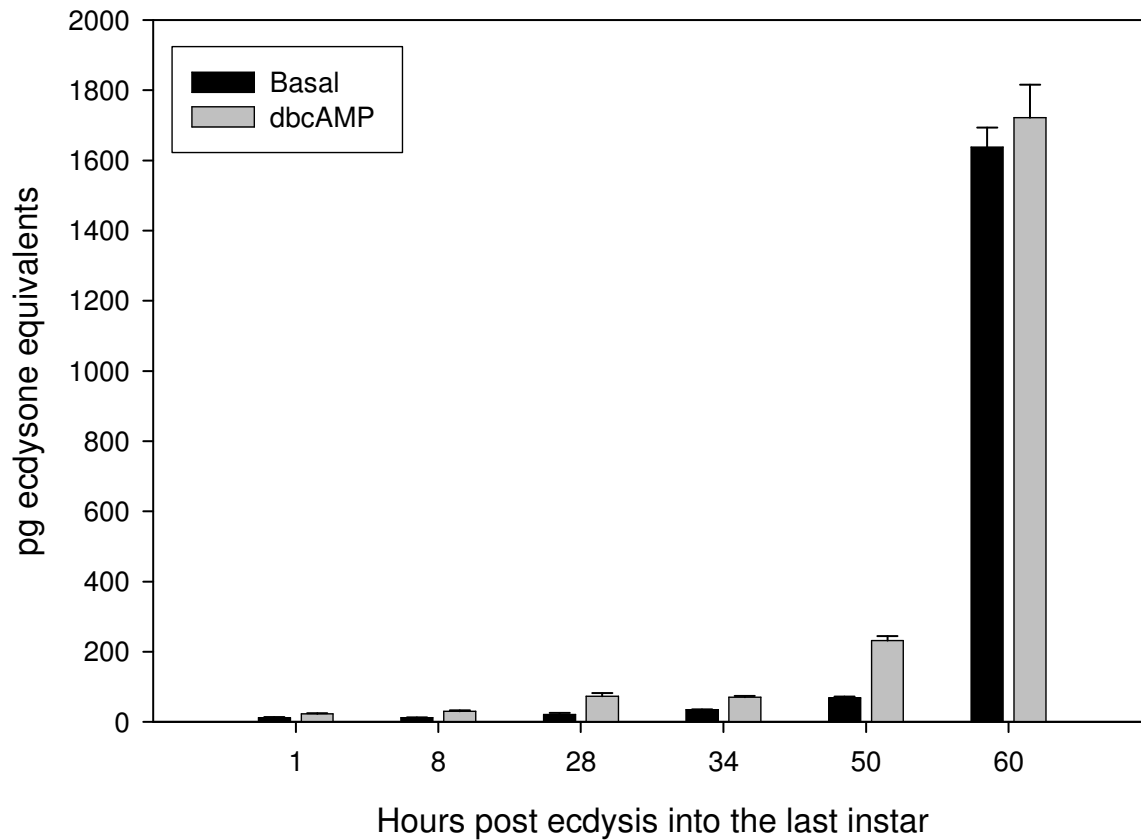


Figure 4.1. Ecdysteroid production by *P. includens* PGs during the fifth instar. Black bars represent the average amount of ecdysone equivalents detected per PG \pm the standard error in the absence of a stimulator (basal condition). Grey bars represent the average amount of ecdysone equivalents produced per PG \pm the standard error in the presence of 10 mM dbcAMP. A significant increase in dbcAMP stimulated ecdysteroid production was detected in glands dissected from larvae at 50h compared to glands dissected from larvae at 34h post-ecdysis (t-test: $t= 6.37$, $p= 0.00008$, $n \geq 7$ PGs from different larvae).

4.3.2 PGs from MdBV infected larvae are unresponsive to stimulation

To test if MdBV infection affects ecdysteroid biosynthesis in last instar larvae, larvae were injected with a physiological dose of calyx fluid in Grace's insect medium. Eighteen hours later, at 50h post ecdysis, PGs were dissected from both infected and uninfected larvae and incubated in a drop of Grace's medium in the presence or absence of 10 mM dbcAMP, followed by analysis of ecdysteroid production by RIA. Our results indicated that PGs from uninfected larvae produced significantly increased amounts of ecdysteroid in response to dbcAMP, but PGs from infected larvae did not (Figure 4.2). We repeated our assay and used crude brain extract (BE) as the inducing stimulus. PGs from uninfected larvae produced significantly more ecdysteroids in response to this stimulus than infected PGs (Figure 4.2). We also noted that the amount of ecdysteroid produced by PGs from infected larvae in the basal (non-stimulated) condition was significantly lower than the basal amount of ecdysteroids produced by glands from mock infected larvae (Figure 4.2). Together, these results indicated that MdBV infection has an inhibitory effect on ecdysteroid production by PGs as early as 18h post infection. Furthermore, MdBV infection reduced both the amount of ecdysteroid produced in the basal condition and in the presence of dbcAMP or BE.

We next asked if inhibition occurred only at the level of gland function, or if the levels of endogenous stimulatory factors in brain extract were affected by infection as well. To this end, we tested the ability of brain extract from infected larvae to stimulate uninfected 50 h old PGs. Interestingly, we did not detect an increase in ecdysteroid production in response to brain extract from infected larvae (Figure 4.2). This result suggested that one or more ecdysteroidogenic factors such as PTTH and insulin-like peptides present in the uninfected larval brain were absent or present in reduced quantities in brains from infected larvae, or that infected

brains contain increased quantities of prothoracicostatic peptides that inhibit PG activation. Taken together, our results suggest that MdBV infection inhibits pupation at two levels: 1) by affecting ecdysteroid production by the PGs and 2) by altering the ecdysteroidogenic activity of brain extract.

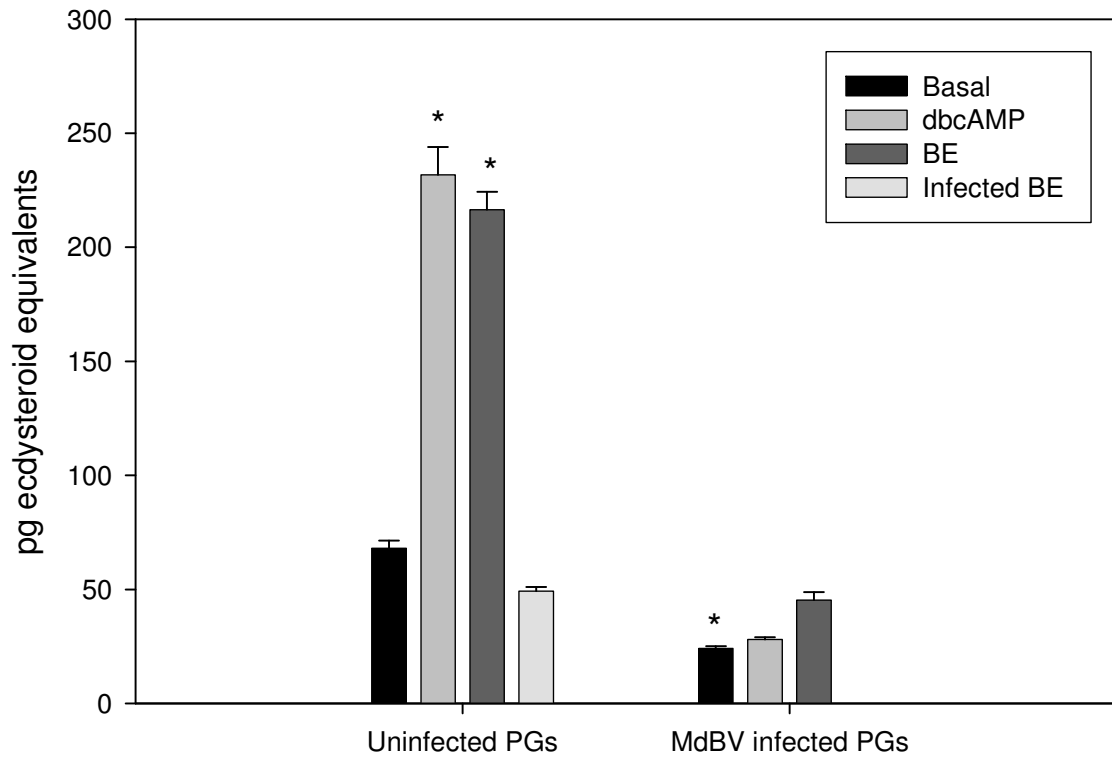


Figure 4.2. Effect of MdBV infection on ecdysteroid production by *P. includens* PGs. Average amounts of ecdysteroids produced per gland \pm the standard error were compared to the basal (non-stimulated) amount of ecdysteroids produced by glands from mock infected control larvae. An asterisk (*) indicates that a given treatment resulted in a significant difference in ecdysteroid production using the Student Newman Keuls (SNK) Multiple Comparison Procedure (overall

model $F_{6, 41} = 47.6$; $P < 0.0001$). Glands from mock infected larvae produced significantly increased amounts of ecdysteroids in response to both dbcAMP and BE, whereas glands from MdBV infected larvae did not. Glands from mock infected larvae did not significantly increase ecdysteroid production in response to stimulation with brain extract from infected larvae. Furthermore, the amount of ecdysteroids produced by glands in the basal condition from infected larvae was significantly lower than the basal amount of ecdysteroids produced by mock injected larvae.

4.3.3 MdBV infection alters host sugar metabolism

Based on the preceding results we further hypothesized that the inability of virus-infected larvae to gain weight could reflect alterations in nutrient mobilization given recent studies showing that, similar to mammals, insulin-like hormones from the insect brain regulate carbohydrate metabolism [206]. To this end, we compared levels of stored versus circulating sugars in MdBV infected and uninfected larvae. Fifth instar *P. includens* larvae were infected with a physiological dose of virus in Grace's or with Grace's medium alone (mock infected control). Hemolymph and fat body samples were collected at three time points post injection, and free sugars in cell-free plasma and glycogen in the fat body were quantified using enzymatic assays. The results indicated that the concentration of free sugar in the plasma and glycogen in the fat body did not change significantly ($P < 0.05$) over time in mock injected larvae (Figure 4.3). MdBV infected larvae, on the other hand, exhibited a significant increase in concentration of free sugar in plasma and a significant decrease in glycogen in the fat body over time. At 24 h post injection with MdBV, the fat body glycogen level dropped roughly two fold, whereas

plasma sugar levels doubled compared to the mock injected control. The fat body glycogen level displayed an additional decrease by 48 h post infection that was not significant ($P < 0.05$) but coincided with an additional increase in the plasma free sugar concentration. Together, these results suggested MdBV infection causes a mobilization of sugars from the fat body stores to the hemolymph.

Simultaneous with the metabolic changes (Figure 4.3), I observed a very strong time versus treatment effect in weight gain in MdBV infected larvae (Figure 4.4a; previously reported in [59]). MdBV infected larvae stopped gaining weight whereas mock injected larvae gained tremendous weight. The reduction in weight gain in MdBV was accompanied by a dramatic decrease in food uptake (Figure 4.4b). I therefore asked if the metabolic shift observed following viral infection is similar to one induced by starvation. Analysis of hemolymph and fat body samples from mock injected and starved larvae suggests that 24h of starvation induced changes in free sugar and glycogen levels that were similar to those observed at 24h post injection with MdBV. Starvation also induced an additional decrease glycogen stores at 48 h after start of the treatment, but this decrease was not accompanied by an increase in plasma sugar concentration (Figure 4.3).

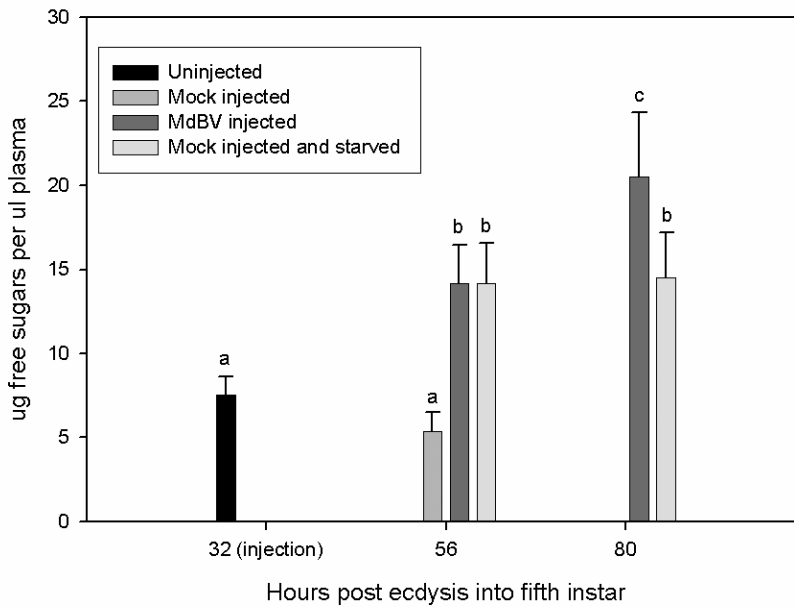
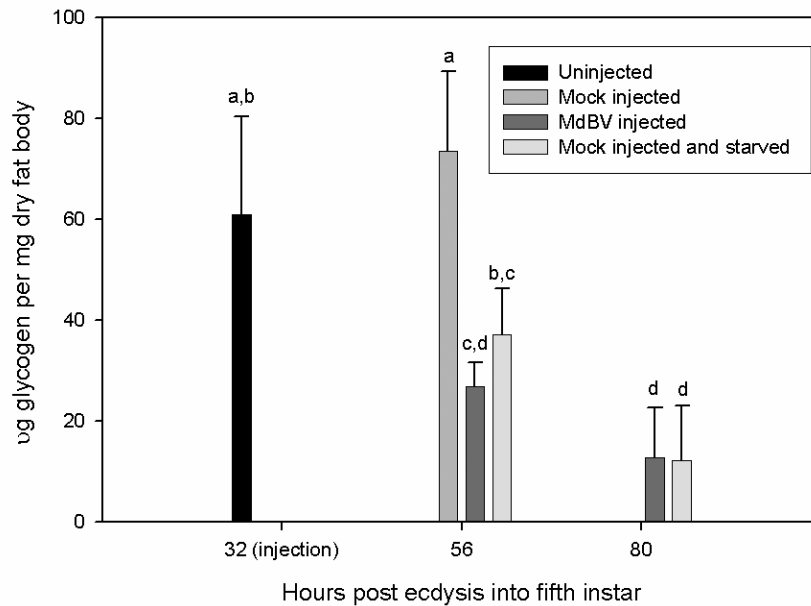
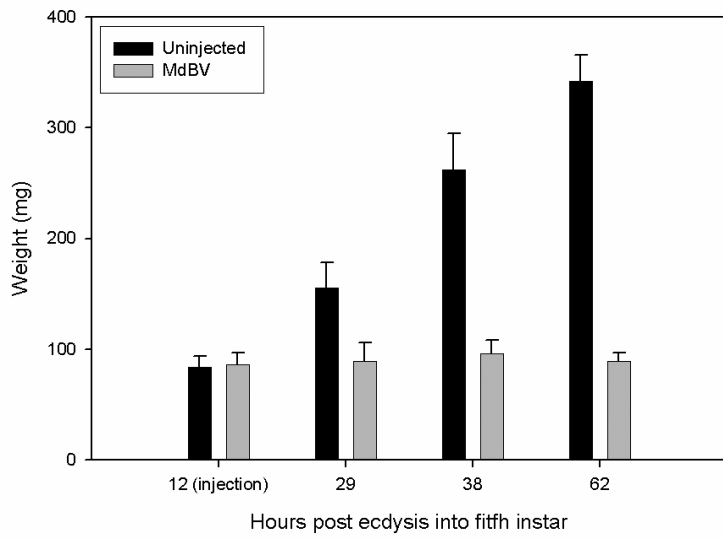
A**B**

Figure 4.3. MdBV infection alters host carbohydrate metabolism. A. Average \pm the standard deviation concentration of free sugars in plasma increased significantly over time in both MdBV infected and starved larvae compared to mock injected larvae (overall model $F_{5,21} = 25.7$; $P < 0.0001$, $n=3$ replicates per treatment). B. Average \pm the standard deviation glycogen

concentration decreased significantly in both MdBV infected and starved larvae compared to mock injected controls (overall model $F_{5, 24} = 18.7$; $P < 0.0001$, $n=4$ replicates per treatment). Averages with the same letter are not significantly different ($P < 0.05$) by the Tukey-Kramer multiple comparison method.

A



B

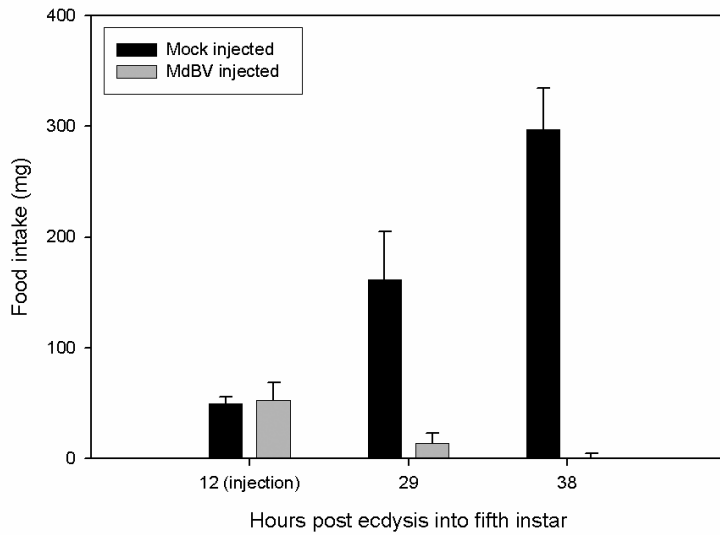


Figure 4.4. MdBV infection causes an inhibition of weight gain and a loss of appetite. A. Average \pm the standard deviation weight gain (treatment * time F= 25.60 P <0.0005, n= 3 replicates). B. Average \pm the standard deviation food uptake (treatment * time F= 15.51 P <0.0028, n= 3 replicates).

4.4 Discussion

In this study, we analyzed the metabolic and hormonal alterations associated with MdBV infected *P. includens*. The results of our metabolic studies suggest that infection of fifth instar larvae with MdBV induced mobilization of glycogen stores from the fat body, leading to a decrease in glycogen in the fat body and an increase in the concentration of free sugars in the plasma over time. The mobilization of sugar reserves coincided with a strong reduction in the uptake of food. Although MdBV infected larvae continued to have access to food, the MdBV induced alterations in carbohydrate metabolism were very similar to those observed in starved larvae. This suggests that the mobilization of sugar reserves was at least initially due MdBV infection. The loss of appetite is therefore likely to be an effect of the hyperglycemic state and could possibly have contributed to the continued mobilization of glycogen stores over time.

The results of our endocrine studies suggest that MdBV infection inhibits the production of ecdysteroids by the PGs, both by inhibiting PG function and by altering the ecdysteroidogenic capacity of the brain. An inhibition of PG activity has also been observed in other host-parasitoid systems such as *Heliothis virescens* parasitized by *Toxoneurin nigriceps*, and also coincide with developmental arrest of this host [207, 208]. Studies with *Manduca sexta* PGs have shown that PTH-activated ecdysteroid production pathway depends on the multiple

tyrosine phosphorylation events [209]. Expression of viral PTP could potentially downregulate hormone induced ecdysteroid synthesis by the PGs. We detected low levels of several PTP-gene transcripts in PGs of infected larvae (data not shown). Studies with TnBV have previously suggested a role for viral PTPs in the inhibition of *H. virescens* prothoracic gland function [210]. Like in our system, *H. virescens* pupation is inhibited after parasitism and infection of the PGs by transcriptionally active TnBV reduced biosynthetic activity of these glands [211]. The authors observed a reduction in overall cellular phosphorylation levels in infected PGs that progressed over time [210]. One TnBV PTP transcript (PTP-7) could be detected in infected *H. virescens* PGs [212]. Direct evidence illustrating the role of viral PTPs in this process has however not been generated. Moreover, considering that TnBV infected glands undergo non-apoptotic cell death at 120 hours post parasitism [210], the reduction of overall phosphorylation levels could potentially be an indicator of cellular decay.

Another interesting result was the inability of brain extract from infected larvae to stimulate uninfected PGs *in vitro*. This suggests that brain extract from infected larvae lacks or contains reduced quantities of PTTH or insulin-like peptides [213, 214] compared to brain extract from uninfected larvae, or brain extract from infected larvae contains an increased concentration of inhibitory factors such as prothoracicostatic peptides [204, 215, 216]. The production and release of PTTH is under controlled by several factors including photoperiod, time of day and physiological factors such as the nutritional state of the animal [217]. It is possible that the virus induced alteration of nutritional state delays the synthesis of ecdysteroidogenic components in the brain. Alternatively, the detection of MdBV gene transcripts in nervous tissue [62, 178] advocates the possibility that virulence factors modulate the production of peptides by the brain.

A growing body of evidence suggests that the signaling pathways regulating growth and developmental processes are interlinked. Studies with *M. sexta* and *Drosophila melanogaster* have generated a detailed understanding of the importance of larval weight in the initiation of molting and metamorphosis. For metamorphosis to be initiated, larvae need to obtain a species-specific critical weight. [218-220]. How the larva determines critical weight remains unclear. Mirth *et. al.* [111] proposed that in *D. melanogaster*, the PGs function as a central tissue that senses the nutritional status of the larva based on its own cell size and integrates this information for correct timing of metamorphosis. By using dominant negative mutations, the authors were able to block the insulin signaling pathway in a PG-specific manner and reduce PG cell growth, leading to a delay metamorphosis and larger than average adult flies. In contrast, acceleration of PG cell growth through PG-specific overexpression of Ras induced premature metamorphosis and smaller than average adult flies [112]. These studies illustrated that the nutritional status in general and the activity of the insulin signaling pathway in particular have a direct effect on the activity of the PGs. Our combined observation that PGs from MdBV infected larvae produce reduced amount of ecdysteroid and that MdBV infection causes a mobilization of stored sugars to the hemolymph points towards a downregulation of the host insulin signaling. MdBV gene products could accomplish this by reducing tissue responsiveness, reducing the production and release of insulin-like hormones in the brain, or both. An interesting avenue for future studies would be to determine which host signaling pathway(s) are directly interfered with by viral factors, and to identify the viral genes responsible.

REFERENCES

1. Whitfield, J.B., *Phylogeny of microgastroid braconid wasps, and what it tells us about polydnavirus evolution*, in *The Hymenoptera: Evolution, Biodiversity and Biological Control*, A.D. Austin, Dowton, M., Editor. 2000, CSIRO Publishing: Melbourne. p. 97-105.
2. Webb B.A., N.E.B., Y. Hayakawa, P. J. Krell, B. Lanzrein, M. R. Strand, D. B. Stoltz, and M. D. Summers, *Polydnaviridae*, in *Virus Taxonomy*, M.H.V.R.e. al, Editor. 2000, Academic Press: San Diego, CA. p. 253-259.
3. Webb B.A. and S. M.R., *The biology and genomics of polydnaviruses*, in *Comprehensive Molecular Insect Science*, K.I.a.S.S.G. L.I. Gilbert, Editor. 2005, Elsevier Press: San Diego p. 260–323.
4. Stoltz, D.B., S.B. Vinson, and E.A. MacKinnon, *Baculovirus-like particles in the reproductive tracts of female parasitoid wasps*. *Can J Microbiol*, 1976. **22**(7): p. 1013-23.
5. Volkoff, A.N., et al., *The Replication of Hyposoter-Didymator Polydnavirus - Cytopathology of the Calyx Cells in the Parasitoid*. *Biology of the Cell*, 1995. **83**(1): p. 1-13.

6. Tanaka, K., et al., *Shared and species-specific features among ichnovirus genomes*. *Virology*, 2007. **363**(1): p. 26-35.
7. Webb, B.A., et al., *Polydnavirus genomes reflect their dual roles as mutualists and pathogens*. *Virology*, 2006. **347**(1): p. 160-74.
8. Kroemer, J.A. and B.A. Webb, *Polydnavirus genes and genomes: emerging gene families and new insights into polydnavirus replication*. *Annu Rev Entomol*, 2004. **49**: p. 431-56.
9. Stoltz, D.B., et al., *Polydnaviridae*, in *Virus Taxonomy*, Murphy F. A., et al., Editors. 1995, Springer-Verlag: New York. p. 143-147.
10. Espagne, E., et al., *Genome sequence of a polydnavirus: Insights into symbiotic virus evolution*. *Science*, 2004. **306**(5694): p. 286-289.
11. Belle, E., et al., *Visualization of polydnavirus sequences in a parasitoid wasp chromosome*. *J Virol*, 2002. **76**(11): p. 5793-6.
12. Desjardins, C.A., et al., *Structure and evolution of a proviral locus of *Glyptapanteles indiensis* bracovirus*. *BMC Microbiol*, 2007. **7**: p. 61.
13. Fleming, J.A.G.W. and M.D. Summers, *Campoletis-Sonorensis Endoparasitic Wasps Contain Forms of Campoletis-Sonorensis Virus-DNA Suggestive of Integrated and Extrachromosomal Poly-Dnavirus Dnas*. *Journal of Virology*, 1986. **57**(2): p. 552-562.

14. Pasquier-Barre, F., et al., *Polydnavirus replication: the EPI segment of the parasitoid wasp Cotesia congregata is amplified within a larger precursor molecule*. Journal of General Virology, 2002. **83**: p. 2035-2045.
15. Drezen, J.M., et al., *Polydnavirus genome: integrated vs. free virus*. Journal of Insect Physiology, 2003. **49**(5): p. 407-417.
16. Marti, D., et al., *Ovary development and polydnavirus morphogenesis in the parasitic wasp Chelonus inanitus. I. Ovary morphogenesis, amplification of viral DNA and ecdysteroid titres*. Journal of General Virology, 2003. **84**: p. 1141-1150.
17. Annaheim, M. and B. Lanzrein, *Genome organization of the Chelonus inanitus polydnavirus: excision sites, spacers and abundance of proviral and excised segments*. Journal of General Virology, 2007. **88**: p. 450-457.
18. Webb, B.A. and L.W. Cui, *Relationships between polydnavirus genomes and viral gene expression*. Journal of Insect Physiology, 1998. **44**(9): p. 785-793.
19. Lapointe, R., et al., *Expression of a Toxoneuron nigriceps polydnavirus-encoded protein causes apoptosis-like programmed cell death in lepidopteran insect cells*. J Gen Virol, 2005. **86**(Pt 4): p. 963-71.
20. Friedman, R. and A.L. Hughes, *Pattern of gene duplication in the Cotesia congregata Bracovirus*. Infection Genetics and Evolution, 2006. **6**(4): p. 315-322.

21. Cerenius, L. and K. Soderhall, *The prophenoloxidase-activating system in invertebrates*. Immunological Reviews, 2004. **198**(1): p. 116-126.
22. Theopold, U., et al., *Coagulation in arthropods: defence, wound closure and healing*. Trends in Immunology, 2004. **25**(6): p. 289-294.
23. Imler, J.-L. and P. Bulet, *Antimicrobial peptides in Drosophila, structures, activities and gene regulation*, in *Mechanisms of epithelial defense*, D. Kabelitz and J.M. Schroder, Editors. 2005: Karger, Basel. p. 1-21.
24. Kanost, M.R. and M.J. Gorman, *Phenoloxidase in insect immunity*, in *Insect immunity*, N.E. Beckage, Editor. 2008, Academic Press: San Diego. p. 69-96.
25. Gillespie, J.P., M.R. Kanost, and T. Trenczek, *Biological mediators of insect immunity*. Annual Review of Entomology, 1997. **42**: p. 611-643.
26. Strand, M.R., *Insect hemocytes and their role in immunity*, in *Insect Immunology*, N.E. Beckage, Editor. 2008, Elsevier: San Diego, CA. p. 25-48.
27. Lavine, M.D. and M.R. Strand, *Insect hemocytes and their role in immunity*. Insect Biochemistry and Molecular Biology, 2002. **32**(10): p. 1295-1309.
28. Ribeiro, C. and M. Brehelin, *Insect haemocytes: What type of cell is that?* Journal of Insect Physiology, 2006. **52**(5): p. 417-429.

29. Gardiner, E.M.M. and M.R. Strand, *Hematopoiesis in larval Pseudoplusia includens and Spodoptera frugiperda*. Archives of Insect Biochemistry and Physiology, 2000. **43**(4): p. 147-164.
30. Nardi, J.B., et al., *Hematopoietic organs of Manduca sexta and hemocyte lineages*. Development Genes and Evolution, 2003. **213**(10): p. 477-491.
31. Nakahara, Y., et al., *In vitro studies of hematopoiesis in the silkworm: cell proliferation in and hemocyte discharge from the hematopoietic organ*. Journal of Insect Physiology, 2003. **49**(10): p. 907-916.
32. Ling, E., et al., *Hemocyte differentiation in the hematopoietic organs of the silkworm, Bombyx mori: prohemocytes have the function of phagocytosis*. Cell and Tissue Research, 2005. **320**(3): p. 535-543.
33. Pech, L.L. and M.R. Strand, *Granular cells are required for encapsulation of foreign targets by insect haemocytes*. J Cell Sci, 1996. **109** (Pt 8): p. 2053-60.
34. Irving, P., et al., *New insights into Drosophila larval haemocyte functions through genome-wide analysis*. Cellular Microbiology, 2005. **7**(3): p. 335-350.
35. Davies, D.H., M.R. Strand, and S.B. Vinson, *Changes in Differential Hemocyte Count and Invitro Behavior of Plasmatocytes from Host Heliothis-Virescens Caused by*

- Campoletis-Sonorensis Polydnavirus*. Journal of Insect Physiology, 1987. **33**(3): p. 143-
&.
36. Lavine, M.D. and N.E. Beckage, *Polydnaviruses - Potent Mediators of Host Insect Immune Dysfunction*. Parasitology Today, 1995. **11**(10): p. 368-378.
37. Strand, M.R. and L.L. Pech, *Immunological Basis for Compatibility in Parasitoid Host Relationships*. Annual Review of Entomology, 1995. **40**: p. 31-56.
38. Schmidt, O., U. Theopold, and M. Strand, *Innate immunity and its evasion and suppression by hymenopteran endoparasitoids*. Bioessays, 2001. **23**(4): p. 344-351.
39. Webb, B.A. and M.R. Strand, *The biology and genomics of polydnaviruses*, in *Comprehensive Molecular Insect Science*, K.I.a.S.S.G. L.I. Gilbert, Editor. 2005, Elsevier Press: San Diego p. 260–323.
40. Strand, M.R., *The insect cellular immune response*. Insect Science, 2008. **15**(1): p. 1-14.
41. Doucet, D. and M. Cusson, *Role of calyx fluid in alterations of immunity in Choristoneura fumiferana larvae parasitized by Tranosema rostrale*. Comparative Biochemistry and Physiology a-Physiology, 1996. **114**(4): p. 311-317.
42. Pennacchio, F. and M.R. Strand, *Evolution of developmental strategies in parasitic hymenoptera*. Annu Rev Entomol, 2006. **51**: p. 233-58.

43. lanzrein, B., R. Pfister-Wilhelm, and F. von Niederhausern, *Effects of an egg-larval parasitoid and its polydnavirus on development and the endocrine system of the host*, in *endocrine interactions of insect parasites and pathogens*. 2001, BIOS Sci. Publishers: Oxford. p. 95-109.
44. Beckage, N.E. and D.B. Gelman, *Wasp parasitoid disruption of host development: Implications for new biologically based strategies for insect control*. Annual Review of Entomology, 2004. **49**: p. 299-330.
45. Thompson, S.N. and D.L. Dahlman, *Aberrant nutritional regulation of carbohydrate synthesis by parasitized *Manduca sexta* L.* Journal of Insect Physiology, 1998. **44**(9): p. 745-753.
46. Balgopal, M.M., et al., *Parasitism by *Microplitis demolitor* induces alterations in the juvenile hormone titers and juvenile hormone esterase activity of its host, *Pseudoplusia includens*.* Journal of Insect Physiology, 1996. **42**(4): p. 337-345.
47. Schafellner, C., R.C. Marktl, and A. Schopf, *Inhibition of juvenile hormone esterase activity in *Lymantria dispar* (Lepidoptera, Lymantriidae) larvae parasitized by *Glyptapanteles liparidis* (Hymenoptera, Braconidae).* Journal of Insect Physiology, 2007. **53**(8): p. 858-868.
48. Dong, K., D.Q. Zhang, and D.L. Dahlman, *Down-regulation of juvenile hormone esterase and arylphorin production in *Heliothis virescens* larvae parasitized by*

- Microplitis croceipes*. Archives of Insect Biochemistry and Physiology, 1996. **32**(2): p. 237-248.
49. Cole, T.J., et al., *Parasitoid-host endocrine relations: self-reliance or co-optation?* Insect Biochemistry and Molecular Biology, 2002. **32**(12): p. 1673-1679.
50. Li, S., et al., *Juvenile hormone synthesis, metabolism, and resulting haemolymph titre in *Heliothis virescens* larvae parasitized by *Toxoneuron nigriceps**. Journal of Insect Physiology, 2003. **49**(11): p. 1021-1030.
51. Hayakawa, Y., *Growth-Blocking Peptide - an Insect Biogenic Peptide That Prevents the Onset of Metamorphosis*. Journal of Insect Physiology, 1995. **41**(1): p. 1-6.
52. Tanaka, T., N. Agui, and K. Hiruma, *The Parasitoid *Apanteles-Kariyai* Inhibits Pupation of Its Host, *Pseudaletia-Separata*, Via Disruption of Prothoracicotropic Hormone-Release*. General and Comparative Endocrinology, 1987. **67**(3): p. 364-374.
53. Kelly, T.J., et al., *Effects of parasitization by *Cotesia congregata* on the brain-prothoracic gland axis of its host, *Manduca sexta**. Journal of Insect Physiology, 1998. **44**(3-4): p. 323-332.
54. Pennacchio, F., M.C. Digilio, and E. Tremblay, *Biochemical and Metabolic Alterations in *Acyrtosiphon-Pisum* Parasitized by *Aphidius-Ervi**. Archives of Insect Biochemistry and Physiology, 1995. **30**(4): p. 351-367.

55. Dover, B.A., T. Tanaka, and S.B. Vinson, *Stadium-Specific Degeneration of Host Prothoracic Glands by Campoletis-Sonorensis Calyx Fluid and Its Association with Host Ecdysteroid Titters*. Journal of Insect Physiology, 1995. **41**(11): p. 947-955.
56. Thompson, S.N., *Redirection of host metabolism and effects on parasite nutrition*, in *Parasites and pathogens of insects*, N.E. Beckage, S.N. Thompson, and B.A. Federici, Editors. 1993, Academic press: New York. p. 125-144.
57. Strand, M.R. and T. Noda, *Alterations in the Hemocytes of Pseudoplusia-Includens after Parasitism by Microplitis-Demolitor*. Journal of Insect Physiology, 1991. **37**(11): p. 839-850.
58. Strand, M.R., et al., *Persistence and expression of Microplitis demolitor polydnavirus in Pseudoplusia includens*. J Gen Virol, 1992. **73**(Pt 7): p. 1627-35.
59. Strand, M.R. and B.A. Dover, *Developmental Disruption of Pseudoplusia-Includens and Heliothis-Virescens Larvae by the Calyx Fluid and Venom of Microplitis-Demolitor*. Archives of Insect Biochemistry and Physiology, 1991. **18**(3): p. 131-145.
60. etc., W.B.S.M., *Polydnavirus genomes reflect their dual roles as mutualists and pathogens*. Virology, 2005.

61. Beck, M. and M.R. Strand, *Glc1.8 from Microplitis demolitor bracovirus induces a loss of adhesion and phagocytosis in insect High Five and S2 cells*. Journal of Virology, 2005. **79**(3): p. 1861-1870.
62. Thoetkiattikul, H., M.H. Beck, and M.R. Strand, *Inhibitor kappa B-like proteins from a polydnavirus inhibit NF-kappa B activation and suppress the insect immune response*. Proceedings of the National Academy of Sciences of the United States of America, 2005. **102**(32): p. 11426-11431.
63. Beck, M.H. and M.R. Strand, *A novel polydnavirus protein inhibits the insect prophenoloxidase activation pathway*. Proc Natl Acad Sci U S A, 2007.
64. Lavine, M.D. and N.E. Beckage, *Temporal pattern of parasitism-induced immunosuppression in Manduca sexta larvae parasitized by Cotesia congregata*. Journal of Insect Physiology, 1996. **42**(1): p. 41-51.
65. Streuli, M., et al., *Distinct Functional Roles of the 2 Intracellular Phosphatase Like Domains of the Receptor-Linked Protein Tyrosine Phosphatases Lca and Lar*. Embo Journal, 1990. **9**(8): p. 2399-2407.
66. Neel, B.G. and N.K. Tonks, *Protein tyrosine phosphatases in signal transduction*. Current Opinion in Cell Biology, 1997. **9**(2): p. 193-204.

67. Jia, Z., et al., *Structural basis for phosphotyrosine peptide recognition by protein tyrosine phosphatase 1B*. Science, 1995. **268**(5218): p. 1754-8.
68. Barford, D., *Colworth Medal Lecture. Structural studies of reversible protein phosphorylation and protein phosphatases*. Biochem Soc Trans, 1999. **27**(6): p. 751-66.
69. Barford, D., A.J. Flint, and N.K. Tonks, *Crystal structure of human protein tyrosine phosphatase 1B*. Science, 1994. **263**(5152): p. 1397-404.
70. Yuvaniyama, J., et al., *Crystal structure of the dual specificity protein phosphatase VHR*. Science, 1996. **272**(5266): p. 1328-31.
71. Dunn, D., et al., *The active site specificity of the Yersinia protein-tyrosine phosphatase*. J Biol Chem, 1996. **271**(1): p. 168-73.
72. Mauro, L.J. and J.E. Dixon, *Zip Codes Direct Intracellular Protein-Tyrosine Phosphatases to the Correct Cellular Address*. Trends in Biochemical Sciences, 1994. **19**(4): p. 151-155.
73. Tonks NK, N.B., *Combinatorial control of the specificity of protein tyrosine phosphatases*. Curr Opin Cell Biol., 2001. **13**(2): p. 182-95.

74. Flint, A.J., et al., *Development of "substrate-trapping" mutants to identify physiological substrates of protein tyrosine phosphatases*. Proc Natl Acad Sci U S A, 1997. **94**(5): p. 1680-5.
75. Xie, L., Y.L. Zhang, and Z.Y. Zhang, *Design and characterization of an improved protein tyrosine phosphatase substrate-trapping mutant*. Biochemistry, 2002. **41**(12): p. 4032-9.
76. Sun, H., et al., *MKP-1 (3CH134), an immediate early gene product, is a dual specificity phosphatase that dephosphorylates MAP kinase in vivo*. Cell, 1993. **75**(3): p. 487-93.
77. Shiozaki, K. and P. Russell, *Cell-cycle control linked to extracellular environment by MAP kinase pathway in fission yeast*. Nature, 1995. **378**(6558): p. 739-43.
78. Furukawa, T., et al., *Specific interaction of the CD45 protein-tyrosine phosphatase with tyrosine-phosphorylated CD3 zeta chain*. Proc Natl Acad Sci U S A, 1994. **91**(23): p. 10928-32.
79. Morrison, D.K., M.S. Murakami, and V. Cleghon, *Protein kinases and phosphatases in the Drosophila genome*. J Cell Biol, 2000. **150**(2): p. F57-62.
80. Andersen, J.N., et al., *A genomic perspective on protein tyrosine phosphatases: gene structure, pseudogenes, and genetic disease linkage*. FASEB J, 2004. **18**(1): p. 8-30.

81. Tonks, N.K., *Protein tyrosine phosphatases: from genes, to function, to disease*. Nat Rev Mol Cell Biol, 2006. **7**(11): p. 833-46.
82. Seifert, R.A., et al., *PTPRQ is a novel phosphatidylinositol phosphatase that can be expressed as a cytoplasmic protein or as a subcellularly localized receptor-like protein*. Exp Cell Res, 2003. **287**(2): p. 374-86.
83. Pils, B. and J. Schultz, *Inactive enzyme-homologues find new function in regulatory processes*. Journal of Molecular Biology, 2004. **340**(3): p. 399-404.
84. Bartlett, G.J., N. Borkakoti, and J.M. Thornton, *Catalysing new reactions during evolution: Economy of residues and mechanism*. Journal of Molecular Biology, 2003. **331**(4): p. 829-860.
85. Oganessian, A., et al., *Protein tyrosine phosphatase RQ is a phosphatidylinositol phosphatase that can regulate cell survival and proliferation*. Proc Natl Acad Sci U S A, 2003. **100**(13): p. 7563-8.
86. Wishart, M.J., et al., *A single mutation converts a novel phosphotyrosine binding domain into a dual-specificity phosphatase*. J Biol Chem, 1995. **270**(45): p. 26782-5.
87. Mochizuki, Y. and P.W. Majerus, *Characterization of myotubularin-related protein 7 and its binding partner, myotubularin-related protein 9*. Proc Natl Acad Sci U S A, 2003. **100**(17): p. 9768-73.

88. Kim, S.A., et al., *Regulation of myotubularin-related (MTMR)2 phosphatidylinositol phosphatase by MTMR5, a catalytically inactive phosphatase*. Proc Natl Acad Sci U S A, 2003. **100**(8): p. 4492-7.
89. Robinson, F.L. and J.E. Dixon, *The phosphoinositide-3-phosphatase MTMR2 associates with MTMR13, a membrane-associated pseudophosphatase also mutated in type 4B Charcot-Marie-Tooth disease*. J Biol Chem, 2005. **280**(36): p. 31699-707.
90. Pearson, A., A. Lux, and M. Krieger, *Expression Cloning of Dsr-Ci, a Class-C Macrophage-Specific Scavenger Receptor from Drosophila-Melanogaster*. Proceedings of the National Academy of Sciences of the United States of America, 1995. **92**(9): p. 4056-4060.
91. Ramet, M., et al., *Drosophila scavenger receptor Cl is a pattern recognition receptor for bacteria*. Immunity, 2001. **15**(6): p. 1027-1038.
92. Michel, T., et al., *Drosophila Toll is activated by Gram-positive bacteria through a circulating peptidoglycan recognition protein*. Nature, 2001. **414**(6865): p. 756-759.
93. Ramet, M., et al., *Functional genomic analysis of phagocytosis and identification of a Drosophila receptor for E-coli*. Nature, 2002. **416**(6881): p. 644-648.
94. Aderem, A. and D.M. Underhill, *Mechanisms of phagocytosis in macrophages*. Annual Review of Immunology, 1999. **17**: p. 593-623.

95. Nathan, C.F. and J.B. Hibbs, *Role of Nitric-Oxide Synthesis in Macrophage Antimicrobial Activity*. *Current Opinion in Immunology*, 1991. **3**(1): p. 65-70.
96. Robinson JM, B.J., *Production of active oxygen species by phagocytic leukocytes*. *Immunol Ser*, 1994(60): p. 159-78.
97. Brennan, C.A. and K.V. Anderson, *Drosophila: the genetics of innate immune recognition and response*. *Annu Rev Immunol*, 2004. **22**: p. 457-83.
98. Belvin, M.P. and K.V. Anderson, *A conserved signaling pathway: the Drosophila toll-dorsal pathway*. *Annu Rev Cell Dev Biol*, 1996. **12**: p. 393-416.
99. Lemaitre, B., et al., *The dorsoventral regulatory gene cassette spätzle/Toll/cactus controls the potent antifungal response in Drosophila adults*. *Cell*, 1996. **86**(6): p. 973-83.
100. Dubé, N. and M.L. Tremblay, *Involvement of the small protein tyrosine phosphatases TC-PTP and PTP1B in signal transduction and diseases: from diabetes, obesity to cell cycle, and cancer*. *Biochim Biophys Acta*, 2005. **1754**(1-2): p. 108-17.
101. Kozma, S.C. and G. Thomas, *Regulation of cell size in growth, development and human disease: PI3K, PKB and S6K*. *Bioessays*, 2002. **24**(1): p. 65-71.

102. Wu, Q. and M.R. Brown, *Signaling and function of insulin-like peptides in insects*. Annual Review of Entomology, 2006. **51**: p. 1-24.
103. Fernandez, R., et al., *The Drosophila Insulin-Receptor Homolog - a Gene Essential for Embryonic-Development Encodes 2 Receptor Isoforms with Different Signaling Potential*. Embo Journal, 1995. **14**(14): p. 3373-3384.
104. Linassier, C., et al., *Molecular cloning and biochemical characterization of a Drosophila phosphatidylinositol-specific phosphoinositide 3-kinase*. Biochemical Journal, 1997. **321**: p. 849-856.
105. Goberdhan, D.C., et al., *Drosophila tumor suppressor PTEN controls cell size and number by antagonizing the Chico/PI3-kinase signaling pathway*. Genes Dev, 1999. **13**(24): p. 3244-58.
106. Oldham, S., et al., *Genetic and biochemical characterization of dTOR, the Drosophila homolog of the target of rapamycin*. Genes & Development, 2000. **14**(21): p. 2689-2694.
107. Gilbert, L.I., R. Rybczynski, and J.T. Warren, *Control and biochemical nature of the ecdysteroidogenic pathway*. Annual Review of Entomology, 2002. **47**: p. 883-916.
108. Priester, J. and W.A. Smith, *Inhibition of tyrosine phosphorylation blocks hormone-stimulated calcium influx in an insect steroidogenic gland*. Mol Cell Endocrinol, 2005. **229**(1-2): p. 185-92.

109. Smith, W.A., et al., *Cyclic AMP is a requisite messenger in the action of big PTTH in the prothoracic glands of pupal Manduca sexta*. *Insect Biochem Mol Biol*, 1996. **26**(2): p. 161-70.
110. Henrich, V.C. and N.E. Brown, *Insect nuclear receptors: a developmental and comparative perspective*. *Insect Biochem Mol Biol*, 1995. **25**(8): p. 881-97.
111. Mirth, C., J.W. Truman, and L.M. Riddiford, *The role of the prothoracic gland in determining critical weight for metamorphosis in Drosophila melanogaster*. *Curr Biol*, 2005. **15**(20): p. 1796-807.
112. Caldwell, P.E., M. Walkiewicz, and M. Stern, *Ras activity in the Drosophila prothoracic gland regulates body size and developmental rate via ecdysone release*. *Curr Biol*, 2005. **15**(20): p. 1785-95.
113. Guan, K.L. and J.E. Dixon, *Protein Tyrosine Phosphatase-Activity of an Essential Virulence Determinant in Yersinia*. *Science*, 1990. **249**(4968): p. 553-556.
114. Rosqvist, R., I. Bolin, and H. Wolfwatz, *Inhibition of Phagocytosis in Yersinia-Pseudotuberculosis - a Virulence Plasmid-Encoded Ability Involving the Yop2b Protein*. *Infection and Immunity*, 1988. **56**(8): p. 2139-2143.

115. Bliska, J.B. and D.S. Black, *Inhibition of the Fc Receptor-Mediated Oxidative Burst in Macrophages by the Yersinia-Pseudotuberculosis Tyrosine Phosphatase*. Infection and Immunity, 1995. **63**(2): p. 681-685.
116. Black, D.S. and J.B. Bliska, *Identification of p130(Cas) as a substrate of Yersinia YopH (Yop51), a bacterial protein tyrosine phosphatase that translocates into mammalian cells and targets focal adhesions*. Embo Journal, 1997. **16**(10): p. 2730-2744.
117. Persson, C., et al., *The PTPase YopH inhibits uptake of Yersinia, tyrosine phosphorylation of p130(Cas) and FAK, and the associated accumulation of these proteins in peripheral focal adhesions*. Embo Journal, 1997. **16**(9): p. 2307-2318.
118. Andersson, K., et al., *Yersinia pseudotuberculosis-induced calcium signaling in neutrophils is blocked by the virulence effector YopH*. Infection and Immunity, 1999. **67**(5): p. 2567-2574.
119. Hamid, N., et al., *YopH dephosphorylates Cas and Fyn-binding protein in macrophages*. Microbial Pathogenesis, 1999. **27**(4): p. 231-242.
120. Black, D.S., et al., *The Yersinia tyrosine phosphatase YopH targets a novel adhesion-regulated signalling complex in macrophages*. Cellular Microbiology, 2000. **2**(5): p. 401-414.

121. Fu, Y. and J.E. Galan, *A salmonella protein antagonizes Rac-1 and Cdc42 to mediate host-cell recovery after bacterial invasion*. Nature, 1999. **401**(6750): p. 293-7.
122. Murli, S., R.O. Watson, and J.E. Galan, *Role of tyrosine kinases and the tyrosine phosphatase SptP in the interaction of Salmonella with host cells*. Cell Microbiol, 2001. **3**(12): p. 795-810.
123. Lin, S.L., T.X. Le, and D.S. Cowen, *SptP, a Salmonella typhimurium type III-secreted protein, inhibits the mitogen-activated protein kinase pathway by inhibiting Raf activation*. Cell Microbiol, 2003. **5**(4): p. 267-75.
124. Rahmouni, S., et al., *Loss of the VHR dual-specific phosphatase causes cell-cycle arrest and senescence*. Nat Cell Biol, 2006. **8**(5): p. 524-31.
125. Liu, K., B. Lemon, and P. Traktman, *The dual-specificity phosphatase encoded by vaccinia virus, VHI, is essential for viral transcription in vivo and in vitro*. J Virol, 1995. **69**(12): p. 7823-34.
126. Andersen, J.N., et al., *Structural and evolutionary relationships among protein tyrosine phosphatase domains*. Mol Cell Biol, 2001. **21**(21): p. 7117-36.
127. Lapointe, R., et al., *Genomic and morphological features of a banchine polydnavirus: Comparison with bracoviruses and ichnoviruses*. Journal of Virology, 2007. **81**(12): p. 6491-6501.

128. Provost, B., et al., *Bracoviruses contain a large multigene family coding for protein tyrosine phosphatases*. Journal of Virology, 2004. **78**(23): p. 13090-13103.
129. Ibrahim, A.M., et al., *Protein tyrosine phosphatases encoded in Cotesia plutellae bracovirus: sequence analysis, expression profile, and a possible biological role in host immunosuppression*. Dev Comp Immunol, 2007. **31**(10): p. 978-90.
130. Gundersen-Rindal, D.E. and M.J. Pedroni, *Characterization and transcriptional analysis of protein tyrosine phosphatase genes and an ankyrin repeat gene of the parasitoid Glyptapanteles indiensis polydnavirus in the parasitized host*. J Gen Virol, 2006. **87**(Pt 2): p. 311-22.
131. Li, Y. and L.K. Miller, *Expression and localization of a baculovirus protein phosphatase*. J Gen Virol, 1995. **76** (Pt 12): p. 2941-8.
132. Li, Y. and L.K. Miller, *Properties of a baculovirus mutant defective in the protein phosphatase gene*. J Virol, 1995. **69**(7): p. 4533-7.
133. Sheng, Z. and H. Charbonneau, *The baculovirus Autographa californica encodes a protein tyrosine phosphatase*. J Biol Chem, 1993. **268**(7): p. 4728-33.
134. Hakes, D.J., et al., *A protein phosphatase related to the vaccinia virus VHI is encoded in the genomes of several orthopoxviruses and a baculovirus*. Proc Natl Acad Sci U S A, 1993. **90**(9): p. 4017-21.

135. Kim, D. and R.F. Weaver, *Transcription mapping and functional analysis of the protein tyrosine/serine phosphatase (PTPase) gene of the Autographa californica nuclear polyhedrosis virus*. *Virology*, 1993. **195**(2): p. 587-95.
136. Takagi, T., et al., *A protein tyrosine phosphatase-like protein from baculovirus has RNA 5'-triphosphatase and diphosphatase activities*. *Proc Natl Acad Sci U S A*, 1998. **95**(17): p. 9808-12.
137. Kamita, S.G., et al., *A baculovirus-encoded protein tyrosine phosphatase gene induces enhanced locomotory activity in a lepidopteran host*. *Proc Natl Acad Sci U S A*, 2005. **102**(7): p. 2584-9.
138. Chen, Y.P., et al., *Quantitative expression analysis of a Glyptapanteles indiensis polydnavirus protein tyrosine phosphatase gene in its natural lepidopteran host, Lymantria dispar*. *Insect Molecular Biology*, 2003. **12**(3): p. 271-280.
139. Strand, M.R., *Microplitis Demolitor Polydnavirus Infects and Expresses in Specific Morphotypes of Pseudoplusia Includens Hemocytes*. *Journal of General Virology*, 1994. **75**: p. 3007-3020.
140. Beck, M. and M.R. Strand, *RNA interference silences Microplitis demolitor bracovirus genes and implicates glc1.8 in disruption of adhesion in infected host cells*. *Virology*, 2003. **314**(2): p. 521-535.

141. Trudeau, D., R.A. Witherell, and M.R. Strand, *Characterization of two novel Microplitis demolitor polydnavirus mRNAs expressed in Pseudoplusia includens haemocytes*. Journal of General Virology, 2000. **81**: p. 3049-3058.
142. Beck, M.H., R. Inman, and M. Strand, *Microplitis demolitor bracovirus genome segments vary in abundance and are individually packaged in virions*. Virology, in press
143. Beck, M.H., R.B. Inman, and M.R. Strand, *Microplitis demolitor bracovirus genome segments vary in abundance and are individually packaged in virions*. Virology, 2007. **359**(1): p. 179-89.
144. Pech, L.L. and M.R. Strand, *Granular cells are required for encapsulation of foreign targets by insect haemocytes*. Journal of Cell Science, 1996. **109**: p. 2053-2060.
145. Lavine, M.D., G. Chen, and M.R. Strand, *Immune challenge differentially affects transcript abundance of three antimicrobial peptides in hemocytes from the moth Pseudoplusia includens*. Insect Biochemistry and Molecular Biology, 2005. **35**(12): p. 1335-1346.
146. Detvisitsakun, C., et al., *Stimulation of cell motility by a viral fibroblast growth factor homolog: Proposal for a role in viral pathogenesis*. Virology, 2005. **336**(2): p. 308-317.

147. Strand, M.R., et al., *Microplitis demolitor bracovirus inhibits phagocytosis by hemocytes from Pseudoplusia includens*. Archives of Insect Biochemistry and Physiology, 2006. **61**(3): p. 134-145.
148. Sall, J.a.A.L., *JMP Start Statistics*. 1996, New York: Duxbury Press.
149. Fallman, M., et al., *Yersinia pseudotuberculosis inhibits Fc receptor-mediated phagocytosis in J774 cells*. Infect. Immun., 1995. **63**(8): p. 3117-3124.
150. Fujimoto, J., et al., *Cloning and characterization of Dfak56, a homolog of focal adhesion kinase, in Drosophila melanogaster*. Journal of Biological Chemistry, 1999. **274**(41): p. 29196-29201.
151. Webb BA, S.M., *The biology and genomics of polydnviruses*, in *Comprehensive Molecular Insect Science*, K.I.a.S.S.G. L.I. Gilbert, Editor. 2005, Elsevier Press: San Diego p. 260–323.
152. Choi, J.Y., et al., *Genomic segments cloning and analysis of Cotesia plutellae polydnvirus using plasmid capture system*. Biochemical and Biophysical Research Communications, 2005. **332**(2): p. 487-493.
153. Strand, M.R., et al., *Persistence and Expression of Microplitis-Demolitor Polydnvirus in Pseudoplusia-Includens*. Journal of General Virology, 1992. **73**: p. 1627-1635.

154. De Gregorio, E., et al., *Genome-wide analysis of the Drosophila immune response by using oligonucleotide microarrays*. Proceedings of the National Academy of Sciences of the United States of America, 2001. **98**(22): p. 12590-12595.
155. Tortorella, D., et al., *Viral subversion of the immune system*. Annual Review of Immunology, 2000. **18**: p. 861-926.
156. Blander, J.M. and R. Medzhitov, *Regulation of phagosome maturation by signals from Toll-like receptors*. Science, 2004. **304**(5673): p. 1014-1018.
157. Gelman, I.H., *Pyk 2 FAKs, any two FAKs*. Cell Biology International, 2003. **27**(7): p. 507-510.
158. Parsons, J.T., *Focal adhesion kinase: the first ten years*. Journal of Cell Science, 2003. **116**(8): p. 1409-1416.
159. Hed, J. and O. Stendahl, *Differences in the Ingestion Mechanisms of Igg and C3b Particles in Phagocytosis by Neutrophils*. Immunology, 1982. **45**(4): p. 727-736.
160. Mustelin, T., T. Vang, and N. Bottini, *Protein tyrosine phosphatases and the immune response*. Nature Reviews Immunology, 2005. **5**(1): p. 43-57.

161. Baeg, G.H., R. Zhou, and N. Perrimon, *Genome-wide RNAi analysis of JAK/STAT signaling components in Drosophila*. *Genes & Development*, 2005. **19**(16): p. 1861-1870.
162. Grabbe, C., et al., *Focal adhesion kinase is not required for integrin function or viability in Drosophila*. *Development*, 2004. **131**(23): p. 5795-5805.
163. Hoffmann, J.A. and J.M. Reichhart, *Drosophila innate immunity: an evolutionary perspective*. *Nature Immunology*, 2002. **3**(2): p. 121-126.
164. Cornelis, G.R., *Yersinia type III secretion: send in the effectors*. *Journal of Cell Biology*, 2002. **158**(3): p. 401-408.
165. Gruenheid, S. and B.B. Finlay, *Microbial pathogenesis and cytoskeletal function*. *Nature*, 2003. **422**(6933): p. 775-781.
166. Singh, R., et al., *Disruption of mptpB impairs the ability of Mycobacterium tuberculosis to survive in guinea pigs*. *Molecular Microbiology*, 2003. **50**(3): p. 751-762.
167. Levashina, E.A., et al., *Conserved role of a complement-like protein in phagocytosis revealed by dsRNA knockout in cultured cells of the mosquito, Anopheles gambiae*. *Cell*, 2001. **104**(5): p. 709-718.

168. Lavine, M.D. and M.R. Strand, *Haemocytes from Pseudoplusia includens express multiple alpha and beta integrin subunits*. *Insect Molecular Biology*, 2003. **12**(5): p. 441-452.
169. Levin, D.M., et al., *A hemocyte-specific integrin required for hemocytic encapsulation in the tobacco hornworm, Manduca sexta*. *Insect Biochem Mol Biol*, 2005. **35**(5): p. 369-80.
170. Celli, J. and B.B. Finlay, *Bacterial avoidance of phagocytosis*. *Trends in Microbiology*, 2002. **10**(5): p. 232-237.
171. Chen, G.-C., et al., *Regulation of Rho and Rac Signaling to the Actin Cytoskeleton by Paxillin during Drosophila Development*. *Mol. Cell. Biol.*, 2005. **25**(3): p. 979-987.
172. Wheeler, G.N. and R.O. Hynes, *The cloning, genomic organization and expression of the focal contact protein paxillin in Drosophila*. *Gene*, 2001. **262**(1-2): p. 291-299.
173. Whitfield, J.B., *Estimating the age of the polydnavirus/braconid wasp symbiosis*. *Proceedings of the National Academy of Sciences of the United States of America*, 2002. **99**(11): p. 7508-7513.
174. Webb, B.A., et al., *Polydnaviridae*, in *Virus Taxonomy*, M.H.V.R.e. al, Editor. 2000, Academic Press: San Diego, CA. p. 253-259.

175. Wertheim, B., et al., *Genome-wide gene expression in response to parasitoid attack in Drosophila*. *Genome Biology*, 2005. **6**(11).
176. Nardi, J.B., et al., *Neuroglian-positive plasmatocytes of Manduca sexta and the initiation of hemocyte attachment to foreign surfaces*. *Dev Comp Immunol*, 2006. **30**(5): p. 447-62.
177. Strand, M.R. and L.L. Pech, *Microplitis demolitor polydnavirus induces apoptosis of a specific haemocyte morphotype in Pseudoplusia includens*. *J Gen Virol*, 1995. **76 (Pt 2)**: p. 283-91.
178. Pruijssers, A.J. and M.R. Strand, *PTP-H2 and PTP-H3 from Microplitis demolitor Bracovirus localize to focal adhesions and are antiphagocytic in insect immune cells*. *J Virol*, 2007. **81**(3): p. 1209-19.
179. Pech, L.L., D. Trudeau, and M.R. Strand, *Separation and Behavior in-Vitro of Hemocytes from the Moth, Pseudoplusia-Includens*. *Cell and Tissue Research*, 1994. **277**(1): p. 159-167.
180. Strand, M.R. and L.L. Pech, *Microplitis-Demolitor Polydnavirus Induces Apoptosis of a Specific Hemocyte Morphotype in Pseudoplusia-Includens*. *Journal of General Virology*, 1995. **76**: p. 283-291.
181. Gorman, A.M., et al., *Use of flow cytometry techniques in studying mechanisms of apoptosis in leukemic cells*. *Cytometry*, 1997. **29**(2): p. 97-105.

182. Clem, R.J., M. Fechheimer, and L.K. Miller, *Prevention of apoptosis by a baculovirus gene during infection of insect cells*. Science, 1991. **254**(5036): p. 1388-90.
183. Clem, R.J. and L.K. Miller, *Apoptosis reduces both the in vitro replication and the in vivo infectivity of a baculovirus*. J Virol, 1993. **67**(7): p. 3730-8.
184. Trudeau, D. and M.R. Strand, *A limited role in parasitism for Microplitis demolitor polydnavirus*. Journal of Insect Physiology, 1998. **44**(9): p. 795-805.
185. Strand, M.R., R.A. Witherell, and D. Trudeau, *Two Microplitis demolitor polydnavirus mRNAs expressed in hemocytes of Pseudoplusia includens contain a common cysteine-rich domain*. Journal of Virology, 1997. **71**(3): p. 2146-2156.
186. Hershberger, P.A., D.J. LaCount, and P.D. Friesen, *The apoptotic suppressor P35 is required early during baculovirus replication and is targeted to the cytosol of infected cells*. J Virol, 1994. **68**(6): p. 3467-77.
187. Gilmore, A.P., *Anoikis*. Cell Death Differ, 2005. **12 Suppl 2**: p. 1473-7.
188. Li, H., et al., *Activation of caspase-2 in apoptosis*. J Biol Chem, 1997. **272**(34): p. 21010-7.
189. Danial, N.N. and S.J. Korsmeyer, *Cell death: critical control points*. Cell, 2004. **116**(2): p. 205-19.

190. Olson, M.R., et al., *Reaper is regulated by IAP-mediated ubiquitination*. J Biol Chem, 2003. **278**(6): p. 4028-34.
191. Abdelwahid, E., et al., *Mitochondrial disruption in Drosophila apoptosis*. Dev Cell, 2007. **12**(5): p. 793-806.
192. Kuranaga, E. and M. Miura, *Nonapoptotic functions of caspases: caspases as regulatory molecules for immunity and cell-fate determination*. Trends Cell Biol, 2007. **17**(3): p. 135-44.
193. Clem, R.J., M. Robson, and L.K. Miller, *Influence of infection route on the infectivity of baculovirus mutants lacking the apoptosis-inhibiting gene p35 and the adjacent gene p94*. J Virol, 1994. **68**(10): p. 6759-62.
194. Huang, Q., et al., *Evolutionary conservation of apoptosis mechanisms: lepidopteran and baculoviral inhibitor of apoptosis proteins are inhibitors of mammalian caspase-9*. Proc Natl Acad Sci U S A, 2000. **97**(4): p. 1427-32.
195. Muro, I., B.A. Hay, and R.J. Clem, *The Drosophila DIAP1 protein is required to prevent accumulation of a continuously generated, processed form of the apical caspase DRONC*. J Biol Chem, 2002. **277**(51): p. 49644-50.
196. Woo, J.H., et al., *Molecular mechanisms of curcumin-induced cytotoxicity: induction of apoptosis through generation of reactive oxygen species, down-regulation of Bcl-XL and*

- IAP, the release of cytochrome c and inhibition of Akt. Carcinogenesis, 2003. 24(7): p. 1199-208.*
197. Wells, B.S., E. Yoshida, and L.A. Johnston, *Compensatory proliferation in Drosophila imaginal discs requires Dronc-dependent p53 activity. Curr Biol, 2006. 16(16): p. 1606-15.*
198. Takada, T., et al., *Induction of apoptosis by stomach cancer-associated protein-tyrosine phosphatase-1. J Biol Chem, 2002. 277(37): p. 34359-66.*
199. Yousefi, S. and H.U. Simon, *SHP-1: a regulator of neutrophil apoptosis. Semin Immunol, 2003. 15(3): p. 195-9.*
200. Gu, F., et al., *Protein-tyrosine phosphatase 1B potentiates IRE1 signaling during endoplasmic reticulum stress. J Biol Chem, 2004. 279(48): p. 49689-93.*
201. Bruckner, S., et al., *Yersinia phosphatase induces mitochondrially dependent apoptosis of T cells. J Biol Chem, 2005. 280(11): p. 10388-94.*
202. Halle, M., et al., *Caspase-3 regulates catalytic activity and scaffolding functions of the protein tyrosine phosphatase PEST, a novel modulator of the apoptotic response. Mol Cell Biol, 2007. 27(3): p. 1172-90.*

203. Strand, M.R., J.A. Johnson, and J.D. Culin, *Developmental Interactions between the Parasitoid Microplitis-Demolitor (Hymenoptera, Braconidae) and Its Host Heliothis-Virescens (Lepidoptera, Noctuidae)*. Annals of the Entomological Society of America, 1988. **81**(5): p. 822-830.
204. Yamanaka, N., et al., *Identification of a novel prothoracicostatic hormone and its receptor in the silkworm Bombyx mori*. J Biol Chem, 2005. **280**(15): p. 14684-90.
205. Gu, S.H., et al., *A deficiency in prothoracicotropic hormone transduction pathway during the early last larval instar of Bombyx mori*. Mol Cell Endocrinol, 1996. **120**(2): p. 99-105.
206. Brown, M.R., et al., *An insulin-like peptide regulates egg maturation and metabolism in the mosquito Aedes aegypti*. Proc. Natl. Acad. Sci. USA, 2008. **In press**.
207. Lewis, W.J. and S.B. Vinson, *Egg and larval development of cardiochiles nigriceps*. Annals of the Entomological Society of America, 1968. **61**(3): p. 561-&.
208. Tanaka, T. and S.B. Vinson, *Depression of prothoracic gland activity of heliothis-virescens by venom and calyx fluids from the parasitoid, cardiochiles-nigriceps*. Journal of Insect Physiology, 1991. **37**(2): p. 139-144.

209. Smith, W., J. Priester, and J. Morais, *PTTH-stimulated ecdysone secretion is dependent upon tyrosine phosphorylation in the prothoracic glands of Manduca sexta*. *Insect Biochem Mol Biol*, 2003. **33**(12): p. 1317-25.
210. Pennacchio, F., et al., *Prothoracic gland inactivation in Heliothis virescens (F.) (Lepidoptera : Noctuidae) larvae parasitized by Cardiochiles nigriceps Viereck (Hymenoptera : Braconidae)*. *Journal of Insect Physiology*, 1998. **44**(9): p. 845-857.
211. Pennacchio, F., P. Falabella, and S.B. Vinson, *Regulation of Heliothis virescens prothoracic glands by Cardiochiles nigriceps polydnavirus*. *Archives of Insect Biochemistry and Physiology*, 1998. **38**(1): p. 1-10.
212. Falabella, P., et al., *Protein tyrosine phosphatases of Toxoneuron nigriceps bracovirus as potential disrupters of host prothoracic gland function*. *Arch Insect Biochem Physiol*, 2006. **61**(3): p. 157-69.
213. King, D.S., et al., *The Secretion of alpha-Ecdysone by the Prothoracic Glands of Manduca sexta In Vitro*. *Proc Natl Acad Sci U S A*, 1974. **71**(3): p. 793-796.
214. Steel, C.G. and X. Vafopoulou, *Ecdysteroidogenic action of Bombyx prothoracicotropic hormone and bombyxin on the prothoracic glands of Rhodnius prolixus in vitro*. *J Insect Physiol*, 1997. **43**(7): p. 651-656.

215. Hua, Y.J., et al., *Identification of a prothoracicostatic peptide in the larval brain of the silkworm, Bombyx mori*. J Biol Chem, 1999. **274**(44): p. 31169-73.
216. Liu, X., et al., *Bombyx mori prothoracicostatic peptide inhibits ecdysteroidogenesis in vivo*. Arch Insect Biochem Physiol, 2004. **56**(4): p. 155-61.
217. Bollenbacher, W.E. and N.A. Granger, *Endocrinology of the prothoracicotropic hormone*, in *Comprehensive Insect Physiology, Biochemistry and Pharmacology*, Kerkut GA and G. LI, Editors. 1985, Pergamon: Oxford p. 109–51.
218. Nijhout, H.F., G. Davidowitz, and D.A. Roff, *A quantitative analysis of the mechanism that controls body size in Manduca sexta*. J Biol, 2006. **5**(5): p. 16.
219. Mirth, C., et al., *Critical weight as a switch in the developmental response to starvation: the role of ecdysone in the maturation of Drosophila wing discs*. Comparative Biochemistry and Physiology a-Molecular & Integrative Physiology, 2007. **148**: p. S9-S9.
220. Mirth, C.K. and L.M. Riddiford, *Size assessment and growth control: how adult size is determined in insects*. Bioessays, 2007. **29**(4): p. 344-355.